GEOLOGIC MAP OF THE NORTH BEND 7.5-MINUTE QUADRANGLE, KING COUNTY, WASHINGTON

by Joe D. Dragovich,
Timothy J. Walsh,
Megan L. Anderson,
Renate Hartog,
S. Andrew DuFrane,
Jeff Vervoot,
Stephanie A. Williams,
Recep Cakir,
Kelsay Davis Stanton,
Fritz E. Wolff,
David K. Norman, and
Jessica L. Czajkowski

WASHINGTON
DIVISION OF GEOLOGY
AND EARTH RESOURCES

Geologic Map GM-73
February 2009

WASHINGTON STATE DEPARTMENT OF
Natural Resources
Peter Goldmark - Commissioner of Public Lands

DISCLAIMER

Neither the State of Washington, nor any agency thereof, nor any of their employees, makes any warranty, express or implied, or assumes any legal liability or responsibility for the accuracy, completeness, or usefulness of any information, apparatus, product, or process disclosed, or represents that its use would not infringe privately owned rights. Reference herein to any specific commercial product, process, or service by trade name, trademark, manufacturer, or otherwise, does not necessarily constitute or imply its endorsement, recommendation, or favoring by the State of Washington or any agency thereof. The views and opinions of authors expressed herein do not necessarily state or reflect those of the State of Washington or any agency thereof.

WASHINGTON DEPARTMENT OF NATURAL RESOURCES

Peter Goldmark—*Commissioner of Public Lands*

DIVISION OF GEOLOGY AND EARTH RESOURCES

David K. Norman—*State Geologist*
John P. Bromley—*Deputy State Geologist*

Washington Department of Natural Resources
Division of Geology and Earth Resources

Mailing Address:
PO Box 47007
Olympia, WA 98504-7007

Street Address:
1111 Washington St SE
Natural Resources Bldg, Rm 148
Olympia, WA 98501

Phone: 360-902-1450
Fax: 360-902-1785
E-mail: geology@dnr.wa.gov
Website: http://www.dnr.wa.gov/AboutDNR/Divisions/GER/

DGER publications are available online at:
http://www.dnr.wa.gov/ResearchScience/Topics/GeologyPublicationsLibrary/Pages/pubs.aspx

The Geology Library catalog is online at:
http://www.dnr.wa.gov/ResearchScience/Topics/GeologyPublicationsLibrary/Pages/library.aspx

Suggested citation: Dragovich, J. D.; Walsh, T. J.; Anderson, M. L.; Hartog, Renate; DuFrane, S. A.; Vervoot, Jeff; Williams, S. A.; Cakir, Recep; Stanton, K. D.; Wolff, F. E.; Norman, D. K.; Czajkowski, J. L., 2009, Geologic map of the North Bend 7.5-minute quadrangle, King County, Washington, with a discussion of major faults, folds, and basins in the map area: Washington Division of Geology and Earth Resources Geologic Map GM-73, 1 sheet, scale 1:24,000, with 39 p. text.

This geologic map was funded in part by the U.S. Geological Survey National Cooperative Geologic Mapping Program.

© 2009 Washington Division of Geology and Earth Resources
Published in the United States of America

Geologic Map of the North Bend 7.5-minute Quadrangle, King County, Washington, with a discussion of Major Faults, Folds, and Basins in the Map Area

Joe D. Dragovich[1], Timothy J. Walsh[1], Megan L. Anderson[2], Renate Hartog[3], S. Andrew DuFrane[4], Jeff Vervoot[4], Stephanie A. Williams[1], Recep Cakir[1], Kelsay Davis Stanton[1], Fritz E. Wolff[1], David K. Norman[1], and Jessica L. Czajkowski[1]

[1] Washington Division of Geology and Earth Resources
PO Box 47007
Olympia, WA 98504-7007

[2] Colorado College
Department of Geology
14 E Cache La Poudre St
Colorado Springs, CO 80903

[3] Pacific Northwest Seismic Network
University of Washington
PO Box 351310
Seattle, WA 98195-1310

[4] Washington State University
School of Earth and Environmental Sciences
Pullman, WA 99164-2812

DESCRIPTION OF MAP UNITS

Information for the unit descriptions was partially compiled from the sources listed at the end of each description. Unconsolidated sediments are classified according to the Udden-Wentworth scale (Pettijohn, 1957). Except for 'volcanic sandstones', the classification of sandstones follows the terminology of Dickinson (1970). Assignment of volcanic rock names was made on the basis of whole-rock geochemistry and the total alkali-silica (TAS) diagram of Le Maitre (1989). See Dragovich and Walsh (2008) and Hammond and Dragovich (2008) for major and trace element geochemical rock data for samples obtained for this study, as well as more regional geochemical data. Clinopyroxenes with moderate birefringence and extinction angles are generally described as 'augite' but may locally include similar minerals such as pigeonite. Thin-section point-count data on the sand-size fractions aids differentiation of several glacial and nonglacial units in the area. One important compositional discriminator for various Quaternary geologic units is the average percentage of monocrystalline quartz (Qm) *versus* quartz mica tectonite/polycrystalline quartz/chert (Qp) versus potassium feldspar (PF). (See $Qm_xQp_xPF_x$ data from the Fall City quadrangle [Dragovich, 2007].) We use the time scale of the U.S. Geological Survey (USGS Geologic Names Committee, 2007) and Wolfe and others (1998). Lidar topographic data (Fig. 1) obtained from the King County Information Technology Division (GIS Products and Services) facilitated our mapping. Age sites and critical sites mentioned below are on the geologic map (on plate); the remaining sites are on Figure 2 (on plate).

Quaternary Sedimentary Deposits

HOLOCENE NONGLACIAL DEPOSITS

af **Artificial fill and modified land (Holocene)**—Mixed earth materials, including sand and gravel fill and natural deposits graded at major construction sites, that obscure the original geologic deposits. Includes fill along major highways (I-90), at landfills and the Seattle Public Utilities lower Cedar (crib) dam along the southeast margin of the map, and construction spoil placed in the Raging River valley in the northeast corner of the map.

Qa **Alluvium (Holocene)**—Sand, silt, gravelly sand, and cobble gravel with lesser peat and organic sediments; dark-gray to black; loose; mostly well stratified and sorted, plane-bedded sands common. Snoqualmie River sands contain monocrystalline quartz (Qm, 17–40%), plagioclase (~15%), volcanic lithic clasts (13–16%), granitic lithic clasts (7–10%), chert/polycrystalline quartz (Qp, 3–4%), and potassium feldspar (PF, 4–10%) and lesser sedimentary and metamorphic lithic clasts. Snoqualmie River alluvium is compositionally similar to the ancient alluvium found in the Olympia beds (unit Qc_o)(Armstrong and others, 1965), both in and northwest of the map area (Dragovich and others, 2007; Dragovich, 2007). Olympia beds along the lower eastern slope of Rattlesnake Mountain are similar to alluvium in the Fall City area, which has an average composition of $Qm_{54}Qp_{38}PF_8$. However, Middle Fork alluvium in the study area, and to a lesser extent the South Fork Snoqualmie River alluvium, has more monocrystalline quartz, potassium feldspar, biotite, hornblende, and granitic lithic clasts and stronger evidence of Snoqualmie batholith provenance as a result of the proximity of the alluvial basin to the Snoqualmie batholith "granite". This unit largely consists of Snoqualmie River alluvium deposited in overbank (flood) and abandoned channel settings that are inferred to overlie Fraser-age glacial deposits in the Snoqualmie valley (cross section on plate). In the northeastern part of the study area (critical site 1, sec. 14, T23N R8E), the Snoqualmie valley has an alluvial fan geomorphology; alluvium there probably overlies a late-glacial delta formed where the ancestral Snoqualmie River entered glacial Lake Snoqualmie. (See, for example, unit Qgl_r.)

Qp **Peat (Holocene)**—Peat, muck, and organic sediment, locally with some thin to very thin beds of tephra; loose or soft; poorly stratified. Peat occurs in abandoned flood-plain channels, in upland swales or closed depres-

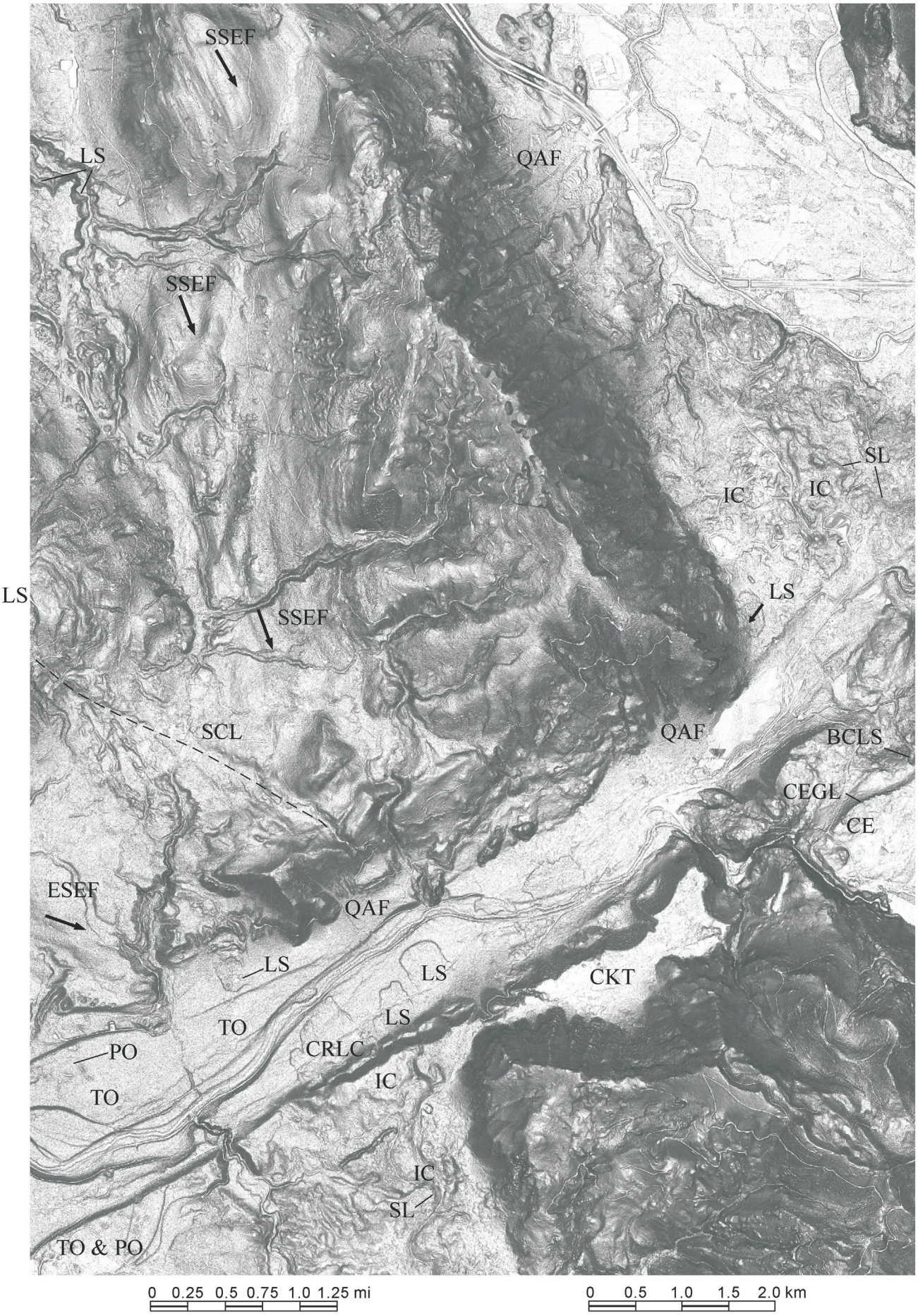
SSEF
LS
QAF
SSEF
SL
IC
IC
LS
LS
SSEF
SCL
QAF
BCLS
CEGL
CE
ESEF
QAF
LS
LS
CKT
LS
TO
CRLC
PO
IC
TO
IC
SL
TO & PO
0 0.25 0.5 0.75 1.0 1.25 mi
0 0.5 1.0 1.5 2.0 km

sions, and in kettles in ice-contact glacial deposits. A marsh-filled depression follows the part of the Steele Creek fault.

Qls **Landslide deposits (Holocene to latest Pleistocene)**—Landslides, including slump-earthflows, debris slumps, debris flows, and rock avalanches; mostly diamicton to sandy boulder gravel; loose or soft; poorly sorted, but some rock avalanches (as mapped, may include talus); moderately sorted; generally nonstratified, except for debris-flow aprons that contain stream-reworked sand or gravel interbeds and slump blocks that may retain disturbed but recognizable original stratigraphy. Clasts are angular to subangular where derived from up-slope bedrock, but the unit also contains rounded clasts derived from slumped older Quaternary deposits. The 1918 Boxley Creek landslide, on the eastern edge of the map area (plate and Fig. 1) in Boxley Canyon, destroyed the town of Edgewick and eventually flowed into the Snoqualmie River. Mackin (1941a) attributed the landslide to increased groundwater flow through gravels of the Cedar embankment as Chester Morse Lake reservoir (1 mi east of the quadrangle) filled. Most of the numerous debris flow/torrent aprons along the lower eastern slopes of Rattlesnake Mountain originated in low-strength, altered volcanic rock and fault gouge of the eastern Rattlesnake Mountain fault zone. Large rock avalanche deposits are mapped around Brewster Lake and north of the Cedar River (Lookout Mountain rock avalanche in the southeastern part of the map). Some landslides may have been seismically induced, particularly the numerous landslide complexes near Little Si along the eastern slopes of Rattlesnake Mountain, and (or) initiated during late Pleistocene deglaciation. For example, the large landslide complex south of the Cedar River likely initially collapsed as its ice buttress melted back during deglaciation and the Cedar kame terrace and Seventeen Creek ice-contact complex failed into the valley. (Walsh, 1984; Tabor and others, 2000)

Qaf **Alluvial fan deposits (Holocene to latest Pleistocene)**—Debris-flow diamicton and alluvial sand, gravel, and (silty) boulder gravel; loose; mostly poorly to moderately sorted; weakly stratified; deposited where streams emerge from confining valleys to areas of reduced stream gradients. Some fans were initiated as fan deltas in late-stage proglacial lakes and were later covered by aggrading Holocene alluvial fans. Several fans may have received high sediment fluxes following seismic events. Alluvial fans have more regular lobate geomorphology than landslide complexes (unit Qls); however, fans are locally gradational with landslide deposits. (Tabor and others, 2000)

PLEISTOCENE GLACIAL AND NONGLACIAL DEPOSITS

Vashon Stade Deposits of the Fraser Glaciation

The southward advance of the Puget lobe during the Vashon Stade blocked ancient rivers, creating an extensive temporary ice-dammed lake or lakes across much of the map area (Porter and Swanson, 1998; Associated Earth Sciences, 2005; Dragovich and others, 2007). The resultant advance glacial-lake deposits (unit Qgl_v) are complexly interlayered with proglacial river and delta sediments (unit Qga_v). These ice-dammed lakes drained generally southward, adjacent to, but more commonly beneath, the eastern margin of the ice sheet. Sands are a mixture of northern exotic and local Cascade detritus and mostly contain volcanic and granitic lithic clasts, chert–polycrystalline quartz, and plagioclase and fewer metamorphic and sedimentary lithic clasts. Vashon advance outwash ($\sim Qm_{40}Qp_{55}PF_5$) is similar to other lithic-rich outwash deposits and contains less monocrystalline quartz and potassium feldspar than Cascade provenance deposits such as the Snoqualmie River alluvium (unit Qa) or Olympia beds (unit Qc_o)(Booth, 1986, 1990; Dragovich and others, 2007; Dragovich, 2007).

The glacial ice limit elevations shown on the plate are probably within ~100 to 300 vertical feet of the actual limit; they were mapped using (1) the maximum local elevation of glacial deposits such as Vashon lodgment till and glacial erratics and (2) ice limit data of Booth (1986). Above the ice limit on Rattlesnake Mountain and southeast of the Cedar embankment, prolonged weathering has produced thick soils that lack exotic clasts.

Some "terraces" on the Cedar embankment are modified ice grounding lines demarking the contact between subglacial ice-contact deposits and ice-covered glacial lake deposits that developed during near-maximum ice advance (Booth, 1986), with later embankment modifications by subaerial kame outwash (Fig. 1). (See Booth, 1986; Mackin, 1941a,b; and Landau Associates, 2006, for information about the Cedar embankment.) Mackin (1941a,b) interpreted the Cedar embankment as a product of grounded ice and subaerial drainage, whereas Booth (1986) emphasized subglacial meltwater dynamics and geomorphic development during the maximum extent of Puget lobe ice. Large areas of stratified ice-contact deposits are commonly bounded on the southeast by relatively flat kames composed of fluvial-deltaic deposits (for example, Cedar kame terrace) and (or) ice dammed-lake deposits reflecting vigorous sedimentation adjacent to stationary ice. Some of the lake deposits that resulted from ice-damming are lateral facies equivalents of the fluvial-deltaic deposits and thus are part of the broader kame complex. Examples of fluvial-deltaic-lake kame complexes are the Cedar kame terrace and the contemporaneous deltaic complex south of the Seventeen Creek ice-contact complex in the southern part of the map area (Fig. 1).

A well-sorted fluvial boulder gravel exposed on an intermediate terrace on the south side of the Cedar River in (critical site 2,

Figure 1. Shaded-relief lidar (light detection and ranging) airborne laser swath mapping image of the North Bend quadrangle with vertical illumination and 6X vertical exaggeration. Prominent geomorphic features discussed in the text are labeled. East-southeast-trending till fluting (ESEF) in the southwestern part of the map area contrasts with the regional south-southeast fluting (SSEF) observed in the northern and central part of the map area. QAF, prominent alluvial fan-landslide complexes; LS, prominent landslide complexes; PO, pitted recessional outwash; TO, terraced outwash; CRLC, Cedar River landslide complex; IC, prominent ice-contact complexes; SL, prominent recessional lake strandlines (former beach positions); CKT, Cedar kame terrace; CEGL, Cedar embankment grounding line (inferred); CE, Cedar embankment; BCLS, Boxley Creek landslide complex; SCL, Steele Creek (fault) lineament.

sec. 23, T22N R7E) and west of the map area contains boulders ranging from 6 to 20 ft in diameter (Walsh, 1984). The boulders are exclusively Western mélange belt peridotite, pyroxenite, and metasandstone. Because of the unmixed provenance of these boulders, we suspect that they (1) were catastrophically scoured from an area near or east of the Cedar embankment where the Mesozoic Western mélange belt crops out or occurs in the near subsurface, (2) originally were deposited as subglacial tunnel ice-contact deposits formed by westward flow along the Cedar River valley, and (3) were later glaciofluvially reworked to produce the present boulder lag in unit Qgof. This model is supported by (1) the unique boulder composition, (2) location of deposit along the axis of the Cedar River valley, and (3) the presumption that jökulhlaups or catastrophic subglacial drainage from ice marginal glacial lakes and englacial water reservoirs were common (Booth, 1986).

Till drumlin and flute elongation directions show that ice flowed south-southeasterly parallel to the Raging River and Snoqualmie valleys. However, fluting in the Cedar River basin west of Rattlesnake Lake records an anomalous southeasterly ice flow that terminates in arcuate ice-contact deposits in the map area (Fig. 1). These arcuate ice contact deposits probably demark a temporary "ice tongue" that occupied the Cedar River valley during ice recession. The ice flow indicators converge in the Cedar River area west of Rattlesnake Lake. We suspect that (1) proglacial lakes had an important local influence on the ice-flow dynamics and (2) the anomalous easterly ice flow is due to late ice flow surge toward one or more of the proglacial lakes in the Cedar River valley that were dammed by this ice tongue. The overall picture for the Cedar River and Raging River valleys during recession is one of interacting proglacial lakes, kame terraces and deltas that dynamically interacted with arcuate ice tongue(s) that occupied these emerging valleys (Dragovich and others, 2007; Booth, 1986; Tabor and others, 2000; Landau Associates, 2006).

Vashon Stade recessional ice-contact, fluvial, deltaic, and lacustrine facies were deposited against and behind the receding Puget lobe. Many of these facies are laterally and vertically gradational, and their contacts are typically gradational and interfingering. The geometry, inset relations, and elevations of these ice-marginal lake and connecting glaciofluvial channel deposits reflect a general lowering of base level as lower valleys successively became deglaciated and new spillways developed during ice recession. The glaciolacustrine lakes and connecting channels migrated westward and northwestward during deglaciation. Inset recessional outwash bodies are graded to a local base level that lowered over time and resulted in younger kame and delta deposits at successively lower elevations. Booth (1986, 1990) and Tabor and others (2000) subdivided recessional outwash deposits into six stages of deglaciation and emphasized the importance of both ice-marginal and subglacial meltwater paths.

Glacial Lake Snoqualmie was long-lived and covered a substantial part of the map area during deglaciation (Mackin, 1941a, b; Booth, 1990). The varying elevation of this lake controlled the altitude of some delta tops, strandlines, and recessional channels, as well as the distribution of some glaciolacustrine deposits.

Recessional sands have a mixed local Cascade and northern metamorphic-granitic provenance, the northern clasts having been transported via Puget lobe ice or scoured from older deposits. Recessional sediments fed westward through the Cedar embankment and kame complex meltwater system contain more local Cascade-provenance clast types.

Deglaciation in this part of the lowland and retreat from maximum ice position commenced about 14,000 yr B.P., and the map area was probably fully deglaciated by about 13,700 yr B.P. (Porter and Swanson, 1998).

Vashon Stade Recessional Deposits

Qgos **Outwash sand (Pleistocene)**—Sand and pebbly sand, with some interbeds of silty sand, silt, or gravel; sands typically grayish brown and weathered or stained brown to yellowish brown; loose or soft; varying from massive to weakly stratified to plane-bedded, laminated, or, rarely, crossbedded. Sands in the Cedar River area contain chert, volcanic, greenstone, and serpentinite grains that indicate their origin in pre-Tertiary mélange belts and Tertiary volcanic rocks east of the deposits. Facies relations, including vertical and horizontal fining trends, suggest that the outwash sands are mostly shallow-water proglacial lake deposits that locally interfinger or are spatially associated with recessional fluvial and deltaic deposits. Some sand bodies are overlain by gravel and underlain by finer lake deposits (unit Qgl_r) due to local deltaic progradation. (Tabor and others, 2000; Dragovich and others, 2007; Dragovich, 2007; Rosengreen, 1965)

Qgl_r **Recessional glaciolacustrine (glacial lake) deposits (Pleistocene)**—Silt, clayey or sandy silt, silty sand, and fine sand typically with scattered dropstones; local layers and lenses of sand or gravel; loose or soft; massive, laminated, or thinly bedded, with some varve-like rhythmites; deposited in small to large proglacial to ice marginal lakes; locally forms upward-coarsening sequences from glacial lake (units Qgl_r and Qgos) to terrestrial environments (units Qgog and Qgof) due to progradation of kames or late-stage fluvial-deltaic complexes; includes sediments of glacial Lake Snoqualmie, late-stage glacial lakes occupying the Cedar and Raging River valleys, and small lakes formed in kettles or small elevated kames. The distribution of glacial-lake sands, silts, strandlines, and some delta tops indicates that glacial Lake Snoqualmie had a persistent level at ~800 ft elevation. Glacial-lake deposits in the Cedar River valley are overlain by fairly thin terraced recessional outwash strata (unit Qgof) as a result of glaciofluvial incision as regional base-level fell during ice recession. (Rosengreen, 1965; Dragovich and others, 2007; Tabor and others, 2000)

Qgof **Fluvial outwash deposits (Pleistocene)**—Boulder cobble gravel, sandy gravel, pebbly sand, sand, and minor silt; loose; moderately to well-stratified; mostly medium- to very thickly bedded, locally cross-bedded. These deposits lack ice-contact features such as kettles or irregular topography and include both outwash plain deposits and remains of less extensive recessional channels incised into older deposits, as well as conspicuous and thin, terraced outwash bodies at intermediate and

low elevations along the Cedar River and around Rattlesnake Lake. The stratigraphy in many erosional terraces indicates that the outwash streams incised older deposits, consistent with a falling base level as ice receded.

Qgic **Ice-contact deposits, undivided (Pleistocene)**—Bouldery cobble gravel, diamicton, silty pebbly gravel, pebbly sand, and lesser sand and silt; loose; mostly moderately stratified; medium- to very thickly bedded; highly varied sorting with abrupt grain-size changes common. Ice-contact primary structures include syndepositional slumps, oversteepened and contorted bedding, and sediment collapse or ice-shear features. Soft melt-out, flow, and water-laid diamictons are interstratified with granular supraglacial, englacial, and subglacial meltwater deposits. The deposit surface is typically hummocky or irregular; numerous kettles or depressions indicate sedimentation in, around, and on stagnant or active ice in controlled moraine and pitted outwash-plain settings. Ice-contact deposits locally are overlain by, or laterally grade to, ice-marginal sandy or silty lake deposits. Although we include densely pitted fluvial outwash terraces in this unit (Fig. 1 and map), most outwash-plain deposits (unit Qgof) are younger and overlie slightly older ice-contact deposits. Some small and subtle linear or sinuous geomorphic features associated with undivided ice-contact deposits in the Cedar River valley may be modified eskers or small eroded moraines. (Walsh, 1984, Tabor and others, 2000; Rosengreen, 1965; Landau Associates, 2006)

Locally divided into:

Qgi **Ice-contact deposits, till (Pleistocene)**—Sandy silty pebble gravel to bouldery gravelly sandy silt locally with lesser sand or gravel beds; includes massive to moderately stratified recessional melt-out, ablation, or flow till deposited near or under melting ice. These deposits are poorly exposed and spatially associated with other moderate- to low-density near-ice deposits.

Qgik **Ice-contact deposits, kames (Pleistocene)**—Sandy gravel, pebbly sand, sand, and cobble gravel, with scattered lenses of diamict; loose; medium- to very thickly bedded; moderately to well-stratified; local till or silt rip-up clasts, crossbedding, cut-and-fill structures, and oversteepened or slumped bedding. These elevated fluvial-deltaic deposits were mapped where sedimentary structures, geomorphology, and (or) geologic setting imply lateral ice buttressing. Broad fluvial (braided) outwash sediments (unit Qgof) deposited in open valley trains generally lack evidence for nearby ice and were generally deposited at lower elevations later in the recessional episode. Some kames grade laterally into kame deltas (unit Qgod) and (or) lake deposits (units Qgos and Qgl_r). For example, the Cedar kame terrace (Fig. 1) grades to the southwest into a kame delta-ice marginal lake complex and is bounded on the west by the Seventeen Creek ice-contact complex (map). The unit includes some moderately pitted or kettled outwash terraces in the southwestern part of the study area. (Dragovich and others, 2007; Walsh, 1984; Mackin, 1941a, b; Tabor and others, 2000; Rosengreen, 1965)

Qgod **Deltaic outwash and kame deltas (Pleistocene)**—Sandy cobble gravel, gravel, and pebbly sand; loose; moderately to well-sorted; thin- to very thickly bedded and well-stratified; includes high-amplitude planar foreset beds graded to temporary ice-dammed lake levels. Cedar River kame deltaic sands are lithic rich and contain significant amounts of serpentinite, granitic, volcanic, amphibolite, and chert lithic clasts and hornblende. This composition indicates a strong local easterly provenance. Deltaic deposits commonly grade laterally to bottomset beds of glaciolacustrine sand (unit Qgos) and (or) silt or clay (unit Qgl_r). This unit includes either large kame deltas or smaller deltas graded to varying proglacial lake levels within the Snoqualmie, Cedar, and Raging River valleys. Small deltas are generally younger than kame deltas because they lack evidence for near-ice deposition and were fed by local upland streams that vigorously incised the newly exposed and unstable upland surfaces.

Qgog **Outwash gravel deposits, undivided (Pleistocene)**—Bouldery pebble cobble gravel to pebbly cobbly sand; loose; massive to crudely bedded; typically poorly exposed. Gravels mapped around late-glacial strandlines are likely beach deposits. The unit may include any of the gravelly Vashon recessional facies described above, but is probably mostly kame deposits, including the prominent perched terraces in the Cedar River valley. (Tabor and others, 2000)

Vashon Stade Advance Proglacial and Subglacial Deposits

Qgt_v **Vashon lodgment till (Pleistocene)**—Clay, silt, sand, and gravel (diamicton), commonly with disseminated cobbles and boulders in a silt-sand matrix; local lenses of sand and gravel; grayish blue to very dark gray; weathers to a mottled yellowish brown; dense to very dense; massive; matrix-supported; friable shear fabric locally; nonstratified; unsorted; northern- and local-source rounded to subangular clasts, but angular where they directly overlie bedrock; generally 10 to 20 ft thick, but ranges from a veneer to ~80 ft thick. The till was deposited as an accretionary bed at the base of Vashon continental ice on a late-glacial topography somewhat similar to today's. Although high-quality boring log information is scant, water well and geotechnical boring information suggests that till locally occurs at a shallow depth in the Snoqualmie valley (cross section). Vashon till unconformably overlies bedrock, advance deposits, and older Quaternary deposits and occurs below ice-contact deposits on and near the Cedar embankment. Unit Qgt_v

diamictons are more compact than the diamictons in unit Qgic. (Dragovich and others, 2007; Booth, 1986; Tabor and others, 2000; Landau Associates, 2006)

Qga_v **Advance outwash deposits (Pleistocene)**—Sand, sandy (pebble) gravel, and cobble gravel with local silt interbeds; sands are gray to reddish gray, weathered yellowish brown; dense; moderately to well-sorted and -stratified; thinly to very thickly bedded; local laminated silt interbeds. Some outcrops contain deltaic foreset beds, cut-and-fill structures, and rip-up clasts or rare ice shear structures. Advance outwash was deposited by streams issuing from the front of the advancing ice and conformably overlies, is complexly interlayered with, or may locally underlie glacial-lake deposits (unit Qgl_v). Advance outwash is overlain by Vashon lodgment till along a sharp contact. Composite sections of fluvial-deltaic advance outwash and glacial-lake deposits are fairly thick in the Raging River valley where deltaic deposits are graded to local proglacial lake elevations as high as ~1700 ft around Canyon Creek in the northwest part of the map area. ^{14}C ages from this unit northwest of the study area are 14,500 ±130 yr B.P. (Associated Earth Sciences, Inc., 2005) and 14,450 to 14,560 yr B.P. (Porter and Swanson, 1998). (Also see limiting ages in unit Qc_o.) (Dragovich and others, 2007; Tabor and others, 2000; Saltonstall and others, 2003; Rosengreen, 1965)

Qgl_v **Advance glaciolacustrine deposits (Pleistocene)**—Silt and clayey silt, locally with scattered dropstones; local beds or lenses of massive diamicton that may be iceberg melt-out till or flow-till; commonly contains laminated to thinly bedded silt ± sand with sparse lenses of gravel; silts or clayey silts typically dark bluish gray, weathered light yellowish brown; stiff or dense; massive to thinly bedded, laminated or varved with slickensided, fractured, contorted folded bedding locally present. This unit is typically overlain by and (or) interbedded with unit Qga_v and was deposited in proglacial lakes in the Raging, Cedar, and Snoqualmie River valleys during ice advance. Elevated advance lake deposits in the Raging River valley (cross section) may be the result of ice damming of the Cedar River valley prior to ice inundation of the Raging River valley. Most outcrops contain dropstones, are interlayered or spatially associated with probable advance outwash, and thus are Vashon-age lake deposits. However, some poorly exposed silt-clay deposits lacking these features but included in unit Qgl_v may be older glacial or nonglacial units. The unit includes some of the advance outwash of Tabor and others (2000). We correlate this unit with the Lawton Clay Member of the Vashon Drift (Mullineaux and others, 1965) and here extend the member into the Snoqualmie 1:100,000-scale quadrangle. (Dragovich and others, 2007; Dragovich, 2007; Saltonstall and others, 2003; Associated Earth Sciences, Inc., 2003; Tabor and others, 2000; Rosengreen, 1965)

Pre-Fraser Glacial and Nonglacial Deposits

Deposits of the Olympia Nonglacial Interval

Qc_o **Olympia beds of Armstrong (1965)(Pleistocene)**—Sand, cobbly and pebbly gravel, with some silty gravel, pebbly sand, and some silt, clay and peat; gray sands typically weathered light to dark brown; dense; laminated to very thickly bedded, locally crossbedded; mostly well stratified; local disseminated organic matter including charcoal. Olympia beds in the Snoqualmie valley are geochemically and petrographically similar to modern Snoqualmie River alluvium. For example, Olympia beds along the eastern slopes of Rattlesnake Mountain are monocrystalline quartz- and potassium feldspar-rich sands ($Qm_{58\text{-}71}Qp_{18\text{-}25}PF_{5\text{-}17}$), similar to both Snoqualmie River alluvium and Olympia beds to the northwest of the area (Dragovich, 2007; Dragovich and others, 2007). Saltonstall and others (2003) Dragovich (2007), and Dragovich and others (2007) also show that Olympia bed sands are geochemically similar to modern Snoqualmie alluvial sand but distinguishable from Vashon glacial sands. The Olympia beds along the eastern slopes of Rattlesnake Mountain (critical site 3, sec. 8, T23N R8E) may be faulted and uplifted within the Rattlesnake Mountain fault zone (cross section). This unit was deposited as Snoqualmie River alluvium, but locally may include alluvial fan, lake, swamp and colluvial deposits of the Olympia nonglacial interval (~20,000–60,000 yr B.P.). Associated Earth Sciences, Inc. (1987, 2003, 2005) obtained nine ^{14}C ages from surface and subsurface Olympia beds around Snoqualmie Ridge[1] north-northwest of the study area; these range from 23,450 ±130 yr B.P. to 41,270 ±1,610 yr B.P. (table 1 in Dragovich and others, 2007). Associated Earth Sciences, Inc. (1998) also obtained a ^{14}C age of 24,060 ±160 yr B.P. from along Boxley Creek in the east-central margin of the study area (age site 1, sec. 35, T23N R8E) where ancient alluvial-alluvial fan sands have a strong local Western mélange belt provenance. We correlate exposures of dense, iron oxide-stained sand and gravel on the eastern slopes of Rattlesnake Mountain with the Olympia nonglacial interval on the basis of sand composition, stratigraphic position, and weathering characteristics. Until we are able to date this unit, we cannot discount the possibility that these some of these deposits may be older interglacial deposits of the Whidbey Formation. (Dragovich, 2007; Dragovich and others, 2007; Associated Earth Sciences, Inc., 1987, 2003, 2005)

Qgn_{pf} **Glacial and nonglacial deposits, pre-Fraser, undivided (Pleistocene to Pliocene?)**—Sand, silt, clay, gravel, peat, and diamicton; dense to very dense; sands weather dark brown. The unit includes pre-Fraser sediments in the subsurface (cross section) and poorly exposed sand ± gravel deposits in the Raging River valley. The Raging River valley sands are strongly oxidized and

[1] Snoqualmie Ridge is an informal geographic name for the ridge extending from the Lake Alice area east to the City of Snoqualmie, north of Interstate-90.

contain significant (~20%) clay weathering products, as well as volcanic and sedimentary lithic clasts, pyroxene, plagioclase, and lesser monocrystalline quartz. The low polycrystalline quartz content and relatively high lithic clast content suggest deposition as an alluvial-alluvial fan nonglacial deposit. Porter (1976) inferred the Evans Creek Stade alpine glaciers extended to or beyond the mountain front and may have advanced down the Snoqualmie valley to as far as the North Bend area early in the Fraser glaciation; thus unit Qgn_{pf} beneath North Bend on the cross section may include Evans Creek glacial deposits. (See "Eastern Rattlesnake Mountain Fault Zone, North Bend Basin, and the Snoqualmie River Anticlinorium", p. 25.) Wood in horizontally bedded sand and silt along the South Fork Snoqualmie River a few miles east of the map area yielded an "infinite" ^{14}C age of >50,000 yr B.P. (Booth, 1986; Porter, 1976). See Tabor and others (2000), Dragovich and others (2007), and Booth (1990) for information about locally oxidized pre-Fraser fluvial, lacustrine, and glacial sediments west, northwest, and north of the map area.

Tertiary Volcanic, Sedimentary, and Intrusive Rocks

Miocene to Eocene rocks in the map area are juxtaposed against pre-Tertiary rocks of the Western mélange belt across the broad Rattlesnake Mountain fault zone (Fig. 2 on plate). Tertiary rocks may be underlain by "basement(?)" west of the Rattlesnake Mountain fault zone (cross section). Exposed Tertiary rocks north of the Steele Creek fault are largely middle Eocene in age in the map area, whereas rocks south of this fault are largely latest Eocene to Miocene in age.

TERTIARY INTRUSIVE ROCKS

ᴍΦigb, ᴍΦigd **Snoqualmie batholith gabbro (Miocene to Oligocene)**—Gabbro (41% SiO_2); contains hypidiomorphic plagioclase and clinopyroxene, and opaque minerals; homogeneous; coarse-grained; grayish green, weathers to a pale brown with red oxide alteration; massive; samples generally altered as indicated by the high geochemical "loss on ignition" and strong alteration of mafic minerals. Gabbro occurs along the western edge of the study area and is coincident with a slight to distinct magnetic high along the Raging River valley that Dragovich and others (2007) correlate with intrusion of Tertiary porphyries and (or) Snoqualmie batholith gabbro northwest of the map area. A tonalite mapped by Tabor and others (2000) east-southeast of the study area may also be an exposed phase of the Snoqualmie batholith; they report a reset 17.6 Ma zircon fission-track age from a rhyolite tuff near this intrusive body. The Snoqualmie batholith intruded from ~15 to 25 Ma; its granodiorite (unit ᴍΦigd; cross section only) is likely exposed directly north and west of the map area (Walsh, 1984; Tabor and others, 1993) and is inferred to be common in the subsurface. Geophysical modeling (Figs. 3A–C) suggests Snoqualmie batholith gabbro occurs below the Raging River valley. The contact and compositional characteristics of the gabbro, tonalite, and granodiorite in and around the map area suggest they are younger than the Puget Group and likely Miocene and (or) Oligocene in age. More work is needed to clarify correlation of these bodies with the Snoqualmie batholith. (Dragovich and Walsh, 2008; Walsh, 1984; Tabor and others, 2000)

ᴍEib **Basaltic andesite dikes (Miocene to Eocene)**—Basaltic andesite to basalt dikes (~46–55% SiO_2); homogeneous; typically greenish black to dark-gray, weather to a yellowish brown; massive, with uniform holocrystalline texture, typically showing eutaxitic (flow) mineral alignment; contains equigranular phenocrysts of plagioclase (0.3–3 mm) and augite ± hypersthene, disseminated opaque minerals, and minor amounts (<5%) of glass. Chloritized grains in a few samples may have been hornblende. Only the most prominent of the widespread dikes in the study area are shown on the map. The protomylonitization of some dikes and dike swarms near faults suggests structural control and faulting during or after intrusion. Because contacts are commonly concealed, we cannot exclude the possibility that some dikes are mafic flows. The uniform geochemical and petrologic composition and widespread occurrence suggests that these rocks are genetically linked intrusive bodies. Dikes intrude most Eocene and (or) Oligocene geologic units in the study area and thus may be locally as young as Miocene (particularly in the southern part of the map area). Dikes are similar to the pyroxene-bearing intermediate and mafic porphyries (21–23 Ma whole-rock K-Ar ages) mapped outside of the study area that Tabor and others (2000; R. W. Tabor, USGS emeritus, written commun., 2008) suggest could be feeder bodies to the Miocene Fifes Peak Formation. We speculate that the two "young" local fission track ages of 17.6 Ma (see unit ᴍΦigb) and 24.7 Ma (age site 2, sec. 21, T22N R8E) in the southeastern part of the map area may be the result of Miocene reheating of country rock near dikes or dike swarms. This hypothesis is particularly relevant for age site 2, where the rock is anomalously young and occurs near mapped dikes. (Dragovich, 2007; Dragovich and Walsh, 2008; Dragovich and others, 2007; Tabor and others, 2000)

ΦEia **Andesite porphyry (Oligocene to Eocene?)**—Sills or dikes of andesite (~57% SiO_2); holocrystalline to porphyritic; massive; typically dark-gray to greenish gray, weathers yellowish brown; contain phenocrysts of plagioclase (2–5 mm long) and smaller grains of euhedral to subhedral augite and local hypersthene. The unit intrudes the Puget Group and (probably) the volcanic rocks of Rattlesnake Mountain (unit $ΦEva_r$). Although contacts are generally concealed, these intrusive rocks are texturally gradational with the extrusive andesites they intrude and are locally difficult to discern; as a result, we map only the most conspicuous bodies. We speculate that some of the porphyry may be the intrusive equivalent of the volcanic rocks of Rattlesnake Mountain (cross section). See Tabor and others (2000) and

Vine (1969) for further descriptions of texturally variable andesite porphyries in the region. (Dragovich and Walsh, 2008; Dragovich and others, 2007)

TERTIARY VOLCANIC AND SEDIMENTARY ROCKS

Ꝧva **Fifes Peak Formation (Miocene)**—Basaltic andesite and basalt flows, flow breccia; flows generally dark reddish, dark green to dark gray or black; local flow banding, columnar jointing, vesicular tops, scoriaceous and amygdaloidal zones, and minor drusy quartz zones. The unit also contains massive to well-bedded polymictic tuff and breccia and rare monolithologic tuff and breccia with andesite clasts. Textures are trachytic, intersertal, or intergranular. Porphyritic to microporphyritic andesite contains plagioclase (20–30%), hypersthene (5–15%), and clinopyroxene in a reddish brown glass. The glass contains plagioclase microlites, pyroxene, opaque minerals, and secondary smectites, hematite, calcite, and quartz. Black basalt contains plagioclase ± pyroxene microphenocrysts and altered olivine in the groundmass. The Fifes Peak Formation occurs in a small area on the south border of the map area. Regionally, the formation also contains interbedded andesite breccia and tuff, mudflow deposits, and minor volcanic sandstone, conglomerate, and siltstone; Fifes Peak rocks are less altered than older volcanic rocks in the study area but locally contain some heulandite, clay, chlorite, and quartz alteration products. The lone mapped contact is largely from Tabor and others (2000). Radiometric age dates nearest the study area indicate that the formation is Miocene (~22–24 Ma) but may be as young as 20 Ma and as old as 27 Ma (Vance and others, 1987; Tabor and others, 2000). (Also see unit ꝦEib.) The unit includes the Fifes Peak Formation and part of the informally named "Snow Creek formation" of Hammond (1963). (Tabor and others, 2000; Fischer, 1970; Hartman, 1973)

ꝦƠva **Volcanic rocks of Eagle Gorge (Miocene and Oligocene)**—Andesite to basaltic andesite (~53% SiO_2) flow and breccia with minor tuff, local tuff breccia with pumice; flows and flow breccia; gray, dark-green to black, weathering light to moderate brown. Regionally, the unit includes basalt flows, sandstone, conglomerate, siltstone, and rare mudflow breccia. In the map area this unit is largely composed of massive flows with some breccia and lapilli tuff. Columnar jointing and vesicular flow tops are locally evident. Breccia is generally monolithologic andesite or basaltic andesite. Phenocrysts include plagioclase and augite with intersertal and intergranular texture. Secondary minerals include smectite, hematite, calcite, and quartz; Tabor and others (2000) report hypersthene phenocrysts. The volcanic rocks of Eagle Gorge were named by Tabor and others (2000); this is a hybrid unit locally present between the Ohanapecosh and Fifes Peak Formations that contains mostly Fifes Peak–equivalent flows, minor breccia and tuff, and Ohanapecosh-equivalent lavas. Tabor and his colleagues were not able to find the diagnostic unconformity between these formations, nor could they find the generally definitive silicic ash-flow tuff at the base of the Fifes Peak in the study area. The unit includes the volcanic rocks of Eagle Gorge of Tabor and others (2000) and part of the "Snow Creek formation" of Hammond (1963). We assign the unit a Miocene to Oligocene age range, given the possibility that the rocks may be correlative with the Fifes Peak Formation (Miocene) or Ohanapecosh Formation (Oligocene). (Hammond, 1963; Tabor and others, 2000)

ƠvT **Tuff of Stampede Pass of Hammond (1963) (Oligocene)**—Dacitic to rhyolitic crystal-vitric to vitric-crystal tuff (63–74% SiO_2), pumiceous tuff-breccia with lesser andesitic (~61% SiO_2) lithic or crystal-lithic tuff-breccia, and rare andesite flows; vitroclastic and eutaxitic textures common. Tuff is pale greenish gray to yellowish gray, and breccia is various shades of greenish gray and brownish gray. Beds are partially welded; bedding is defined by flattened pumice lapilli or rare aligned coalified sticks and logs. Crystal-vitric tuff matrix typically consists of plagioclase (~10–25%), quartz (typically embayed; 5–10%), with scattered augite crystals (~1–4%) in a clear to greenish brown vitroclastic glass (to ~80%) that locally contains microlites and altered red, brown, and black lithic lapilli (to ~25%). Pumice lapilli are conspicuous except in the lithic breccia where andesitic lithic clasts dominate.

Unit ƠvT is a composite ignimbrite with as many as six individual thick to very thick tuff beds. We do not show the single lensoidal andesite flow interbed mapped by Hammond (1963, pl. 1) that suggests the tuff in the map area is a composite of at least two very thick tuff beds. Compositional trends noted in the field suggest that individual pyroclastic flows and (or) surge

Figure 3A. *(opposite page)* Gravity anomaly and aeromagnetic map of the North Bend quadrangle with isostatic gravity anomaly contours (Anderson and others, 2006) superimposed on the aeromagnetic map of the North Bend quadrangle. Locations for profiles modeled in Figure 3B and 3C are labeled A–A′ and B–B′, respectively. Blue crosses, gravity stations; NBB, North Bend basin (gravity low); GB, Snoqualmie batholith gabbro (slight magnetic high); RS, Rattlesnake Mountain (magnetic high); WMB, Western mélange belt (magnetic high above serpentinites); LS, Lindsay syncline (magnetic high and gravity low). Gravity contours indicate a Tertiary basin in the southern part of the map area. Bedding contours around the Lindsay syncline follow this Tertiary basin. See Figures 3B and 3C for gravity and magnetic modeling cross sections. See the geologic map (plate) for fault and fold symbols and their definitions not shown in the explanation.

Figure 3B. *(page 12)* Gravity and magnetic modeling cross section A–A′. Profile A is near and mostly subparallel to the geologic cross section on the plate. The model is assumed to extend to infinity in both directions perpendicular to the profile. $\Delta\rho$ is the density contrast relative to normal crust (2670) in kg/m^3; χ is magnetic susceptibility in SI units multiplied by 1000.

Figure 3C. *(page 13)* Gravity and magnetic modeling cross section B–B′. The model is assumed to extend to infinity in both directions perpendicular to the profile. $\Delta\rho$ is the density contrast relative to normal crust (2670) in kg/m^3; χ is magnetic susceptibility in SI units multiplied by 1000.

3A

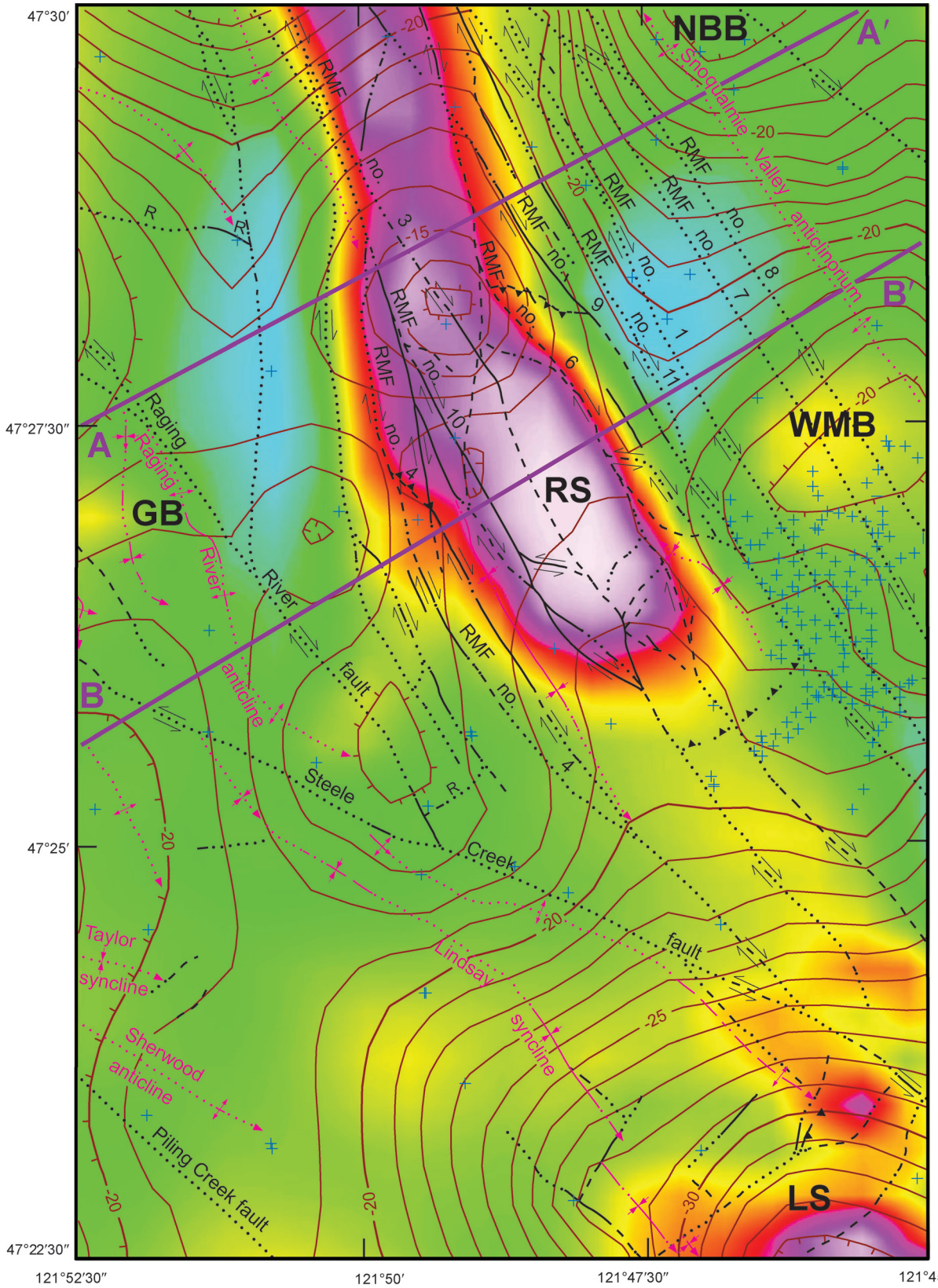

EXPLANATION

+	Gravity measurement locations used to control interpolation of gravity data
—— -20	Gravity contours—hachures point in the direction of decreasing gravity values; contour interval 1 milligal
A ——	Cross section line
NBB	North Bend basin
RS	Rattlesnake Mountain
LS	Lindsay syncline
WMB	Western mélange belt
GB	Snoqualmie batholith gabbro

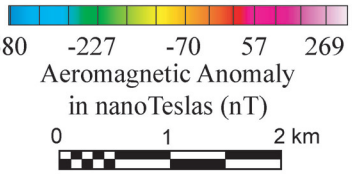

Note: fault and fold symbology simplified from geologic map (plate) for clarity. See plate for fault and fold symbol definitions.

3B

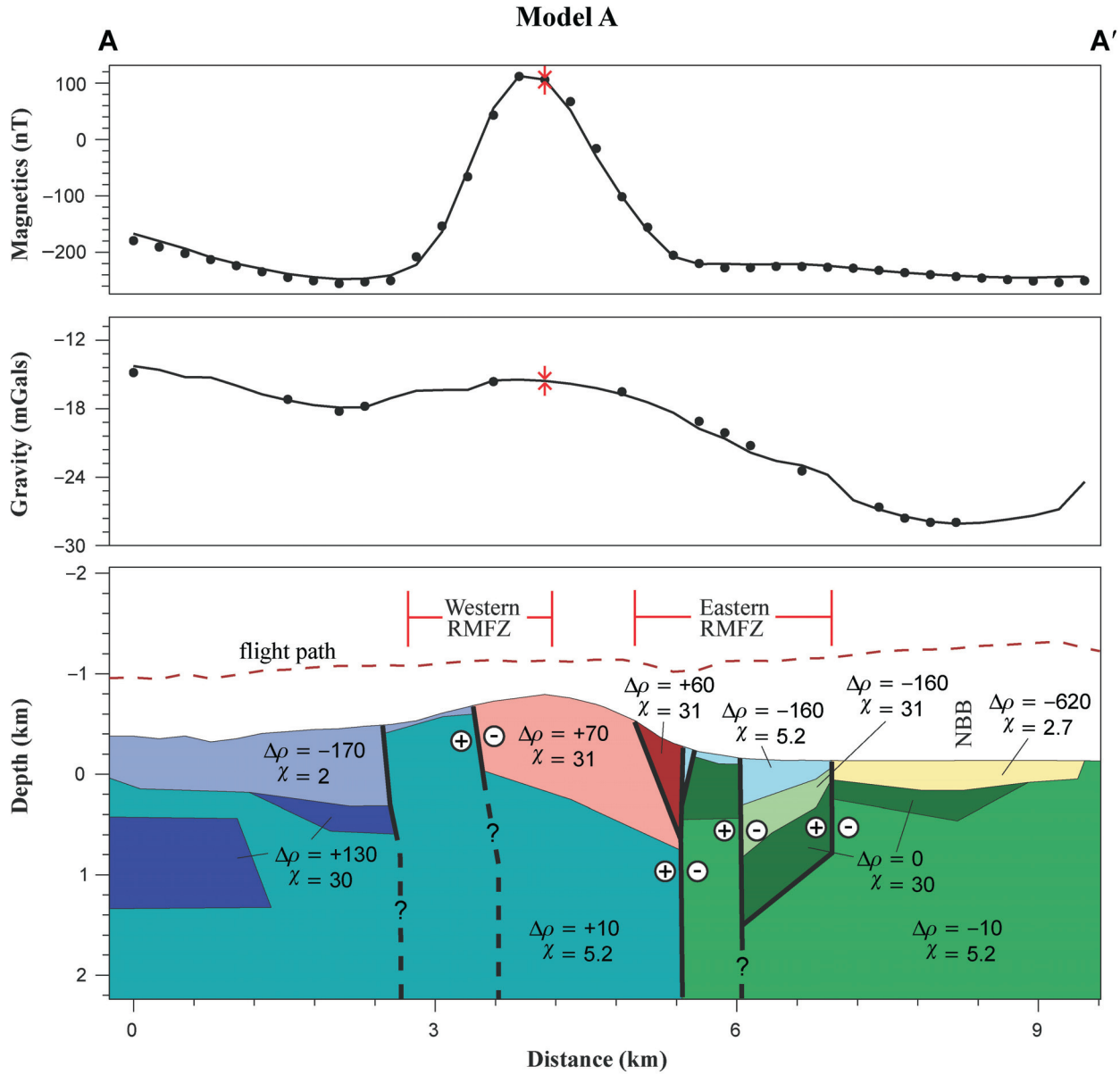

Anomalies:

- ● Observed
- —— Calculated
- Geophysical datum
- ——?– – – Fault; dashed where inferred
- ⊕ Strike-slip movement away from viewer
- ⊖ Strike-slip movement toward viewer
- $\Delta\rho$ density contrast relative to normal crust, in kg/m^3
- χ magnetic susceptibility in SI units x 100

Quaternary deposits	Volcanic rocks of Rattlesnake Mountain (undifferentiated)	Basement?
Puget Group and Raging River Formation	Western mélange belt	Snoqualmie batholith gabbro
Metagabbro	RMFZ Rattlesnake Mountain fault zone	NBB North Bend basin

Eastern Rattlesnake Mountain fault zone cataclasites

Volcanic rocks of Rattlesnake Mountain	Western mélange belt	Gabbro

3C

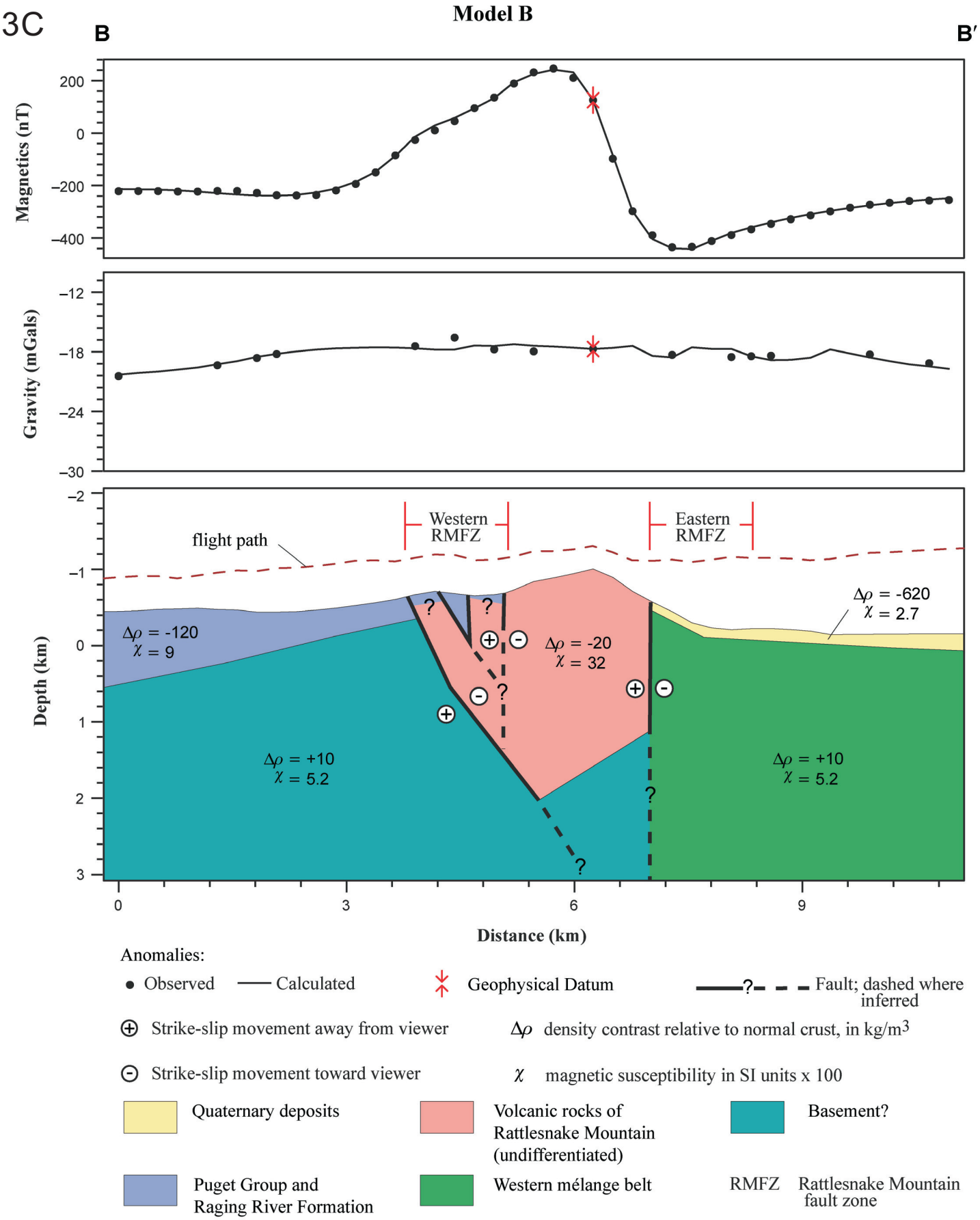
Model B
B
B′
Magnetics (nT)
200
0
–200
–400
Gravity (mGals)
–12
–18
–24
–30
Depth (km)
–2
–1
0
1
2
3
flight path
Western RMFZ
Eastern RMFZ
Δρ = -120
χ = 9
Δρ = -20
χ = 32
Δρ = -620
χ = 2.7
Δρ = +10
χ = 5.2
Δρ = +10
χ = 5.2
0
3
6
9
Distance (km)
Anomalies:
Observed
Calculated
Geophysical Datum
Fault; dashed where inferred
Strike-slip movement away from viewer
Δρ density contrast relative to normal crust, in kg/m3
Strike-slip movement toward viewer
χ magnetic susceptibility in SI units x 100
Quaternary deposits
Volcanic rocks of Rattlesnake Mountain (undifferentiated)
Basement?
Puget Group and Raging River Formation
Western mélange belt
RMFZ Rattlesnake Mountain fault zone

deposits are compositionally zoned from dacite tuff and tuff-breccia to lithic andesite breccia with dacitic rocks dominating individual flow units (Dragovich and Walsh, 2008; Hammond and Dragovich, 2008). Unit ⦶vt may unconformably overlie the "Huckleberry Mountain formation" of Hammond (1963). The dated dacitic tuff (age site 3, sec. 21, T22N R8E) contains conspicuous semi-flattened pumice constituting about 15 percent of the rock. Pumice clasts are as much as 22 cm long and are slightly welded. The rock contains broken pumice grains and fragments in a light greenish brown glass with significant darker lithic clasts. Lithic clasts contain a dark-brown, black, and reddish brown glass and of are of varied texture and composition; most lithic clasts are microlitic and probably andesitic in composition. One clast contains a biotite-like mineral after hornblende(?), and another contains clinopyroxene microphenocrysts. The tuff matrix also contains a few small clinopyroxene (augite?) grains, a few small angular grains of quartz, and ash-size pumice with well-formed concentric bubble walls. The tuff has a fragmented glass (vitroclastic) texture similar to that of the tuff of Stampede Pass of Hammond (1963) and that Hammond and Dragovich (2008) observed in exposures east of the map area. Unit ⦶vt was mapped as part of the Ohanapecosh Formation by Tabor and others (2000). We follow Hammond (1963) and Hammond and Dragovich (2008) and tentatively correlate unit ⦶vt with the tuff of Stampede Pass near Stampede Pass and Lake Keechelus. An age span of a few million years for unit ⦶vt may be expected, given (1) the composite or compound nature of this ignimbrite and (2) the andesite flow interbeds that suggest punctuated pyroclastic deposition over a period of time. The tuff of Stampede Pass was mapped by Hammond (1963) and Hammond and Dragovich (2008) as a discontinuous pyroclastic unit; it is presently mapped on the west to the southern edge of the map area. If the mapped beds are correlative, then the unit is a marker bed that helps define several plunging folds in the region. The tuff likely originated from an elliptical vent on the east shore of Lake Keechelus; the vent area was mapped as the tuff member of Lake Keechelus by Tabor and others (2000). (Hammond, 1963; Hammond and Dragovich, 2008; Dragovich and Walsh, 2008; Tabor and others, 2000; P. E. Hammond, Portland State University emeritus, written communs., 2007–2008)

Tuff units correlated with unit ⦶vt by Hammond and Dragovich (2008) have regional ages of ~27 to 32 Ma. Tabor and others (2000) obtained a zircon fission-track age of 24.7 ±1.7 Ma from this unit near Taylor Creek (age site 2) in the southeast part of the map area; this is probably too young and may be reset. Tabor and others (1984, 2000) also reported a zircon fission-track age of 30.4 ±1.2 Ma for the tuff member of the Lake Keechelus vent area; this age is similar to a plagioclase Ar-Ar plateau age of 27.87 ±0.06 Ma from unit ⦶vt in the southeastern part of the map area (age site 3; Hammond and Dragovich, 2008). These ages are also similar to the 29.38 ±0.06 Ma plagioclase Ar-Ar plateau age from the Stampede Pass type section (Hammond and Dragovich, 2008) where Tabor and others (1984, 2000) reported fission track zircon ages of 30.2 ±1.1 and 32.4 ±0.6 Ma. We obtained U-Pb zircon age of 29.0 ±1.4 Ma from unit ⦶vt in the southeastern part of the study area (age site 4, sec. 23, T22N R8E; Appendix A, Table A1 and Fig. A2). We suspect that the other Eocene, Cretaceous, and Proterozoic zircons obtained from this sample (Appendix A, Table A1, and Figs. A3–A4) were incorporated during magmatic ascent and catastrophic extrusion, possibly from (1) the Eocene Naches Formation (Appendix A and Fig. A3) mapped around the vent area and (2) pre-Tertiary intrusions and basement rocks underlying the vent area (such as mid-Cretaceous plutons common in the Cascades).

Ohanapecosh Formation of Tabor and others (2000)

Tabor and others (2000) included parts of the informally named "Enumclaw formation" and "Huckleberry Mountain formation" of Hammond (1963) in the Ohanapecosh Formation in the map area. We have subdivided those rocks into proximal (unit ⦶Eva) and distal volcanic (unit ⦶Evs) facies in the study area. This subdivision is somewhat similar to the "Enumclaw and Huckleberry Mountain formation" mapping of Hammond (1963) in that these two formations are flow-dominated and volcaniclastic-dominated, respectively. Interbedding of our mapped volcanic facies probably reflects paleogeographic controls such as paleodrainage evolution and (or) waxing and waning volcanism around volcanic center(s). The volcanic center for the proximal volcanic facies may be south of the map area (Hammond, 1998).

⦶Eva **Proximal volcanic facies – andesite (Oligocene to Eocene)**—Andesite, basaltic andesite to dacitic flows (52–67% SiO_2) and tuff breccia with lesser amounts of tuff and minor volcanolithic tuffaceous sandstone and siltstone and rare possible basalt flows or dikes; andesite flows typically dark gray to greenish gray, weather to shades of brown. Flows are glomerophyric to eutaxitic and locally exhibit well-formed columns and contain amygdules. Phenocrysts include plagioclase, augite ± hypersthene, with some local subhedral quartz (in dacite flows or tuffs) and accessory opaque minerals including magnetite with glass (≤60%). Microlites of plagioclase are common. Tuffs are mostly vitric crystal to crystal vitric, and breccias are mostly lithic rich. Pumice is locally conspicuous in some tuffs and breccias. Breccias were deposited as pyroclastic flows and flow breccias. Deposition near a volcanic center is implied by the prominence of flows and coarse breccias. The contact between the distal volcanic facies (unit ⦶Evs) and the underlying Renton Formation (unit Ec_r) along Williams Creek appears to be either conformable or disconformable and parallel. Tabor and others (2000) also note the parallel and gradational nature of some contacts between the correlative Ohanapecosh Formation and the Puget Group in outcrops near the area, but they contend that regional differences in severity of deformation between the two units make the contact mostly an unconformity.

Tabor and others (2000) consider the Ohanapecosh Formation to be mostly Oligocene in age, although on the basis of paleontological data, Fiske and others (1963) concluded that the rocks of the Ohanapecosh in Mount Rainier National Park to the south ranged in age from middle Eocene to early Oligocene, but were mostly late Eocene. Southwest of the map area, Ohanapecosh Formation beds ~500 to 1000 ft above the contact with the Puget Group were K-Ar dated as latest Eocene (35.2 ±2.2 Ma) (Turner and others, 1983), and rocks ~250 ft above the base have fossil plant remains assigned to the Kummerian Stage (late Eocene to earliest Oligocene; Wolfe, 1968, 1981; Wolfe and others, 1998; Vine, 1969). We obtained U-Pb zircon age of 34.75 ±0.68 Ma (Appendix A, Table A1 and Fig. A5) from a light-colored felsic tuff containing euhedral zircons from the northern part of unit directly south of the Steele Creek fault in the south-central part of the map area (age site 5, NE¼ sec. 7, T22N R8E). This latest Eocene magmatic age helps confirm (1) our latest Eocene to early Oligocene age assignment for unit ΦEva (33.9 Ma Eocene/Oligocene boundary) and (2) our mapping of the Steele Creek fault. Older dated zircons in this sample (Appendix A, Table A1 and Fig. A6) may reflect assimilation or erosion of basement during intrusion or pyroclastic deposition of this tuff. (Vine, 1969; Walsh, 1984; Tabor and others, 2000; Hammond, 1963, 1998; Hammond and Dragovich, 2008)

ΦEvs **Distal facies – volcanic sedimentary rocks (Oligocene to Eocene)**—Lithic to lithofeldspathic volcanic sandstone locally with pumice clasts, tuffaceous siltstone, andesite to dacite tuff, lapilli breccia, lapilli tuff and tuff breccia with lesser non-cohesive lahar diamictite and rare conglomerate. Volcanic sandstones are typically gray and weathered to olive gray. Fluvial volcaniclastic rocks are mostly laminated to medium bedded and locally display graded bedding, cross-beds, or soft-sediment deformational features. Hammond (1963; sample #UWA 2300) identified leaf fossils from the unit east-southeast of Cedar Falls (SW¼NW¼SE¼ sec. 3, T22N R8E). Crystal-lithic, vitric-crystal, crystal-vitric, and lithic tuffs contain pumice and (or) lithic clasts. Lithic clasts are mostly are mostly andesitic in composition. Phenocrysts in lithic clasts and crystals in tuff are plagioclase ± augite and rare hornblende(?). Some dacitic tuffs contain quartz. The unit was deposited primarily as volcaniclastic fluvial lahar with pyroclastic deposits in a distal volcanic setting; some unit ΦEvs bodies occur as lenses in proximal volcanic rocks (unit ΦEva), implying fairly high-gradient channel or flood-plain deposits eroded into the ΦEva volcanic apron. The overall increased thickness of fluvial volcaniclastic sediments upward within units ΦEva and ΦEvs implies waning or shifting volcanism over time; regional relations suggests volcanic centers shifted away from the study area in the early Oligocene. The apparent lack of unit ΦEvs fluvial conglomerate and dominance of fluvial sandstone to pebbly sandstone suggest (1) more distal sedimentation along lower gradient streams or broad flood plains, (2) poor preservation of fluvial deposits near the volcanic center(s), or (3) lack of diagnostic exposures. This unit is older than the tuff of Stampede Pass (~29 Ma) and probably latest Eocene to early Oligocene in age. See units ΦvT, ΦEva, and Ecr for further age constraints. Hammond (1963) reports latest Eocene to early Oligocene leaf fossil ages from this unit. A component of north-side-up vertical offset for the Steele Creek fault is necessitated by the juxtaposition of the middle Eocene Tukwila Formation (unit Evs_t) and unit ΦEvs north of the Cedar River. (See "Major Cenozoic Faults, Folds, and Basin in the Map Area", p. 24.) (Hammond, 1963; Walsh, 1984; Tabor and others, 2000; Shannon & Wilson, 1978)

Volcanic Rocks of Rattlesnake Mountain of Walsh (1984)

The volcanic rocks of Rattlesnake Mountain are dominated by a proximal andesite package (unit $ΦEva_r$) consisting mostly of andesitic flows and tuffs. Unit $ΦEva_r$ is locally divided into an andesitic volcanic tuff breccia unit ($ΦEvbx_r$) and a volcanic sediment-tuff unit ($ΦEvt_r$). The proximal package is a ~1- to 3-km-thick body that is bounded by the western and eastern Rattlesnake Mountain fault zones (Figs. 3A–C and cross section). These dislocation zones contain fault-imbricated bodies of proximal to distal volcanic rocks that we correlate with the volcanic rocks of Rattlesnake Mountain, as well as rocks of the Puget Group and Western mélange belt. The dominance of flows and breccias in the volcanic rocks of Rattlesnake Mountain combined with our age, structural, and geophysical observations indicate that the unit is predominantly a fault-bounded proximal volcanic accumulation or volcanic center within the broad Rattlesnake Mountain fault zone. Unit $ΦEvt_r$ appears to be dominantly a distal volcanic package that also occurs as fault-bounded imbricate masses but contains significant volcanic sedimentary rocks. We were unable to directly date the proximal package atop Rattlesnake Mountain, and thus the relationship between this volcanic center and more distal volcanic rocks occurring in the bounding fault zones remains uncertain. Tabor and others (1982) correlated the rocks of Rattlesnake Mountain with the Ohanapecosh or Fifes Peak Formations. Subsequently, Tabor and others (2000) tentatively correlated the volcanic rocks of Rattlesnake Mountain with the volcanic rocks of Mount Persis of Tabor and others (1993), 20 mi northeast of the map area. They also suggested that the poorly dated volcanic rocks of Mount Persis may be late(?) Eocene, roughly the same age as the Tukwila Formation (~42 Ma). However, the lack of strong deformation in the Mount Persis rocks north-northwest of the map area suggested to Tabor and others (1993, 2000) that the unit is younger than the Tukwila, but it cannot be younger than the 34-Ma Index batholith that intrudes the Mount Persis unit in the Skykomish Pass 1:100,000-scale quadrangle.

Eva_r **Volcanic rocks of Rattlesnake Mountain, andesite (Eocene to Oligocene)**—Andesite and basaltic andesite flows (53–62% SiO_2) and crystal-lithic to crystal-vitric tuff, with some lapilli tuff and tuff breccia; flows typically composed of phenocrysts of subhedral to euhedral plagioclase (~2–4 mm), subhedral augite, and locally possible accessory hornblende altered to chlorite or clay

minerals, as well as hypersthene with augite (R. W. Tabor, USGS emeritus, written commun., 2008); typically gray to greenish black, weather to light gray, and commonly altered to dark reddish gray. Plagioclase microlites are common (~10–40%) in glass and define a eutaxitic (flow) texture. Some samples contain accessory quartz microphenocrysts that may be secondary. Massive flows locally contain amygdules and display rare columns. Very thick bodies of massive plagioclase-phyric tuff are commonly difficult to distinguish in the field from flows. The volume of flows and coarse breccia (below) indicates that this unit represents a volcanic center. East of Rattlesnake Mountain faults nos. 6 and (or) 11, the unit thins significantly to a 50- to 200-ft-thick volcanic layer that unconformably overlies the Western mélange belt rocks (cross section). Tertiary volcanic rocks overlying the mélange belt basement may thicken to the north along the axis of the inferred Snoqualmie Valley anticlinorium and toward Snoqualmie Falls, which are composed of Tertiary volcanic rocks. (See "Eastern Rattlesnake Mountain Fault Zone, North Bend Basin, and the Snoqualmie River Anticlinorium", p. 25.) Stratigraphic thinning of the volcanic rocks of Rattlesnake Mountain in and west of the eastern Rattlesnake Mountain fault zone is evidenced by the outcrop distribution and the geophysical signature, which is best modeled as thin Tertiary volcanic rocks over a shallow pre-Tertiary mélange basement. (See "Magnetic and Gravity Anomaly Analyses", p. 20.) (Walsh, 1984; Tabor and others, 2000; Dragovich and Walsh, 2008)

Locally divided into:

$\Phi Evbx_r$ **Volcanic rocks of Rattlesnake Mountain, tuff breccia (Eocene to Oligocene)**—Andesite and basaltic andesite (52–56% SiO_2) crystal-lithic and lithic tuff breccia and breccia with lesser lapilli breccia with minor flows and tuffs; typically dark gray to dark reddish gray; massive. Breccia clasts are angular, rarely subrounded, and locally as much as 2.6 ft in diameter; they include rare pumice lapilli. Vesicular clasts are common, particularly in flow breccia. Clast and matrix mineralogy is similar to that of the plagioclase-augite-phyric andesites in unit ΦEva_r, including rare chloritized hornblende. Some breccias are pyroclastic deposits laid down near the volcanic center(s). Only the very thick and mappable breccia units are shown on the plate. (Walsh, 1984; Dragovich and Walsh, 2008)

ΦEvt_r **Volcanic rocks of Rattlesnake Mountain, tuff (Eocene to Oligocene)**—Andesitic (55–61% SiO_2) crystal-vitric to crystal-lithic tuff, lapilli tuff, local lithic to feldspatholithic volcanic sandstone, tuffaceous siltstone with some beds of crystal lithic tuff breccia; massive to very thickly bedded; laminated or cross-bedded. Dominant phenocrysts in tuff or tuff breccia are plagioclase ± augite, locally with some interstitial quartz grains and rare resorbed quartz phenocrysts in breccia clasts. Most lithic clasts are andesite but may locally include dacite or basaltic andesite; rarely includes pumiceous tuffs (ignimbrites). We obtained a U-Pb zircon age of 45.17 ± 0.62 Ma (Appendix A, Table A1 and Fig. A7) from distinctly pumiceous volcaniclastic sandstone at age site 6 (sec. 28, T23N R8E) near Brewster Lake in the east-central portion of the study area. This age indicates that (at least locally) volcaniclastic fluvial and tuffaceous rocks in the eastern Rattlesnake Mountain fault zone correlate with the Tukwila Formation. (See unit Evt_t below for further information.) Unit ΦEvt_r is interpreted to be more distal volcanic rocks of the Rattlesnake Mountain complex (unit ΦEva_r) that are fault-imbricated with the proximal flows and breccias that dominate the axial region of Rattlesnake Mountain, but we cannot exclude the possibility that some of these fault-bounded bodies are distal Tukwila Formation equivalents imbricated with the proximal volcanic rocks of Rattlesnake Mountain.

Puget Group and Raging River Formation

The Puget Group in the map area includes the Renton, Tukwila, and Tiger Mountain Formations. The middle? to late Eocene Renton and middle Eocene Tiger Mountain Formations were deposited as meandering-river fluvial-deltaic sediments on a coastal plain. Johnson and O'Connor (1994) modeled the depositional environment of the Puget Group as a delta plain complex prograding over the shallow marine strata of the Raging River Formation. In their model the fluvial Renton Formation was deposited on an upper delta plain that may locally include shallow marine deposits. The andesitic Tukwila Formation volcanic complex is intermediate in age between the bulk of the Renton and Tiger Mountain Formations in the map area. This volcanism brought voluminous volcaniclastic fluvial and volcanic deposits onto this coastal plain and interrupted the fluvial feldspathic sediment deposition characteristic of the enveloping formations. The Tukwila Formation represents an andesitic stratovolcano complex with one or possibly more volcanic centers. The most prominent intrusive equivalent of the mostly extrusive Tukwila Formation crops out west of the map area (Vine, 1969), and if this represents the volcanic center, its location is consistent with overall fining trends away from it. The upper sedimentary beds of the Tiger Mountain Formation interfinger with the Tukwila Formation; interstratification of these formations is particularly evident around Kerriston where generally east-derived mature feldspathic sandstones of the Tiger Mountain Formation interfinger with generally west-derived volcanic and volcaniclastic fluvial rocks of the Tukwila Formation (cross section).

The Puget Group is locally fault imbricated with the volcanic rocks of Rattlesnake Mountain within the Rattlesnake Mountain fault zone (cross section). We cannot exclude the possibility that the volcanic rocks of Rattlesnake Mountain might be a Tukwila

Formation proximal volcanic package or center. (See unit ΦEva$_r$.) (Walsh, 1984; Tabor and others, 2000; Vine, 1962, 1969; Dragovich and others, 2007)

Ec$_r$ **Renton Formation (middle? to late Eocene)**—Nonmarine feldspathic to lithofeldspathic subquartzose sandstone, with interbedded carbonaceous claystone, siltstone, subbituminous coal beds, and felsic tuff. Sandstone is light gray to white, typically well-stratified, micaceous, fine to medium grained, crossbedded, and laminated to massive; it contains quartz (30–45%), plagioclase and potassium feldspar (40–50%), and lithic grains (10–20%). The Renton Formation occurs in the north-central (sec. 12, T23N R7E) and southwestern parts of the study area (sec. 12, T22N R7E). Abandoned coal mines occur north of the map area, directly north of critical site 4 (sec. 12, T23N R7E), as well as directly west of the map area (west of Williams Creek). We suspect the distal facies of the Ohanapecosh Formation (unit ΦEvs) is locally latest Eocene in age because its contact with the Renton Formation along Williams Creek is concordant or disconformable but parallel. A very thick bed of altered felsic crystal-vitric tuff interbedded with Renton sandstone directly west of Williams Creek contains mostly plagioclase (~45%) and lesser quartz in a highly altered light-colored matrix containing zeolites; we speculate that this tuff is a distal correlative of the Mount Catherine rhyolite member of Tabor and others (2000). Plant fossils were assigned by Wolfe (1968) to the Ravenian and Kummerian (late Eocene) stages; the unit conformably overlies the Tukwila Formation dated by Turner and others (1983) at ~42.0 ±2.4 Ma. (Dragovich and Walsh, 2008; Dragovich and others, 2007; Frizzell, 1979; Vine, 1969; Walsh, 1983, 1984; Yount and Gower, 1991; Tabor and others, 2000)

Evs$_t$ **Tukwila Formation, sedimentary and volcanic rocks (middle Eocene)**—Nonmarine lithofeldspathic to feldspatholithic volcanic sandstone, tuff, lapilli tuff and tuffaceous siltstone with some intercalated volcanic conglomerate, feldspathic sandstone, carbonaceous shale, siltstone, impure coal beds, and minor (pumiceous) tuff breccia; generally bluish gray to greenish gray; weathered or altered to various shades of brown to olive-gray; local laharic mudflow deposits (subrounded andesite clasts to ~6 ft in diameter); typically thinly to very thickly bedded and moderately to well-stratified and -sorted. Exposures are dominantly volcaniclastic sedimentary rock types. Coalified organic debris, sticks and logs and thin to thick beds of coal are common. An abandoned coal mine at critical site 5 (SE¼ sec. 29, T23N R8E) is in a sedimentary interbed in the stratified volcaniclastic rocks of the Tukwila within the western Rattlesnake Mountain fault zone. Volcanic sandstones contain andesite lithic clasts (~30–40%), plagioclase (~30%), monocrystalline quartz (~10%), with local sedimentary lithic clasts, polycrystalline quartz, chert, and opaque minerals. Andesitic to dacitic vitric to vitric?-crystal tuffs contain mostly glass and blocky plagioclase (≤25%), typically with smaller grains of quartz, and local chloritized pyroxene. Most of the unit is broad lenticular bodies hundreds of feet thick that (1) consist of interbedded hyperconcentrated flood, lahar, alluvial fan, alluvial, and pyroclastic deposits and some airfall beds and (2) represent either discrete drainages emanating from the Tukwila volcanic center(s) to the west or more distal aprons of volcaniclastic sedimentary rocks that interfinger with the compositionally mature fluvial deposits of the Tiger Mountain Formation (unit Ec$_t$). (Dragovich and Walsh, 2008; Dragovich and others, 2007; Vine, 1962, 1969; Walsh, 1983, 1984; Yount and Gower, 1991; Tabor and others, 1993, 2000)

Evt$_t$ **Tukwila Formation, tuff (middle Eocene)**—Nonmarine andesitic lapilli tuff, tuff, tuff breccia, lesser volcaniclastic sandstone and siltstone, and rare possible vesicular flows; tuffs typically gray to greenish gray, weathered or altered to brown, light olive-brown or olive-gray; mostly massive to poorly or moderately stratified with thick to very thick beds. Exposures are dominantly volcanic rock types. Sedimentary interbeds or aligned welded clasts in pyroclastic beds locally indicate bedding structure. Tuff or tuff breccia matrix is typically lithic, crystal vitric, or crystal rich with abundant plagioclase ± augite and rare hornblende crystals. This matrix surrounds scattered lithic breccia clasts of dacitic to andesitic composition. Pumice is locally conspicuous. Chemical analyses indicate andesitic to almost dacitic compositions for most of the lithic clasts and the tuffaceous matrix (57–62% SiO_2); some quartz phyric tuffs may be dacitic in composition. Coarse block-and-ash flow deposits are more common west and northwest of the area, nearer the inferred volcanic center. In the map area, tuff and lapilli tuff predominate, and the formation contains more fluvial volcaniclastic rock (unit Evs$_t$). The lower part of the formation is interstratified with unit Ec$_t$ (cross section). The formation is overlain by unit Ec$_r$ fluvial deposits. Fossil leaves are referable to the Ravenian (late Eocene) floral stage (Wolfe and others, 1998). Turner and others (1983) reported middle Eocene fission-track and K-Ar ages of 39.4 ±2.4 to 45.7 ±2.7 Ma (avg. 42.0 ±2.7 Ma) near the top of the formation west of the map area. At age site 6 directly west of Brewster Lake in the east-central portion of the map area, we obtained a U-Pb zircon age of 45.17 ± 0.62 Ma (Appendix A, Table A1 and Fig. A7) from a gritty lapilli tuff or pumiceous volcaniclastic sandstone with abundant pumice clasts as much as a few inches long. This age indicates that (at least locally) some of the rocks previously included with volcanic rocks of Rattlesnake Mountain (unit ΦEvt$_r$) by Walsh (1984) correlate with the Tukwila Formation. The age site contains well-bedded volcaniclastic sandstone, siltstone, tuff, and andesitic tuff breccia that dip moderately west; beds are generally 7 to 15 ft thick, and some tuffaceous siltstone contains plant fossils. Some rocks are cross bedded or laminated or contain coalified log fragments and leaf impressions. The interbedded lapilli tuffs are mostly lithic rich with some dark lithic clasts as much as 2 cm long. Volcanic tuff breccia

occurs higher in the stratigraphic section at age site 6. These rocks are dark colored and have varied amounts of andesite lithic clasts in a light-brown disorganized glassy matrix containing plagioclase (~50%) and a few subhedral to anhedral quartz grains and accessory black lithic grains. This crystal-lithic tuff breccia contains microlitic andesite clasts with augite or rare green pleochroic hornblende grains, clasts of Western mélange belt sandstone, and dark volcanic lithic clasts displaying plagioclase microlites, hornblende, and vesicles. Other volcanic clasts are spherulitic or contain possible vesicles. The occurrence of fragments of Western mélange belt foliated or mylonitic metasandstone or polycrystalline quartz grains in this breccia suggests that the mélange belt was exposed or occurred in the shallow subsurface as country rock during deposition of this pyroclastic deposit. Tabor and others (2000) also observed inclusions of mélange belt metagabbro in Tertiary volcanic breccia near Chester Morse Lake (1 mi east of the quadrangle), suggestive of near-surface(?) basement involvement during deposition. Similarly, we suspect the mélange belt basement occurs at a shallow depth in the Brewster Lake area. Older dated zircons in sample 07-14E (Appendix A, Table A1 and Fig. A8) may be detrital zircons derived from the Western mélange belt or other basement that were acquired as this volcaniclastic unit was deposited. Following Tabor and others (2000), we suspect that the proximal volcanic rocks that dominate the axial region of Rattlesnake Mountain are younger than the Puget Group and thus latest Eocene to early Oligocene in age. Alternatively, the proximal flows and breccias atop Rattlesnake Mountain are correlative with the Tukwila Formation and represent an in-faulted proximal volcanic complex. (Vine, 1962, 1969; Walsh, 1984; Yount and Gower, 1991; Tabor and others, 1993, 2000)

Ec_t **Tiger Mountain Formation (middle Eocene)**—Nonmarine micaceous feldspathic to feldspatholithic subquartzose to rare quartzose sandstone interbedded with carbonaceous siltstone and shale, siltstone, minor pebble conglomerate, and coal beds; sandstone typically light gray; siltstone typically light olive-brown; well-stratified; laminated to thickly bedded and cross-bedded. Sandstones contain subequal amounts of monocrystalline quartz (~25–30%) and plagioclase feldspar (~25–30%), volcanic lithic and sedimentary lithic clasts (~5–30%), polycrystalline quartz and chert (~5%), biotite or white mica (~3%), and a trace of metamorphic lithic clasts and potassium feldspar. Sandstones in the map area are compositionally mature feldspathic sandstones with a low (<~3%) volcanic lithic content, even where interstratified with the Tukwila Formation, probably as a result of different paleoflow directions for the Tukwila and Tiger Mountain Formations. We suggest a prodelta shelf setting for the lower part of the formation because of the interfingering of the marine Raging River and nonmarine Tiger Mountain Formations (Dragovich and others, 2007; Johnson and O'Connor, 1994). Unit Ec_t is widely exposed in the Raging River valley west of the Rattlesnake Mountain fault zone. We include in this unit the feldspathic sandstones with coal stringers that are interbedded with volcanic breccia in test pits within the eastern Rattlesnake Mountain fault zone (Associated Earth Sciences, Inc., 1992); we suspect that these rocks are a small fault-imbricated body of interstratified Tiger Mountain and Tukwila Formation (unit Ec_t directly north of critical site 6, sec. 8, T23N R8E) near the main strand of the Rattlesnake Mountain fault zone as illustrated on the cross section. Our suggestion that Puget Group imbricate bodies occur in the eastern Rattlesnake Mountain fault zone is supported by our U-Pb zircon age of 45.17 ±0.62 Ma on Tukwila Formation volcaniclastic rocks near at age site 6. See units Evt_t and Em_r for age constraints; the Tiger Mountain Formation contains fossil leaves referable to the Fultonian floral stage (Wolfe, 1968). (Dragovich and others, 2007; Vine, 1962, 1969; Walsh, 1984; Yount and Gower, 1991; Tabor and others, 1993, 2000)

Em_r **Raging River Formation (early? to middle Eocene) (cross section only)**—Subquartzose lithic to feldspatholithic volcanic sandstone, siltstone, and shale; local chert- or volcanic rock-pebble conglomerate; medium to very thickly bedded; at least 3300 ft thick (base not exposed). Unit Em_r is exposed in the core of the Raging River anticline directly west of the study area where Johnson and O'Connor (1994) assigned a shallow marine to fluvial depositional environment to the lower part of the formation, a fluvial environment to the middle part, and a bathyal to outer-shelf marine depositional environment to the uppermost part. Johnson and O'Connor (1994) described the age, stratigraphy, and sedimentology of the lithologies observed in the Amoco oil and gas exploration boring B-83-4 (DNR permit no. 364, boring WC-83-4, unique no. 041-00159) shown on the cross section. Strata in this boring dip consistently east at ~50° and have spaced subparallel faults and fractures that we suspect are bedding-parallel shear zones as a result of flexural slip during folding. This unit contains locally abundant fossil plants and marine mollusks and radiolarians. Foraminifera in the upper part of the formation are of the *Bulimina* cf. *B. jacksonensis* zone, which correlates with the lower part of the Narizian (middle Eocene) benthic foraminiferal stage (Johnson and O'Connor, 1994). See Johnson and O'Connor (1994) and Dragovich and others (2007) for composition, provenance, and sedimentary structures in the unit. (Vine, 1962, 1969; Walsh, 1984; Yount and Gower, 1991; Tabor and others, 1993, 2000)

Tertiary to Recent Tectonic Zones

tz **Tectonic zone (Tertiary to Recent)**—Cataclasite, fault breccia, clay-rich fault gouge, protomylonite, and strongly slickensided and fractured rocks in fault zones; variously colored or mottled as a result of local hydrothermal alteration or strong weathering. Some tectonic zones display siliceous, propylitic, argillic, and (or) fer-

ric hydrothermal alteration; the most prominent zones of hydrothermal alteration occur near Williams Creek (critical site 8, sec. 13, T22N R7E) and around Steele Creek, as well as in outcrops along I-90. Most kinematic indicators, such as shallow slickenlines on steep shear planes and (or) en echelon vein arrays, suggest strike-slip or oblique-slip faulting within the broad Rattlesnake Mountain fault zone (see Fig. 5B). Some tectonic zones align with transfer faults between master strands in this fault zone. We map unit tz only where the zones are large enough to plot at this map scale. (See "Major Cenozoic Faults, Folds, and Basins in the Map Area", p. 24, for more information.) (Dragovich and others, 2007; Walsh, 1984; Vine, 1969)

Mesozoic Low- to Medium-Grade Metamorphic Rocks of the Western Mélange Belt

The Western mélange belt of Frizzell and others (1987) and Tabor and others (2000) in the map area consists of metamorphosed argillite and sandstone (unit $KJms_w$) with generally lesser amounts of volcanic rocks (unit $KJmv_w$), conglomerate (unit $KJmcg_w$), gabbro (unit $KJigb_w$), and rare ultramafite such as serpentinite (unit KJu_w). We did not observe the metachert and marble found in the belt more regionally by Tabor and others (2000) and Fuller (1925); they described outcrop- to mountain-size phacoids of metagabbro, metadiabase, and metatonalite and megaclasts of sandstone, chert, and marble in a matrix of poorly foliated or disrupted argillite or thin-bedded argillite and sandstone. We have also mapped a gneissic amphibolite unit (unit $KJgn_w$) as part of the mélange belt. The mélange belt occurs east of Rattlesnake Mountain fault no. 9, is unconformably overlain by the volcanic rocks of Rattlesnake Mountain, and is fault imbricated with small bodies of the Puget Group. However, the geophysical anomaly pattern (Fig. 3A) suggests that the mélange belt basement occurs as far east as Rattlesnake Mountain fault no. 6 (cross section), particularly along the southeastern part of Rattlesnake Mountain. Tabor and others (2000, 1993) report that most metasedimentary components of the mélange are Late Jurassic to Early Cretaceous in age on the basis of megafossils in argillite and radiolarians in chert pods found regionally (Frizzell and others, 1987; Miller, 1989; Tabor and others, 1993). They also report (1) mid- and Late Permian fusulinids in marble blocks (Danner, 1966) that may be olistostromes, (2) four U-Th-Pb zircon Jurassic ages (~150–170 Ma) from metatonalite-metagabbro, and (3) a Jurassic (~160 Ma) hornblende K-Ar age from metagabbro. Mixing and emplacement of the Western mélange belt may have been as early as mid-Cretaceous and as late as mid-Eocene. On the basis of metamorphic fabric and mineral relations, we concur with Jett and Heller (1988) that a majority of the tectonic mixing of the mélange occurred in a subduction-zone accretionary wedge environment during the Cretaceous.

$KJms_w$ **Western mélange belt metasedimentary rocks (Cretaceous to Jurassic)**—Marine lithofeldspathic, feldspatholithic subquartzose metasandstone and meta-argillite; minor metaconglomerate, chert pebble metaconglomerate, and metatuff; metasandstone typically greenish gray to dark gray and weathered to brown; ranges from metasandstone to metawacke with subrounded to angular clasts; meta-argillite typically black to dark greenish gray; graded bedding and load casts locally preserved. Meta-argillite is erosionally recessive, forms thin to very thick tectonized interbeds in metasandstone, and is the dominant component of the mélange matrix. Most of the unit is moderately to well foliated; rootless isoclinal folds have meta-argillite bedding transposed into the foliation in a few areas. Relict clasts include feldspar, monocrystalline quartz, chert (locally with radiolarians), polycrystalline quartz, and volcanic and sedimentary lithic clasts that include rip-up clasts of meta-argillite. Detrital biotite or muscovite is locally conspicuous. Provenance corresponds most closely to the lithic and cherty petrofacies of Jett and Heller (1988). Rocks are partly recrystallized and display a mostly synkinematic metamorphic fabric. Dominant metamorphic minerals are actinolite/tremolite, epidote or clinozoisite, chlorite ± pumpellyite; rarer prehnite and perhaps stilpnomelane are present. More work is required to document the metamorphic grade of the mélange belt argillic rocks, which may have been insheared with the other metasedimentary rocks of the mélange belt in a nonmetamorphic environment (R. W. Tabor, USGS emeritus, written commun., 2008). Units $KJms_w$ and $KJmcg_w$ were probably deposited as turbidites. C. D. Blome (USGS, *in* Walsh, 1984) reported Cretaceous or Jurassic radiolarians (*Sethocapsa* from a chert clast in metasandstone (age site 7 in sec. 16, T23N R8E, southwest of North Bend). (Tabor and others, 1993, 2000; Walsh, 1984; Fuller, 1925; Jett and Heller, 1988)

$KJmcg_w$ **Western mélange belt metaconglomerate (Cretaceous to Jurassic)**—Polymictic cobble metaconglomerate with minor feldspatholithic to lithic metasandstone or metawacke; dark gray to greenish gray; well-sorted and clast-supported to moderately sorted and matrix-supported; very thick, massive to crudely stratified with some local graded bedding; scattered lenticular beds of metasandstone or wacke that form bold outcrops. Some metaconglomerate also occurs as thick beds within metasandstone or metatuffaceous greenstone. Relict clasts are subangular to rounded and include chert (locally with radiolarians), volcanic lithic clasts (including vesicular basalt to andesite containing pyroxene), sandstone and argillite, and some greenstone, gabbro, and pyroxene quartz diorite clasts and are set in a matrix of mostly polycrystalline quartz, feldspar, and monocrystalline quartz fragments. Some metaconglomerate also contains minor clasts or grains of augite, serpentinite, and actinolized hornblende. Metaconglomerate has an overall chert-basalt-granitic rock provenance and contains the same metamorphic minerals as unit $KJms_w$. Most of this unit occurs as steeply dipping, fault-bounded blocks within the Rattlesnake Mountain fault zone. Although the relationship to unit $KJms_w$ is mostly obscured by faulting, we suspect that these rocks are proximal fan turbidites and genetically related to the

finer metasandstone facies. (Tabor and others, 2000; Jett and Heller, 1988)

$KJmv_w$ **Western mélange belt metavolcanic rocks (Cretaceous to Jurassic)**—Greenstone representing metamorphosed flows, tuff, and minor volcanic breccia; greenish gray; dominantly massive to moderately foliated metabasaltic andesite (~54% SiO_2); local metabasalt to meta-andesite; typically contains plagioclase (≤2 mm) and actinolized pyroxene in a chloritic matrix (~50%) with local minor quartz and opaque minerals. (Walsh, 1984; Tabor and others, 2000; Fuller, 1925)

$KJigb_w$, KJu_w **Western mélange belt metagabbro and ultramafite (Cretaceous to Jurassic)**—Metagabbro; greenish gray; medium- to coarse-grained; massive to slightly foliated; rare local amphibolite. Protomylonitized metagabbro is finer grained and locally aphanitic. The unit contains plagioclase (~50%) with intergranular to euhedral actinolized clinopyroxene or hornblende (to 1 cm long) and opaque minerals. Metamorphic minerals include actinolite, chlorite ± epidote, sphene, and calcite. Metagabbro is associated with serpentinite and serpentinized pyroxenite (unit KJu_w) along the east-central part of the map area at critical site 7 (sec. 22, T23N R8E). The slight magnetic high that overlies the lone exposure of ultramafite in the map area is likely the result of the abundance of magnetite in serpentinites. (Compare unit KJu_w on the plate and the WMB anomaly on Fig. 3A.) Metagabbro in the Snoqualmie 7.5-minute quadrangle and ~1 mi directly north of Little Si in the northeast corner of the map area yielded a U-Pb age of ~150 Ma (Tabor and others, 1993). (Tabor and others, 1993, 2000; Walsh, 1984; Fuller, 1925)

$KJgn_w$ **Western mélange belt gneiss (Cretaceous to Jurassic)**—Gneissic amphibolite and amphibolite; rare thin serpentinite or chloritic pods along the South Fork Snoqualmie River; gneiss banding dark greenish black to greenish white, locally to 1 in. thick; medium- to coarse-grained; moderate to very strong foliation; contains crystalloblastic subhedral to euhedral hornblende (~50–80%) and plagioclase (~20–40%) and accessory opaque minerals, locally with prehnite or pumpellyite in veins. These rocks are exposed on the eastern slope of Rattlesnake Mountain and along the south fork of the Snoqualmie River (secs. 21–22, T23N R8E). Tabor and others (2000) did not describe gneissic amphibolite in the Western mélange belt on the Snoqualmie 1:100,000-scale geologic map but do note minor gneissic amphibolite on the Skykomish 1:100,000-scale geologic map (Tabor and others, 1993) north of the map area. Gneiss is locally tectonically interleaved with minor tectonic lenses of greenstone and metasandstone in fault zones. The rocks could be gneissose meta-intrusive rocks or completely recrystallized mafic volcanic rocks. The lack of synmetamorphic epidote allows for the possibility of a gneissic fabric of magmatic origin (E. Brown, Western Wash. Univ. emeritus, written commun., 2008). This possibility, and the observation by Tabor and others (2000) that amphibolites are spatially associated with metagabbros of the Western mélange belt, suggest that the gneisses may be an intrusive border phase of the metagabbros (unit $KJigb_w$). The strong development of the amphibolite facies(?) gneissose fabric contrasts with the intensity and grade of the metamorphic fabric in most other mélange rocks and awaits further study. We speculate that (1) these amphibolite facies metamorphic rocks were completely recrystallized and tectonized within a thermally zoned subduction zone environment, and (2) they were later tectonically mixed with lower grade rocks of the mélange belt that display a much less well developed tectonic foliation.

GEOPHYSICAL ANALYSES OF THE MAP AREA

Magnetic and Gravity Anomaly Analyses

METHODS

Geophysical Map

Aeromagnetic data come from a survey contracted by the U.S. Geological Survey in 1997. Flight lines are oriented north–south and have a 250-m spacing (Blakely and others, 1999). Magnetic anomalies for the map area are strongly asymmetric with respect to the source of the magnetic anomaly. Therefore we present a reduced-to-pole aeromagnetic anomaly grid, calculated using standard procedures (Blakely, 1995). This filter moves magnetic anomalies directly over the magnetic source units. New data constrain the gravity anomalies for this region (Anderson and others, 2006; Megan Anderson, Colorado College, Department of Geology, unpub. data, 2007), and we used standard formulas and reduction procedures (Blakely, 1995), as well as a reduction density of 2670 kg/m^3, to produce the isostatic gravity anomaly contours.

Geophysical Modeling

Geophysical cross-section models were calculated with GM-SYS Geophysical Modeling software (NGA, Inc.). Rock magnetic and density properties used in two-dimensional geophysical modeling are supported by hand sample and outcrop magnetic susceptibility measurements, as well as density measurements from hand samples (Anderson and others, 2006; Megan Anderson, unpub. data, 2006). Geophysical properties of "combined" units (for example, Western mélange belt) are averaged from hand samples of each component, based on the percentage of each component exposed in outcrops in the area. For example, greenstone is estimated to compose about 15 percent of the Western mélange belt in the map area, an estimate that may be too high for the mélange belt as a whole (R. W. Tabor, written commun., 2008). Our one density measurement of cataclasite in the eastern Rattlesnake Mountain fault zone may not be representative. Sampling of the magnetic and gravity grid for the model profile is at 250 m, similar to the spacing of flight lines on the aeromagnetic survey. Magnetic measurements in the profile are matched to the airplane altitude recorded by radar altimeter during the aeromagnetic survey. Gravity constraint is considerably sparser, more on the order of 1.5 km; therefore, some of the small details based on geologic mapping, though matching the gravity, are not well constrained. Mapped lithologic boundaries are honored first, and depth to basement

across the profile attempts to follow well data within the quadrangle. Deeper boundaries are based solely on the geophysics. Basement properties are based on modeling from areas farther west in the Puget Lowland; Crescent Formation volcanic rocks, exposed west of the Puget Sound, were not used in the section because of differences in geophysical properties observed between the North Bend quadrangle and areas where Crescent volcanic rocks crop out to the west (Anderson and others, 2006).

INTERPRETATIONS

Geophysical Map

The strongest geophysical anomaly in the North Bend quadrangle is related to the volcanic rocks of Rattlesnake Mountain (RS on Fig. 3A, p. 11), which create a strong magnetic high trending north-northwest over the region. The simplicity of the magnetic anomaly indicates that Rattlesnake Mountain is cored by a simple wedge of volcanic rocks that has steeply dipping boundaries (faults). Lack of a corresponding gravitational high is borne out by density measurements of hand samples across the region; these indicate that many of the basement and volcanic rocks have similar densities. Magnetic highs in the southeastern corner of the map correspond to magnetic volcanic rocks that are likely part of the Tertiary fill within the south-southeast–plunging Lindsay syncline that extends to the southeast of the quadrangle (Fig. 3A, LS). This interpretation is also supported by a gravitational low in that corner of the quadrangle. Another gravitational low crosses the North Bend basin (Fig. 3A, NBB) in the northeastern corner of the map under North Bend, and it corresponds to a region where there are both slightly less dense basement rocks ($\Delta\rho = 20$ kg/m^3) and a small basin filled with Quaternary deposits. Small gravitational highs on the map (for example, Western mélange belt, WMB) that correspond to minor magnetic highs are likely due to small zones within the basement or Western mélange belt rocks that contain serpentinites and spatially associated metagabbros that have high magnetic susceptibility and, for the gabbros, higher densities.

Geophysical Modeling

The strongest magnetic contrast is between volcanic rocks of Rattlesnake Mountain and surrounding basement/Western mélange belt/Puget Group lithologies. The strongest density contrast is between Western mélange belt rocks and Quaternary deposits/Puget Group rocks; there is a smaller contrast between volcanic rocks of Rattlesnake Mountain and Western mélange belt rocks. Therefore, vertical boundaries based on these contrasts exert maximum control on the model. Depth to the base of volcanic rocks of Rattlesnake Mountain under Rattlesnake Mountain is strongly dependent on the magnetic properties of volcanic rocks of Rattlesnake Mountain; therefore, there is some uncertainty in this boundary. Basement and nonmagnetic parts of the Western mélange belt are nearly geophysically indistinguishable and are therefore the most speculative. Gabbro bodies at depth are postulated solely off the geophysics, as necessary to fit the data, though the gabbro properties used in modeling follow measurements of only a few outcrops in the quadrangle area. (See Fig. 3A and compare with the cross section on the plate.)

Model A

Snoqualmie batholith gabbro modeled at depth below the western side of the profile is well controlled by the shape of the magnetic anomaly on the western side of the profile (Figs. 3A–B and cross section). This body should extend into the quadrangle west of North Bend, a concept supported by a magnetic high observed over Tiger Mountain northwest of the map area. The dip of the boundary between Puget Group rocks and basement on the western side of Rattlesnake Mountain is not well constrained. Complicated fault blocks on the eastern side of Rattlesnake Mountain are also not fully constrainable by the gravity or magnetic properties, and therefore several geometries are possible. However, magnetic basement is necessary to fit the aeromagnetic profile, and some lower density cataclasite is necessary to match the gravity. A slight transition in basement density is necessary under Rattlesnake Mountain to match a cross-profile trend in the gravity data, which is supported by a slight north–south gradient in the gravity across the map area. The thickness of Quaternary deposits under North Bend depends on the density of those deposits, though the modeled depth generally matches well data in the region (Associated Earth Sciences, Inc., 1996).

Model B

Little change in basement properties is expected across this profile (Fig. 3C) on the basis of the low amplitude of the gravity anomaly profile and the simple nature of the magnetic anomaly profile. Quaternary deposits in the Snoqualmie valley are necessarily thin, also based on the flat gravity profile. The position, near-vertical dip, and abrupt transition between volcanic rocks of Rattlesnake Mountain and the Western mélange belt on the eastern side of Rattlesnake mountain is well constrained by the geophysics, in particular the magnetic anomaly, and is best modeled as a fault or faults. Similarly, the western boundary of the volcanic rocks of Rattlesnake Mountain is necessarily less abrupt; the boundary is east-dipping at depth, and the volcanic rocks are intermixed with the Puget Group in the near-surface. The exact geometry of the structural mixing of Puget Group and Rattlesnake Mountain lithologies in the western Rattlesnake Mountain fault zone is not well constrained by the geophysics, and the position of faults and geologic unit boundaries shown in the model is constrained partly by the geophysics and partly by the mapped faults at the surface (map and cross section). In addition, the magnetic volcanic rocks included with the volcanic rocks of Rattlesnake Mountain are not well identified; they were not identified at the surface during our geophysical investigation. Other intrusive lithologies such as a subvolcanic intrusive complex to the volcanic rocks of Rattlesnake Mountain or perhaps anomalous Tukwila volcanic rocks are also possible in this region. Although it is poorly constrained, we cannot exclude the possibility that the "basement?" shown on the cross section is the Western mélange belt exposed both in and east of the eastern Rattlesnake Mountain fault zone or is perhaps the Eastern mélange belt exposed northeast of the map area.

Seismicity in the Map Area

Most of the microseismicity in the North Bend quadrangle occurs in the mid-crust (~20 km depth); shallow crustal earthquakes have been much less frequent. To investigate the relation between mod-

ern seismicity and the location of mapped faults, earthquakes from the Pacific Northwest Seismic Network (PNSN) catalog (accessed Dec. 2007 at www.psn.org) that occurred between 1980 and 2007 within the North Bend quadrangle have been relocated using the double-difference algorithm of Waldhauser and Ellsworth (2000). The algorithm uses the facts that (1) ray paths from two closely located earthquakes to a common station are almost identical and (2) difference in observed travel time can therefore be attributed to the spatial offset of the two earthquakes with a high degree of certainty. We used analyst picks and did not re-pick arrival times. Furthermore, only three network stations are located close to the source region, and the accuracy of the earthquake locations is therefore limited due both to station distribution and possible picking errors. We relocated earthquakes that occurred below and above 10 km depth as two separate clusters.

A few shallow (depth <10 km) earthquakes have occurred in the quadrangle. To select shallow earthquakes, we included only those events for which we have waveform data (to be able to verify quality of picks) and that were recorded by more than five stations. Only 14 events matched these criteria, and we were able to successfully relocate ten of them. First-motion focal mechanisms for the two largest shallow events (Md [duration magnitude] = 2.9; both were felt and occurred in February 2006) are well constrained and consistent with oblique right-lateral slip on a steep northwest-trending plane, suggesting they occurred on a deeper (~7 km) part of the eastern Rattlesnake Mountain fault zone (Figs. 4A–B).

To select the better constrained events in the mid-crust, we included only events with magnitude 1.0 and larger for which we have waveform data. We thus selected 166 events, of which we successfully relocated 164. Well-constrained focal mechanisms indicate north-northeast–south-southwest compression, mostly on oblique reverse faults. Slip direction varies among events. For example, two small earthquakes on Jan. 21, 1996, occurred in almost the same location within a few hours of each other; however, their focal mechanisms are quite different. Cross sections through the seismicity (Figs. 4A–F) suggest steep reverse faults at mid-crustal depths. There is no clear direct evidence for a mid-crustal décollement (below) as proposed by some previous studies. However, most earthquakes do occur in the 17- to 20-km depth range, which can be considered indirect evidence for a horizontal décollement.

How the mid-crustal seismicity connects to shallower seismicity and mapped faults is difficult to determine due to the lack of earthquakes in the depth range of 8 to 15 km. Therefore our stipulations concerning fault geometry using the earthquake data should be considered speculative. (For example, see "Steele Creek Fault and the Olympic–Wallowa Lineament", p. 30.) The correlation of individual fault strands mapped at the surface with hypocenters at depth depends upon the subsurface geometry of the faults, including the fault dip and curvature, which has many degrees of freedom and thus is poorly constrained. Fault dip can be estimated for the uppermost crust by combining the surface fault trace (map) with possible fault dips inferred from our geophysical modeling (Figs. 3B and C). This combined dataset provides these first-order constraints on the geometry of some of the fault zones: (1) the fault strands in the western Rattlesnake Mountain fault zone dip to the east, and (2) most fault strands in the eastern Rattlesnake Mountain fault are subvertical. Correlation of individual strands with individual hypocenters is partly driven by

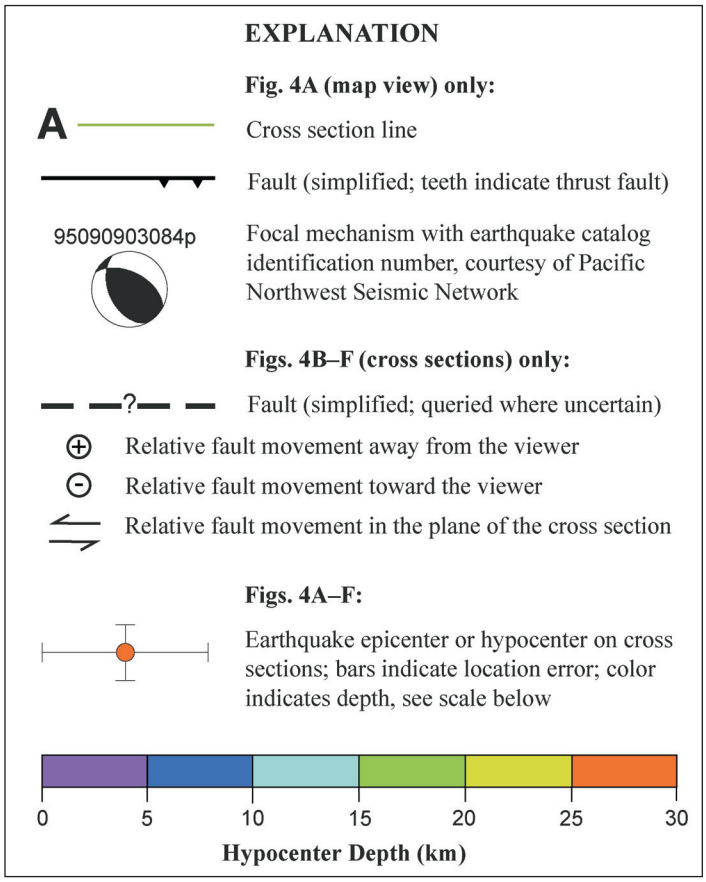

Figure 4. Relocated hypocenter and focal mechanism earthquake data for the study area (Figs. 4A–F). The relocated hypocenters include only moderate- to high-quality data, as discussed in "Seismicity in the Map Area", p. 21. Earthquakes are shown as circles with diameter proportional to magnitude and color graded to depth. Location errors are shown by the bar symbols.

Figure 4A. *(opposite page)* Epicenter map. Note the dominance of focal mechanisms with flat focal plane solutions at depth (>15 km). Two shallow earthquakes with dextral strike-slip solution focal mechanism solutions occur within the eastern Rattlesnake Mountain fault zone near RMF-1 and (or) RMF-11. See "Steele Creek Fault and the Olympic–Wallowa Lineament", p. 30, for a discussion of the "Southeast Rattlesnake Mountain earthquake cluster" and OWL (Olympic–Wallowa lineament), which aligns with the Steele Creek fault. Locations of sections are indicated by lines A–A′, B–B′, C–C′, North–South, and West–East.

Figures 4B–F. Hypocenter cross sections showing major mapped faults in the North Bend quadrangle. See "Major Cenozoic Faults, Folds, and Basins in the Map Area", p. 24, for our interpretation of some of the presented data. Cross sections "North–South" and "West–East" contain projected hypocenters within 5 km of the profile line; the remaining profiles show only the hypocenters located with 1 km of the profile line shown on Figure 4A. Inferred fault geometries are speculative at depth. Figure 4B is the best profile orientation for comparing the shallow hypocenter locations with the inferred strands of the Rattlesnake Mountain fault zone. Figures 4C–E are the best profile orientations for comparing the hypocenter locations with the Steele Creek fault, which is a strand of the OWL. The orientation of 4F is oblique to the majority of the faults in the study area but provides a second profile compilation of a broad band of seismicity in the map area.

4A

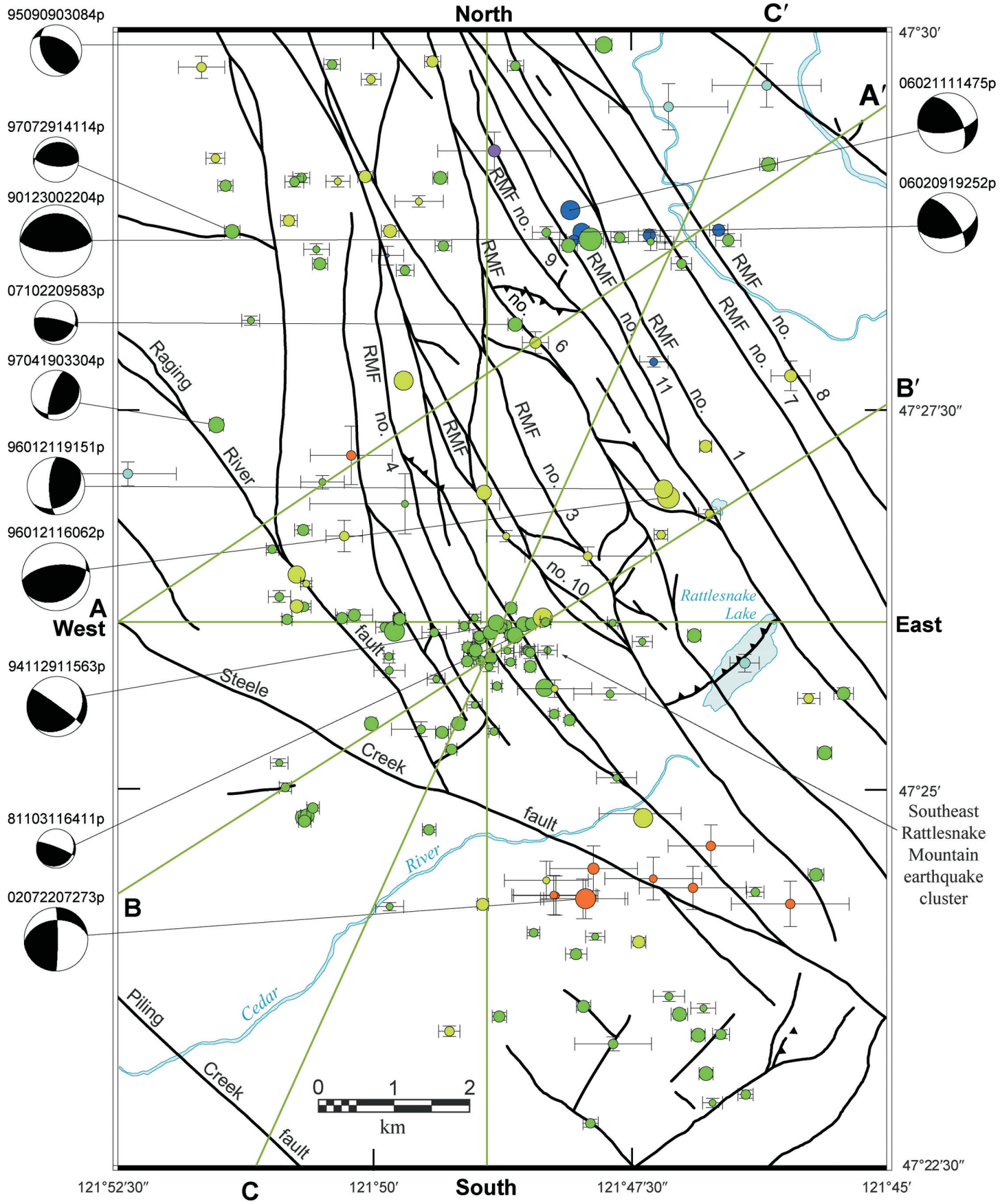
North
South
West
East
A
A′
B
B′
C
C′
47°30′
47°27′30″
47°25′
47°22′30″
121°52′30″
121°50′
121°47′30″
121°45′
95090903084p
97072914114p
90123002204p
07102209583p
97041903304p
96012119151p
96012116062p
94112911563p
81103116411p
02072207273p
06021111475p
06020919252p
RMF no. 1
RMF no. 3
RMF no. 4
RMF no. 6
RMF no. 7
RMF no. 8
RMF no. 9
RMF no. 10
RMF no. 11
Raging River fault
Steele Creek fault
Piling Creek fault
Cedar River
Rattlesnake Lake
Southeast Rattlesnake Mountain earthquake cluster
0 1 2
km

these general constraints and partly driven by our model of the Rattlesnake Mountain fault zone as a strike-slip fault zone containing positive flower structures.

MAJOR CENOZOIC FAULTS, FOLDS, AND BASINS IN THE MAP AREA

Here we report on the major Cenozoic faults and related structural features in the map area that have regional significance and (or) provide evidence for on-going local deformation. We also discuss some of the folding and basin development in the Snoqualmie River valley. Faults are mapped on the basis of our interpretation of geographic, geophysical, geomorphic, and stratigraphic lineaments and anomalies, as well as our interpretation of deformational features observed both locally and regionally. (See "Geophysical Analyses of the Map Area", p. 20, and Fig. 2 on plate.) Many of the faults follow linear tectonic zones (unit tz) or fault lineaments noted on lidar. We have queried faults where (1) the evidence of faulting is indirect (for example, geophysical lineaments) and (or) (2) the evidence for faulting is made on the basis of information gained from poorly exposed outcrops. Although more work is warranted, available information indicates that some of these structures have been active in the Pleistocene and Holocene.

Rattlesnake Mountain Fault Zone

Dragovich and others (2007) divided the Rattlesnake Mountain fault zone (RMFZ) into five strands in the Fall City 7.5-minute quadrangle directly northwest of the map area (Fig. 2 on plate). We have preserved their naming convention and have extended Rattlesnake Mountain faults nos. 1, 3, and 4 into this quadrangle, broadly similar to earlier compilations by Dragovich and others (2007) and Walsh (1984). Rattlesnake Mountain faults nos. 2 and 5 (Fig. 2 on plate, site 1) of Dragovich and others (2007) are not mapped in the North Bend 7.5-minute quadrangle and are not discussed here. Within the North Bend quadrangle, we have named Rattlesnake Mountain faults nos. 6 through 11 for prominent fault strands in the RMFZ. We divide the RMFZ into eastern and western belts to emphasize that volcanic rocks along the top of Rattlesnake Mountain are commonly less tectonized than rocks along faulted border zones (cross section).

Overall strike-slip offset is indicated for the RMFZ by (1) the outcrop structures, (2) the fault strand linearity, (3) its resemblance to a positive flower structure, and (4) the along-strike variation in structural features. The bedding in Tertiary rocks (Fig. 5A) is generally folded around southeast-plunging fold axes such as the Raging River anticline and Lindsay syncline. This general pattern is strongly modified near some faults where steeply to vertically dipping beds in Tertiary and pre-Tertiary rocks strike parallel to nearby faults (plate). Strike-slip to oblique-slip deformation in or near the various RMFZ strands is also evidenced by the dominance of subhorizontal to gently inclined, northwest-trending slickenlines on steep to vertical frac-

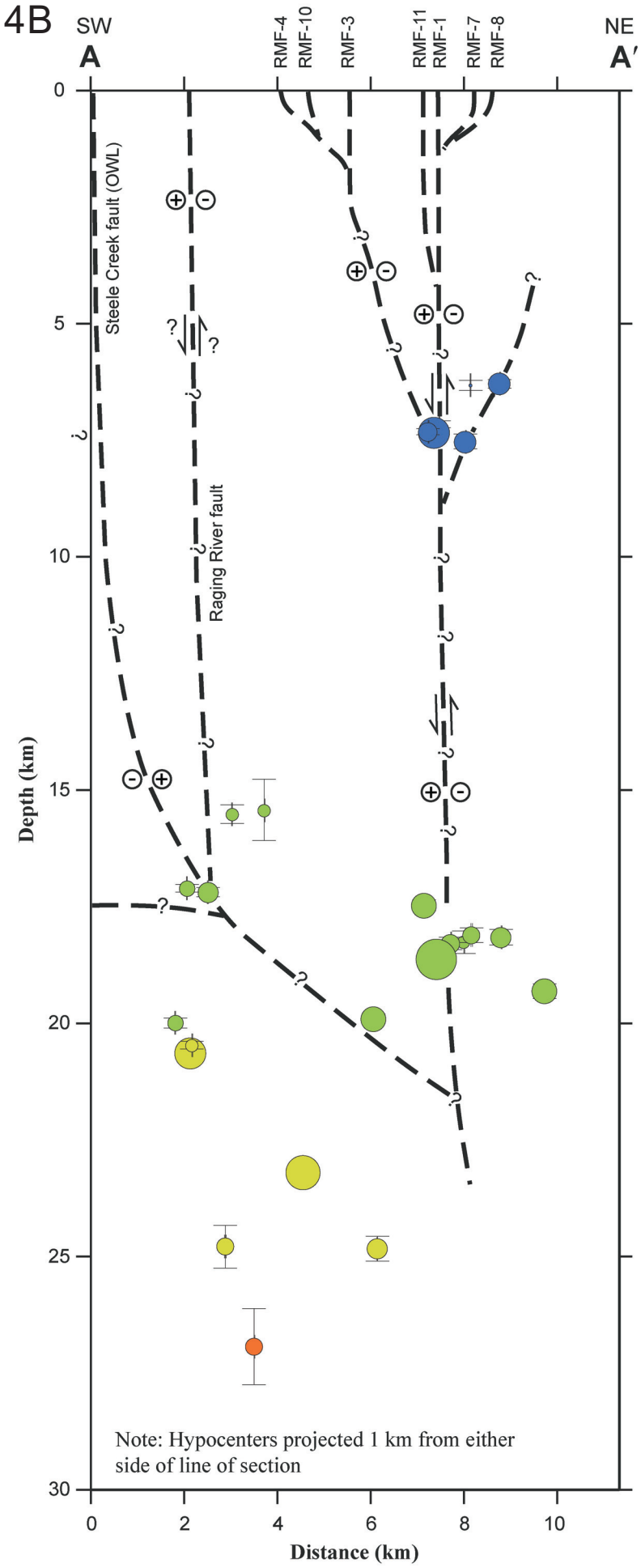

tures in gouge, cataclasite, and protomylonite in tectonic zones (Fig. 5B) that are locally strongly hydrothermally altered (this study, Dragovich and others, 2007; Walsh, 1986; Walsh and Logan, 1985). Transfer faults connect the various strands of the RMFZ in the map area; transfer faults are generally high-angle faults with shallow slickenlines, but they locally include thrusts and reverse faults with more steeply plunging slickenlines. Strike-slip offset is also consistent with the along-strike variation in geologic features between the major strands of the fault zone. For example, Rattlesnake Mountain is a precipitous geomorphic feature that exposes a disrupted volcanic center. We infer that the proximal volcanic rocks of Rattlesnake Mountain are bounded by strike-slip faults that have a normal component of slip. We suspect this volcanic center intruded an earlier version of the RMFZ. To the northwest, Dragovich and others (2007) and Associated Earth Sciences, Inc. (1987, 2003, 2005) infer that this volcanic complex is overlain by thick pre-Fraser glacial and nonglacial deposits including uplifted ancient (pre-Vashon) Snoqualmie valley fluvial deposits that are mapped as Olympia beds (Fig. 2 on plate, site 2, south of Fall City). We interpret uplift to be the result of vertical cannibalization of basin sediments due to migrating growth folding and (or) general exhumation within an evolving and locally active strike-slip fault zone. Current work suggests that much of the Snoqualmie valley is structurally controlled by RMFZ fault strands, strike-slip basins, and en-echelon fold axes. Included are the informally named Snoqualmie valley basin and the Tolt Hill anticline of Dragovich and others (2007) northwest of the map area (Fig. 2 on plate, site 4).

Dragovich and others (2007) correlated the RMFZ with the Southern Whidbey Island fault zone, mostly consistent with Rogers and others (1996) and Sherrod and others (2008). Quaternary faulting along the Southern Whidbey Island fault zone (Johnson and others, 1996) near Woodinville (Blakely and others, 2004; Brocher and others, 2005; Sherrod and others, 2005) occurs along our projection of the RMFZ (Fig. 2 on plate, site 3). The alignment, width, pre-Tertiary basement geometry, and apparent modern activity of both the RMFZ and the Southern Whidbey Island structures provide a compelling case for the correlation of these fault zones.

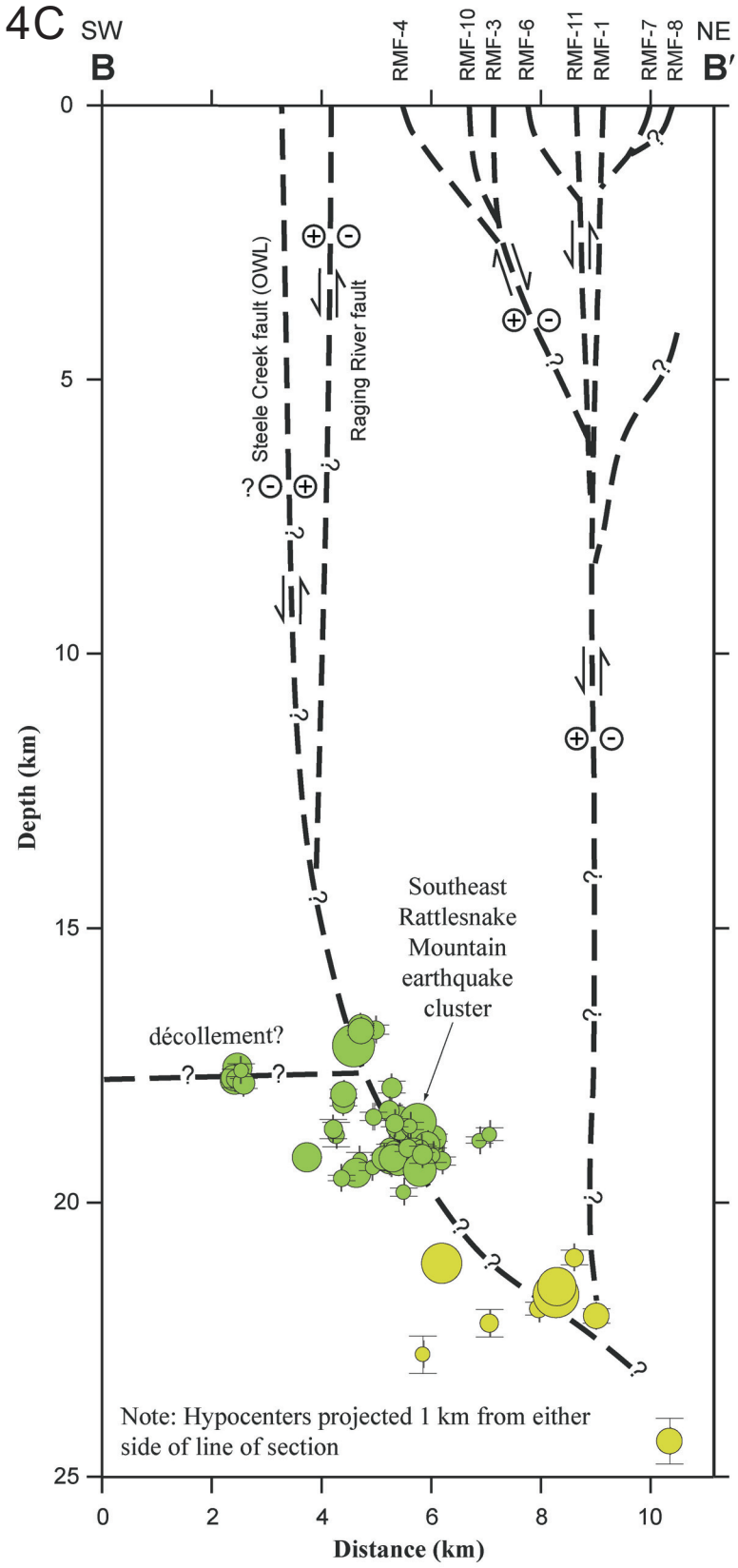

EASTERN RATTLESNAKE MOUNTAIN FAULT ZONE, NORTH BEND BASIN, AND THE SNOQUALMIE RIVER ANTICLINORIUM

Rattlesnake Mountain fault no. 1 (RMF-1) is the main strand of the RMFZ in that it appears to be a regional fault (Fig. 2 on plate). Western mélange belt pre-Tertiary basement occurs on both sides of this fault in the study area (map and cross section). Dragovich and others (2007) infer that RMF-1 regionally juxtaposes Tertiary and pre-Tertiary basement rocks. Newer mapping and geophysical analyses in the North Bend quadrangle suggest that the boundary between basement and Tertiary rocks occurs along RMF-6, west of the main strand. RMF-1 bounds the Snoqualmie valley basin gravity low just east of Fall City where it is colinear with buried bedrock escarpments. Dragovich and others (2007) mapped this fault across the Snoqualmie valley basin in the northern part of the Fall City quadrangle and projected this structure toward a strong lineament that is colinear with stratigraphic anomalies in the Carnation quadrangle (Fig. 2 on plate, site 5). This portion of the projected fault also follows a long linear magnetic low that separates moderate magnetic highs evident on upward-continued magnetic maps of the area (Blakely and others, 1999; Dragovich and others, 2007). Di-

rectly to the northwest of the linear magnetic low, the RMF-1 aligns with the Cottage Lake lineament, an active strand of the Southern Whidbey Island fault zone in the Woodinville area west of the Carnation 7.5-minute quadrangle (Blakely and others, 2004; Sherrod and others, 2005, 2008)(Fig. 2 on plate, site 3). Deformed recessional outwash along the main strand in the Carnation quadrangle implies local Holocene RMF-1 offset (Fig. 2 on plate, site 6), although further work is required to discount landslides or glacial deformation as possible causes of structural features at that site (Dragovich and others, 2007).

Deformed Quaternary sediments both southwest of North Bend (critical site 6) and southeast of Rattlesnake Lake (critical site 9, sec. 2, T22N R8E) are possible evidence for tectonic activity along the main strand. Associated Earth Sciences, Inc. (1992) described fractured glaciolacustrine deposits (unit Qgl_v) exposed in a test-pit at critical site 6 near the main strand. We infer that unit Qgl_v is faulted against unit Ec_t along the main strand in this area (cross section). Also, Landau Associates (2006) described fractured and slickensided clay deposits from a geotechnical boring 283 to 295 ft below the Cedar embankment at critical site 9 and near our projection of RMF-1 in the southeastern part of the map area. Stratigraphic position suggests that these clays are unit Qgl_v or older glacial or nonglacial deposits (unit Qgn_{pf}). Pleistocene activity on the eastern part of the RMFZ zone is also implied by apparently uplifted Olympia-age nonglacial deposits along the eastern lower slopes of Rattlesnake Mountain (critical site 3, SW corner of sec. 8, T23N R8E). These ancient Snoqualmie River sands and gravels appear to be anomalously high, given a lower sea level (base level) during the Olympia nonglacial interval. (See the description of unit Qc_o and Dragovich and others, 2007.) A component of westside-up offset across RMF-1 and (or) nearby faults in the Pleistocene and (or) Holocene may explain (1) the elevated ancient Snoqualmie River alluvium and (2) the North Bend basin east of the main strand in the study area (cross section). This sense of motion is opposite to the westside-down component of RMF-1 offset inferred by Dragovich and others (2007) in the Fall City quadrangle where the main strand bounds the eastern part of the Snoqualmie valley basin. This along-strike variation in vertical tectonism is not unexpected in strike-slip fault zones and may be related to en echelon folding or faulting or transfer or scissor faulting and is generally consistent with the along-strike variation of other RMFZ structures. Right-lateral strike-slip to oblique-slip

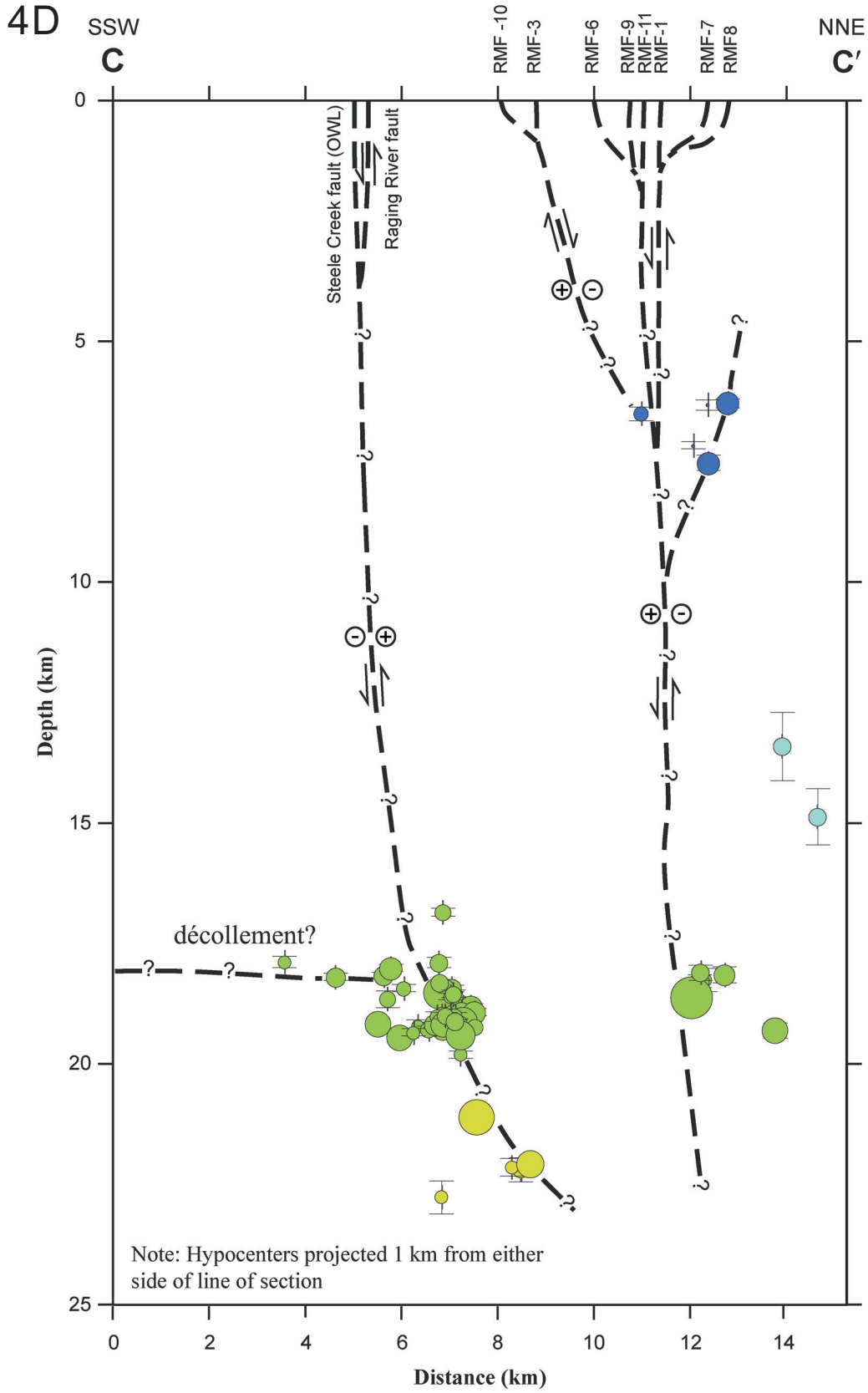

focal mechanism solutions for some relatively shallow seismic events within the eastern RMFZ (Figs. 4A–B) are consistent with our structural model. These seismic events occur near our projection of RMF-1 or RMF-11 (cross section).

Although further work is required, we are intrigued by the possibility that Snoqualmie Falls, an anomalous geographic feature in the Puget Lowland, is related to neotectonic movements within the RMFZ. We forward this as an addendum to the widely accepted glacial-pinning hypothesis of Mackin (1941b). In Mackin's hypothesis, the falls were created by the pinning of the Snoqualmie River onto a bedrock spur by the late glacial Tokul Creek delta; this delta prograded into glacial Lake Snoqualmie, resulting in diversion of the trunk Snoqualmie River around the delta and onto volcanic bedrock. In the Snoqualmie 7.5-minute quadrangle, RMF-1 projects to a large landslide complex directly west of Snoqualmie Falls (Dragovich and others, unpub. data) and may explain other possibly related geomorphic and stratigraphic anomalies around the falls including (1) the anomalously thick (400^{+} ft) ancient Snoqualmie River alluvium (Olympia beds) directly east of the falls (Dragovich and others, 2007, cross section A) and (2) the wide transpressional Snoqualmie and North Bend basins(?) north and south of the falls. (See Fig. 2 on plate and the discussion of North Bend basin below.)

We accept the glacial-pinning hypothesis as a factor in the growth of the falls, but on the basis of local and regional geology suggest that the anomalous position of the high falls at Snoqualmie is the result of Pleistocene to recent tectonism around Snoqualmie. Active faulting, growth folding, or tectonic tilting may be a factor in the development of this high falls along the edge of the Puget Lowland.

Rattlesnake Mountain faults nos. 7 and 8 (RMF-7 and RMF-8) lie east of the main strand (map and cross section). Recent mapping (Dragovich and others, unpub. data) suggests that these two faults may merge with the main strand north of the study area. These faults are mapped on the basis of lineaments and locally strongly tectonized Tertiary and pre-Tertiary bedrock observed both at the surface or reported in geotechnical borings along I-90. For example, a Snoqualmie valley hillock ~0.75 mi north of the quadrangle contains

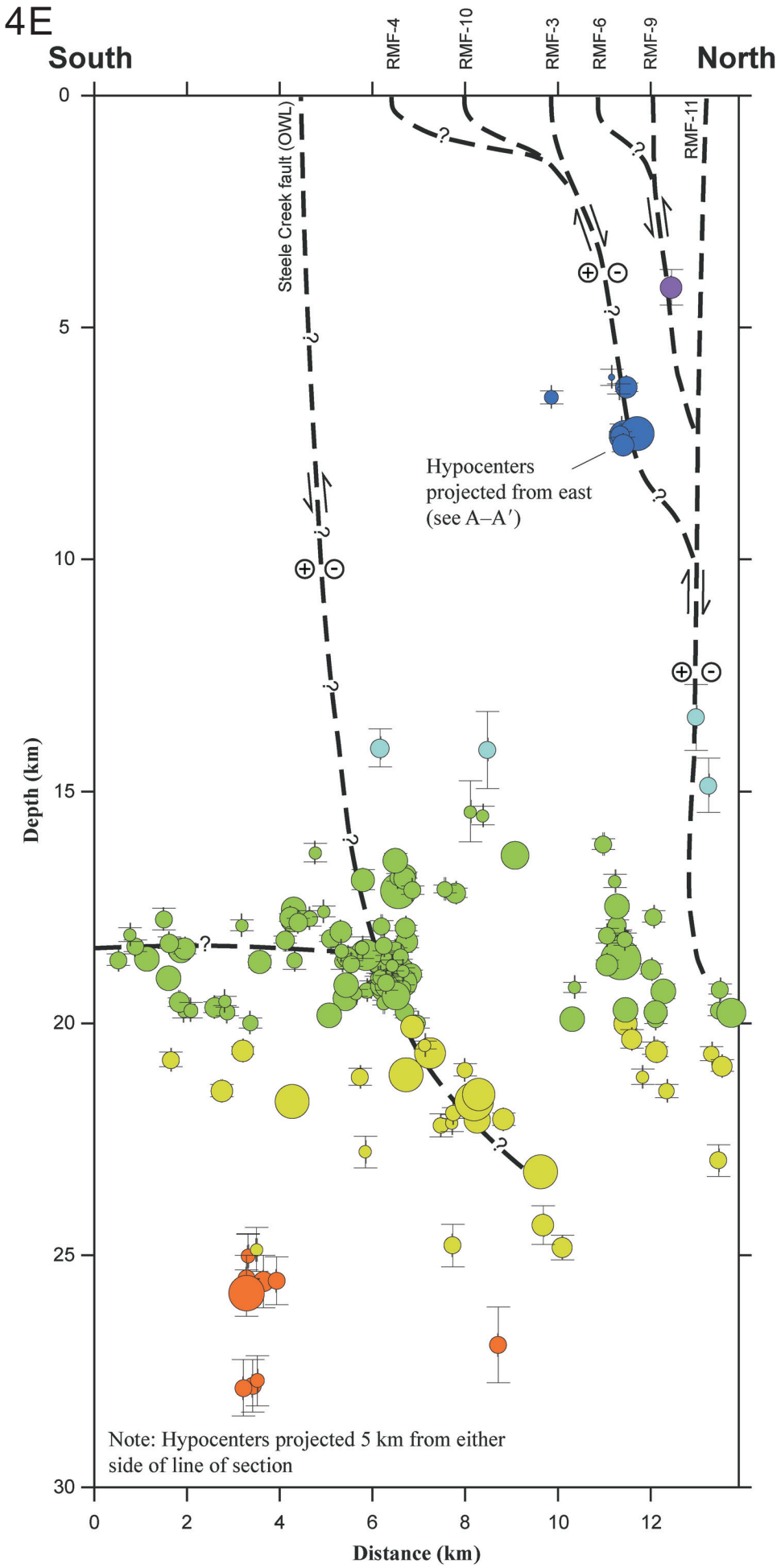

protomylonitized and faulted Western mélange belt greenstone (Tabor and others, 1993; this study) directly east of the projection on RMF-8. RMF-7 and RMF-8 appear to structurally bound the basin below North Bend; we have named this thick Quaternary sediment fill and corresponding gravity low the North Bend basin (cross section). Subsurface data indicate that this basin is 300+ ft deep. However, geotechnical boring data from north of the map area (Associated Earth Sciences, Inc., 1996) combined with our geophysical modeling (Fig. 3A–B) suggest a much greater thickness (~1000 ft). This basin may be a long-lived structural feature that is floored by Pliocene or Miocene rocks. This conjecture may be supported by the 22.26 ±0.57 Ma U-Pb zircon magmatic age (Appendix A, Table A1 and Fig. A1) from rhyolite directly north of Snoqualmie Falls located on Figure 2 on the plate. This date (1) indicates that the Tertiary volcanic rocks directly east of the main strand are locally significantly younger than Tertiary volcanic rocks west of the main strand, including the volcanic rocks of Rattlesnake Mountain or the volcanic rocks Mount Persis of Tabor and others (1993, 2000) and (2) may indicate that the North Bend basin south of Snoqualmie Falls contains Miocene rocks at depth. The Snoqualmie and North Bend basins straddle RMF-1 and are tentatively interpreted by us to be restricted transtensional(?) basins within a major strike-slip fault zone.

We have also named the Snoqualmie River anticlinorium[2] (plate), a complex fold or faulted fold that plunges to the north-northwest toward the Miocene volcanic rocks exposed at Snoqualmie Falls (Fig. 2 on plate). These rocks were initially mapped as the late Eocene to earliest Oligocene rocks of Mount Persis by Tabor and others (1993, 2000), although we have obtained a Miocene age for rocks at the base of Snoqualmie Falls. This anticlinorium is cored by the Western mélange belt basement rocks and is bordered by Tertiary rocks along the lower slopes of Rattlesnake Mountain where Tertiary rocks thinly overlie or are faulted against the mélange basement east of RMF-6 (cross section). Further surface and subsurface structural and stratigraphic work is required to elucidate the nature of this proposed anticlinorium.

Rattlesnake Mountain fault no. 11 (RMF-11) traverses the lower east side of Rattlesnake Mountain and trends to the southeast where it is inferred to underlie the Cedar embankment. Rattlesnake Mountain fault no. 9 (RMF-9) appears to be a transfer fault between RMF-6 and RMF-11. Dropstone-bearing, laminated glaciolacustrine deposits (unit Qgl_v) are fractured near RMF-11 in two exposures along North Bend Way in the Snoqualmie 7.5-minute quadrangle about 1 mi north of the study area (NAD 27: 47°30.97′, 121°50.12′ and 47°30.92′, 121°49.99′). These fractures are steeply dipping to vertical and strike predominantly north–south, subparallel to RMF-11 at both locations. These structures are not consistent with glacial ice shear mechanisms that typically produce shallowly dipping thrust-style structures. We cannot discount a landslide mechanism for these structures; however, most bedding offsets in these glacial sediments seem to be inconsistent with downslope movements related to landsliding. Pleistocene to recent activity along RMF-11 is also suggested by fractured and slickensided clay deposits described

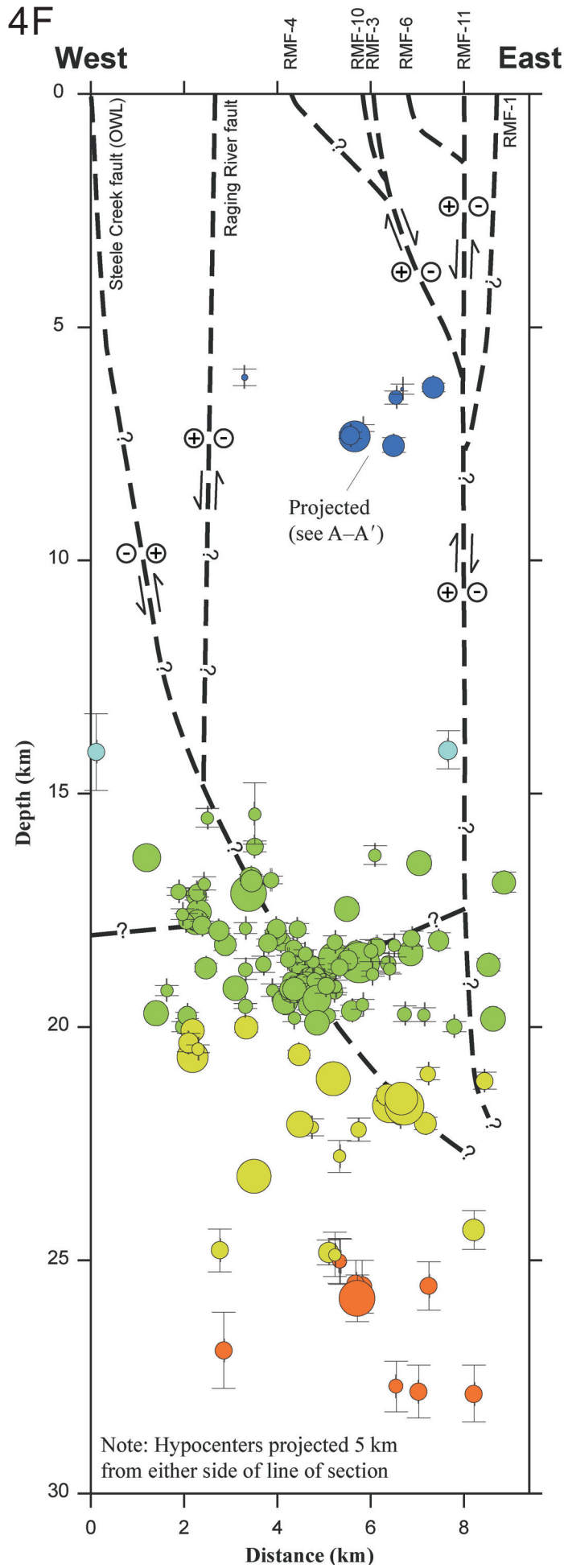

[2] More recent detailed mapping in the north-adjacent Snoqualmie 7.5-minute quadrangle indicates that Miocene transtensional basins occur within the eastern Rattlesnake Mountain fault zone. This finding suggests that the younging Snoqualmie Valley anticlinorium possibly results from pull-apart basin formation and not folding.

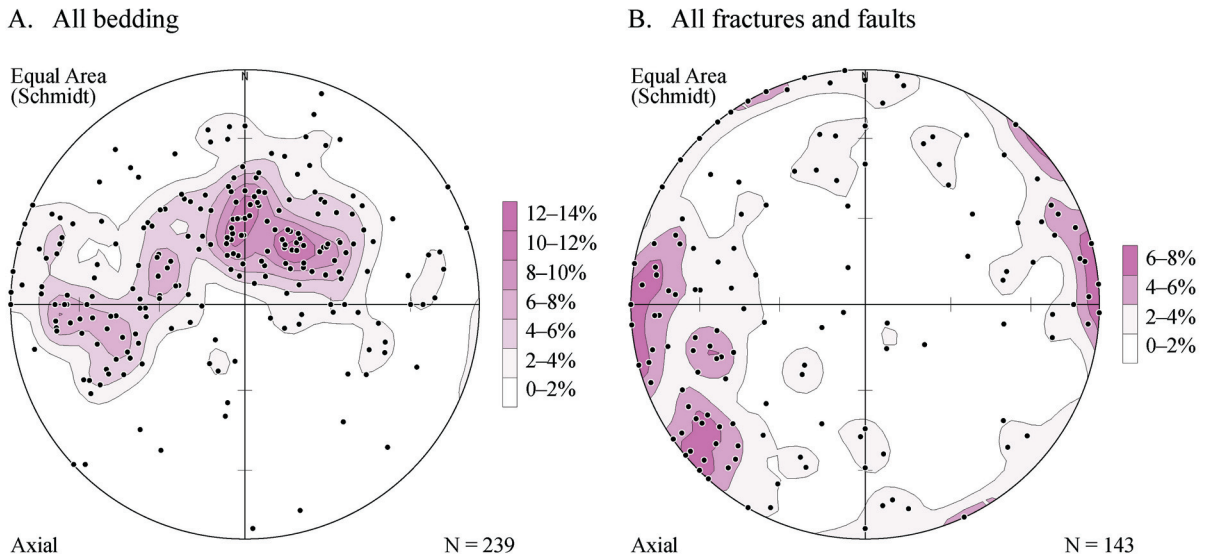

Figure 5. Stereonet using the Gaussian (k=100) method with contour intervals of 0, 2, 6…10 percent/1 percent area. **A**, Poles to bedding of Tertiary rocks; includes all bedding attitudes for rocks younger than those of the Western mélange belt, most of which are shown on the plate. Data are from this study, Walsh (1984), Warren and others (1945), Tabor and others (2000), Vine (1969), Evans (1912), Shannon & Wilson (1978), and Hammond (1963). The data defines southeast-plunging folds such as the Lindsay syncline and Raging River anticline. The figure also shows a dominance of northwest-trending, vertical to subvertical bedding orientations that are common near faults or in tectonic zones (unit tz). **B**, Our data for fractures and faults in the map area show the dominance of steep to vertical fracturing or faulting subparallel to north- to northwest-trending faults. Included are some fractures along steep to shallow transfer faults that are oblique to the main north- to northwest-trending faults. Slickenlines on these discontinuities are typically shallowly plunging to the north-northwest.

by Landau Associates (2006) near our projection of the RMF-11 on the Cedar embankment in the southeastern part of the map area (critical site 10, sec. 2, T22N R8E). These deposits were penetrated in a geotechnical boring from 392 to 400 ft below the surface and are likely pre-Fraser deposits (unit Qgn_{pf}) that may correlate with the Olympia beds (unit Qc_o). We cannot discount glacial ice shear or mass-wasting origins for the deformational features observed along RMF-11. However, the common occurrence of deformed Quaternary sediments along this fault warrants further detailed investigation. (Also see discussion of the Chester Morse Lake earthquake below.)

Rattlesnake Mountain fault no. 11B (RMF-11B) occurs directly west of RMF-11 in the northern part of the map area and may be a short subsidiary strand of the longer RMF-11 structure. R. L. Logan (Wash. Div. of Geology and Earth Resources, oral commun., 2007) observed possible faulted Holocene colluvium at critical site 11 (sec. 8, T23N R8E) near this fault. We were unable to relocate this small exposure; the area is now a residential development.

Rattlesnake Mountain fault no. 6 (RMF-6) occurs along the mid- to upper eastern slope of Rattlesnake Mountain (map and cross section). RMF-6 is a subvertical fault (Fig. 3) that separates magnetically prominent rocks of Rattlesnake Mountain from the Western mélange belt pre-Tertiary basement. (See "Geophysical Analysis of the Map Area", p. 20.) Significant offset along this fault is implied by the juxtaposition of a thick proximal volcanic assemblage west of the fault and mélange basement bearing only a thin carapace of Tertiary volcanic rocks east of the fault (cross section). Inclusions of metagabbro in Tertiary volcanic breccia observed by Tabor and others (2000) suggest that the Western mélange belt occurs in the subsurface at least as far southwest as Chester Morse Lake. We map the fault as an oblique strike-slip fault, but this fault could be a steep normal fault. We map thrusts between RMF-3, RMF-6, and RMF-11 near Rattlesnake Lake to tectonically divide unit ΦEva from the magnetically prominent volcanic rocks of Rattlesnake Mountain (Fig. 3A).

On April 29, 1945, a moderate earthquake occurred near our projection of RMF-6 or RMF-11 near Chester Morse Lake directly east-southeast of the study area. The "Chester Morse Lake earthquake" (M 5.5–5.7) was felt over an area of ~50,000 mi^2 and had a maximum reported intensity of MM VII on the Modified Mercalli scale (Noson and others, 1988). It was followed by two felt aftershocks, suggesting that it was fairly shallow. Minor damage was sustained in North Bend, Snoqualmie, Palmer, Cle Elum, Elma, Greenwater, Index, Leavenworth, and Stampede Pass (Coffman and others, 1982). Plaster, windows, and chimneys were cracked, and large rock avalanches occurred on the west side of Mount Si, 0.5 mi northeast of the quadrangle.

WESTERN RATTLESNAKE MOUNTAIN FAULT ZONE

Rattlesnake Mountain faults nos. 3 and 4 (RMF-3 and -4) were mapped by Dragovich and others (2007) on the basis of several stratigraphic, geomorphic, and geophysical anomalies across these structures in the Fall City area (Fig. 2 on plate). The Renton Formation occurs as a fault-imbricate body between these faults along the northern boundary of the study area (critical site 4, sec. 12, T23N R7E) (Walsh, 1983, 1984). These major faults almost merge in the northern part of the present map area (Walsh, 1984). The steep magnetic gradient in this northern area indicates a subvertical fault separating the volcanic rocks of Rattlesnake Mountain from the Puget Group (Figs. 3A–B). South of this area, the southwestern RMFZ splays into several faults that follow well-exposed major and minor tectonic zones (unit tz). This wide fault zone separates the volcanic rocks on Rattlesnake Mountain from the Tukwila Formation on southwestern Rattlesnake Mountain. Some high-angle, strike-slip fault imbrication of the Tukwila and the rocks of Rattlesnake Mountain is evident within this part

of the RMFZ. RMF-10 is mapped between RMF-3 and RMF-4. RMF-10 and RMF-4 locally separate the Tukwila Formation from the magnetically prominent volcanic rocks of Rattlesnake Mountain (Figs. 3A–C). A moderately steep northeasterly to easterly dip for some of the faults in the southwestern part of the RMFZ is indicated by fault trace geometries and geophysical anomaly patterns (Fig. 3C). We infer that some of the faults in the western RMFZ merge at depth (cross section).

In the Fall City quadrangle, RMF-4 locally bounds steep subsurface bedrock escarpments (fig. 3 in Dragovich and others, 2007), and both RMF-3 and -4 bound an ancient Snoqualmie River channel that was first documented by Associated Earth Sciences, Inc. (1987). These faults are inferred by Dragovich and others (2007) to be strike-slip to oblique-slip faults bounding the west side of the Snoqualmie valley basin near Fall City (Fig. 2). Olympia-age sands (unit Qc_o), consisting of ancient Snoqualmie River alluvium, at 480 ft above present sea level on Snoqualmie Ridge are very similar both geochemically and modally to modern Snoqualmie River alluvium (Dragovich, 2007; Dragovich and others, 2007). The thickening of the Olympia beds to at least 430 ft on Snoqualmie Ridge south of Fall City was attributed to ancient valley fluvial aggradation in a Snoqualmie River structural basin. This observation, combined with the overall thickening of the Olympia beds in the basin, argues for Quaternary tectonism along basin-margin faults to account for all the stratigraphic, structural, and geophysical anomalies across Snoqualmie Ridge in the Fall City area. Shifting tectonism within a strike-slip fault zone apparently uplifted these deposits. Otherwise, Dragovich and others (2007) had difficulty explaining the anomalies by normal valley aggradation in the Quaternary; alluvial river deposits along major rivers in western Washington are typically only tens of feet thick. Furthermore, sea level was about 160 to 260 ft lower during the deposition of the nonglacial Olympia beds (Lambeck and others, 2002), and thus Snoqualmie River entrenchment should have occurred instead of Olympia bed aggradation.

In the northern part of the Fall City quadrangle, RMF-3 and RMF-4 may merge along the eastern side of Tolt Hill. Tertiary to Pleistocene stratigraphic relations across RMF-3 indicate a long-lived component of eastside-down fault displacement from Rattlesnake Mountain to near Tolt Hill north of the present study area The fault juxtaposes younger volcanic rocks of Rattlesnake Mountain with the probably older Puget Group. Dragovich and others (2007) suggest the fault forms the boundary between the Snoqualmie valley basin and Tolt Hill (growth fold?) anticline. Dragovich and others (2007) also infer that RMF-3 and RMF-4 offset Olympia bed sediments north of the study area, but found no evidence for post-Olympia offset and regarded these faults as dormant strands. (See discussion of Southeast Rattlesnake Mountain earthquake cluster below.)

Steele Creek Fault and the Olympic–Wallowa Lineament

The Steele Creek fault is best exposed north of the Cedar River where a fault lineament separates Ohanapecosh (unit ⦶Eva) from older rocks of the Puget Group (Tukwila Formation, unit Evs_t). This stratigraphic and structural relation indicates a north-side-up component of offset for the Steele Creek fault. This fault follows a west-northwest–trending lineament northeast of Williams Creek (Fig. 1, SCL), as well as highly tectonized rocks along Steele Creek (unit tz). The fault is tentatively projected to the east-southeast to align with tectonic zones (unit tz) in the southwest part of the map area near Fish Creek and to the west-northwest to align with a prominent deep-seated landslide directly west of the map area. Hydrothermal alteration associated with tectonic zones around Williams Creek (critical site 8, near the north margin of sec. 13, T22N R7E) and Steele Creek is apparently coincident with a broad zone of structural disruption, although some of this disruption may be related to deformation along the Raging River fault. On the basis of known structural relations west of the study area (Vine, 1969), we suspect that this fault splays into bedding-parallel faults within the Puget Group with offset being transferred subparallel to the Hobart fault of Vine (1969) and the Piling Creek fault of Hammond (1963) or other faults that bound the southern part of the Seattle uplift.

The Steele Creek fault aligns with the Olympic–Wallowa lineament (OWL) of Raisz (1945) and is subparallel to a family of regional faults (for example, White River fault) and folds that define a strong OWL structural grain along, and south of, the study area (Tabor and others, 2000). Raisz (1945) originally mapped the east-southeast–trending OWL from the headwaters of the Cedar River and Chester Morse Lake directly east of the study area, through Fish Creek in the map area and projected the OWL west-northwest across the map area to the headwaters of Issaquah Creek to the west (Fig. 2 on plate, site 7). As mapped, the Steele Creek fault closely follows the OWL of Raisz (1945). The Taylor syncline, Sherwood anticline (Vine, 1969), the northern part of the Lindsay syncline (Hammond, 1963), and the southern part of the Raging River anticline have anomalous west-northwest– or east-southeast–trending fold axes proximal to the Steele Creek fault. Although speculative, the curvature of fold axes (plate) is consistent with a component of left-lateral slip along this fault. We suspect that the RMFZ follows Chester Morse Lake and curves to the east-southeast into alignment with the OWL structural grain southeast of the study area. The fault lineament observed on lidar (Fig. 1, SCL) and the Southeast Rattlesnake Mountain earthquake cluster (Figs. 4C–F) may be evidence that the Steele Creek fault in the map is an active north-northeast–dipping reverse fault that may interact in a complex way with the décollement (below) and the eastern RMFZ. The most distinct portion of the lineament is mostly in glacial deposits and partly defined by a peculiar bend in Williams Creek that could be glacial derangement (R. W. Tabor, USGS emeritus, written commun., 2007). We were unable to evaluate the possibility of Holocene offset of this structure in this area because of general lack of exposure west of Steele Creek. Also, the lack of obvious strike-slip offset of the Snoqualmie batholith along the OWL east of the map area implies limited translational movement along this structure since the Miocene (R. W. Tabor, written commun., 2007).

We informally give the name Southeast Rattlesnake Mountain earthquake cluster to a tight grouping of earthquake hypocenters that occurs in the mid-crust below RMF-4 (Figs. 4C–E). Hypocenter cluster geometry best fits a north-northeast–dipping fault that if projected to the surface may be the currently mapped Steele Creek fault (Fig. 4C). However, hypocenter distribution could imply two intersecting faults involving a steep fault such as RMF-4 and the more gently dipping Steele Creek fault. We tentatively in-

terpret this cluster to be located along the down-dip extension of the Steele Creek fault. If this interpretation is correct, we estimate that the Steele Creek fault has an average dip of ~86º north-northeast (the cluster is ~1.2 km horizontally from the exposed Steele Creek fault at a depth of ~19 km); however, we suspect it is subvertical near the surface and becomes a listric curving structure near the hypocenters and thus may dip more gently at depth. This steep dip is consistent with the linear nature of this mapped fault. This fault and the Piling Creek fault of Hammond (1963), which is collinear with the Hobart fault of Vine (1969), form part of a series of west-northwest-trending faults exposed in coal mines in May Creek Valley and Maple Valley (Walsh, 1984) that broadly bound the Seattle fault uplift on its south side.

Regional Décollement and Flat Faulting

Pratt and others (1997) argued that the Seattle uplift occurs above north-verging reverse faults or thrusts that taper down into a regional décollement (detachment) at a mid-crustal level. This décollement may regionally connect many of the active fault zones in western Washington that are a result of active north-south compression; these include the Tacoma and Southern Whidbey Island faults, and possibly the Darrington–Devils Mountain fault. Although other interpretations are possible (for example, Brocher and others, 2001; Blakely and others, 2002), this regional detachment is suggested by the relatively high density of ~17- to 28-km-deep hypocenters that cannot easily be correlated with surface faults. Conversely, Van Wagoner and others (2002) state that, "the seismicity pattern and velocity structure shows no direct evidence for this mid-crustal feature, so if decoupling occurs on a sub-horizontal décollement, it has no apparent effect on the contemporary earthquake activity and is without clear structural manifestation". The Seattle and Rattlesnake Mountain fault zones (Fig. 2 on plate) intersect northwest of the map area (Dragovich and others, 2007) where the RMFZ forms the eastern tectonic boundary of the Seattle uplift. Our conceptual model is that dextral strike-slip offset along the high-angle RMFZ accommodates northerly vergence on the south-dipping Seattle fault zone. The two shallow micro-earthquakes along the eastern part of the RMFZ with a strike-slip focal mechanisms solution (Figs. 4A–B) are interpreted to be dextral-slip tears due to north–south shortening. Whether or not there is a regional décollement, the relatively high density of relocated hypocenters below the study area at a depth of ~17 to 28 km with reverse or thrust focal mechanism solutions is consistent with activity along thrusts or reverse faults at depth that are accommodating north–south compression (Figs. 4A–F).

ACKNOWLEDGMENTS

This geologic map was funded in part by the U.S. Geological Survey (USGS) National Cooperative Geologic Mapping Program under award no. 07HQAG0142. We thank many people for assistance: Paul Hammond (Portland State Univ., emeritus) for geologic input and unpublished data; Rowland Tabor (USGS emeritus) for a review of the map and text and other geologic input; Jennifer Saltonstall (Associated Earth Sciences, Inc.) and James Johnson (Golder Associates) for subsurface geotechnical information; Russ Steele and Eric Dingeldein (Wash. Dept. of Transportation), Stephen Bottheim (King County), Daniel Huang and Martin Hansen (Seattle Public Utilities), Ed Heavey (Landau Assoc., Inc.), and Myrtle Jones (USGS, Water Resources Division, Tacoma) for subsurface geologic information; Jeff Grant (Green Crow Management Services) and Dwayne Paige and Darin Davis (Seattle Public Utilities) for providing property access; and Brian Ballard (Wash. Dept of Natural Resources, South Puget Region) for providing logistical support. We also thank Albert Gonzales and Mike Leathers (King County Information Technology Division, GIS Products and Services) for the lidar data; Brian Sherrod (USGS) for providing in-press geologic information; and Diane Cornelius, Rick Conrey, and Charles Knaack (Wash. State Univ.) for geochemical analysis of our samples. We thank Washington Division of Geology and Earth Resources colleagues Josh Logan for map and text reviews, Jessica Hicks and Debbie Grant for clerical support, and Lee Walkling for assistance with references. Thanks also to staff members Eric Schuster, Jari Roloff, Anne Heinitz, and Chuck Caruthers for cartographic support on the map and figures, Katherine Reed and Jari Roloff for editorial help, and Jessica Czajkowski and Jari Roloff for drafting of figures.

REFERENCES CITED

Anderson, M. L.; Blakely, R. J.; Brocher, T. M.; Pratt, T. L.; Wells, R. E.; Haugerud, R.; Bush, M., 2006, Structure of the Seattle uplift from seismic, gravity, magnetic, geologic, and geomorphic data [abstract]: Eos (American Geophysical Union Transactions), v. 87, no. 52, abstract T41A-1554.

Armstrong, J. E.; Crandell, D. R.; Easterbrook, D. J.; Noble, J. B., 1965, Late Pleistocene stratigraphy and chronology in southwestern British Columbia and northwestern Washington: Geological Society of America Bulletin, v. 76, no. 3, p. 321-330.

Associated Earth Sciences, Inc., 1987, Snoqualmie Ridge project, King County, Washington—Soils, geology, geologic hazards and ground water hydrogeology: Associated Earth Sciences, Inc. [Kirkland, Wash., under contract to] Snoqualmie Ridge Associates, Inc., 2 v., 4 plates.

Associated Earth Sciences, Inc., 1992, Forster Woods phase II—North Bend, Washington: Associated Earth Sciences, Inc., 1 v.

Associated Earth Sciences, Inc., 1996, Snoqualmie North Valley well field, Snoqualmie, Washington—Hydrogeologic evaluation for source approval of group A public water systems, WAC 246-290-130: Associated Earth Sciences, Inc., 1 v.

Associated Earth Sciences, Inc., 1998, Review draft—Results of preliminary investigations, Cedar Moraine Monitoring Improvements Project, Cedar River watershed, King County, Washington: Associated Earth Sciences, Inc., 1 v.

Associated Earth Sciences, Inc., 2003, Proposed Snoqualmie Ridge II project—Environmental impact statement—Technical report on geology, soils, and groundwater: Associated Earth Sciences, Inc, [Kirkland, Wash., under contract to] Quadrant Corporation, 1 v.

Associated Earth Sciences, Inc., 2005, Proposed Snoqualmie Ridge II N1 and N2 infiltration ponds—Technical report on geology and groundwater: Associated Earth Sciences, Inc, [Kirkland, Wash., under contract to] Quadrant Corporation, 1 v.

Black, L. P.; Kamo, S. L.; Allen, C. M.; Davis, D. W.; Aleinikoff, J. W.; Valley, J. W.; Mundil, Roland.; Campbell, I. H.; Korsch, R. J.; Williams, I. S.; Foudoulis, Chris, 2004, Improved $^{206}Pb/^{238}U$ microprobe geochronology by the monitoring of a trace-element-related matrix effect—SHRIMP, ID-TIMS, ELA-ICP-MS and oxygen isotope documentation for a series of zircon standards: Chemical Geology, v. 205, no. 1-2, p. 115-140.

Blakely, R. J., 1995, Potential theory in gravity and magnetic applications: Cambridge University Press, 441 p.

Blakely, R. J.; Sherrod, B. L.; Wells, R. E.; Weaver, C. S.; McCormack, D. H.; Troost, K. G.; Haugerud, R. A., 2004, The Cottage Lake aeromagnetic lineament—A possible onshore extension of the Southern Whidbey Island fault, Washington: U.S. Geological Survey Open-File Report 2004-1204, 60 p.

Blakely, R. J.; Wells, R. E.; Weaver, C. S., 1999, Puget Sound aeromagnetic maps and data: U.S. Geological Survey Open-File Report 99-514, version 1.0. [http://geopubs.wr.usgs.gov/open-file/of99-514/]

Blakely, R. J.; Wells, R. E.; Weaver, C. S.; Johnson, S. Y., 2002, Location, structure, and seismicity of the Seattle fault zone, Washington—Evidence from aeromagnetic anomalies, geologic mapping, and seismic-reflection data: Geological Society of America Bulletin, v. 114, no. 2, p. 169-177.

Booth, D. B., 1986, The formation of ice-marginal embankments into ice-dammed lakes in the eastern Puget Lowland, Washington, U.S.A., during the late Pleistocene: Boreas, v. 15, no. 3, p. 209-264.

Booth, D. B., 1990, Surficial geologic map of the Skykomish and Snoqualmie Rivers area, Snohomish and King Counties, Washington: U.S. Geological Survey Miscellaneous Investigations Series Map I-1745, 2 sheets, scale 1:50,000, with 22 p. text.

Brocher, T. M.; Blakely, R. J.; Wells, R. E.; Sherrod, B. L.; Ramachandran, Kumar, 2005, The transition between N–S and NE–SW directed crustal shortening in the central and northern Puget Lowland—New thoughts on the Southern Whidbey Island fault [abstract]: Eos (American Geophysical Union Transactions), v. 86, no. 52, p. F1459.

Brocher, T. M.; Parsons, T. E.; Blakely, R. J.; Christensen, N. I.; Fisher, M. A.; Wells, R. E.; SHIPS Working Group, 2001, Upper crustal structure in Puget Lowland, Washington—Results from the 1998 Seismic Hazards Investigations in Puget Sound: Journal of Geophysical Research, v. 106, no. B7, p. 13,541-13,564.

Chang, Zhaoshan; Vervoort, J. D.; McClelland, W. C.; Knaack, Charles, 2006, U-Pb dating of zircon by LA-ICP-MS: Geochemistry, Geophysics, Geosystems, v. 7, p. 1-14.

Coffman, J. L.; von Hake, C. A.; Stover, C. W., editors, 1982, Earthquake history of the United States; revised edition (through 1970), reprinted 1982 with supplement (1971–80): U.S. National Oceanic and Atmospheric Administration–U.S. Geological Survey Publication 41-1, 268 p.

Danner, W. R., 1966, Limestone resources of western Washington; with a section on the Lime Mountain deposit, by G. W. Thorsen: Washington Division of Mines and Geology Bulletin 52, 474 p.

Dickinson, W. R., 1970, Interpreting detrital modes of greywacke and arkose: Journal of Sedimentary Petrology, v. 40, no. 2, p. 695-707.

Dickinson, W. R.; Gehrels, G. E., 2003, U-Pb ages of detrital zircons from Permian and Jurassic eolian sandstones of the Colorado Plateau, USA—Paleogeographic implications: Sedimentary Geology, v.163, no. 1-2, p. 29-66.

Dragovich, J. D., 2007, Sand point count and geochemical data in the Fall City and Carnation 7.5-minute quadrangles, King County, Washington—Supplement to GM-64: Washington Division of Geology and Earth Resources Open File Report 2007-3, 1 CD zip archive containing 4 files: Microsoft Word, Microsoft Excel, and Adobe PDF formats, 144 kb. [http://www.dnr.wa.gov/ResearchScience/GeologyEarthSciences/Pages/Home.aspx]

Dragovich, J. D.; Anderson, M. L.; Walsh, T. J.; Johnson, B. L.; Adams, T. L., 2007, Geologic map of the Fall City 7.5-minute quadrangle, King County, Washington: Washington Division of Geology and Earth Resources Geologic Map GM-67, 1 sheet, scale 1:24,000. [http://www.dnr.wa.gov/Publications/ger_gm67_geol_map_fallcity_24k.zip]

Dragovich, J. D.; Logan, R. L.; Schasse, H. W.; Walsh, T. J.; Lingley, W. S., Jr.; Norman, D. K.; Gerstel, W. J.; Lapen, T. J.; Schuster, J. E.; Meyers, K. D., 2002, Geologic map of Washington—Northwest quadrant: Washington Division of Geology and Earth Resources Geologic Map GM-50, 3 sheets, scale 1:250,000, with 72 p. text.

Dragovich, J. D.; Walsh, T. J., 2008, Geochemical sample analyses of Tertiary and pre-Tertiary volcanic rocks in and around the North Bend 7.5-minute quadrangle, King County, Washington: Washington Division of Geology and Earth Resources Open File Report 2008-4, 1 Microsoft Excel file with 4 p. text. [http://www.dnr.wa.gov/Publications/ger_ofr2008-4_northbend_geochem.zip]

Evans, G. W., 1912, The coal fields of King County: Washington Geological Survey Bulletin 3, 247 p., 13 plates.

Fischer, J. F., 1970, The geology of the White River–Carbon Ridge area, Cedar Lake quadrangle, Cascade mountains, Washington: University of California at Santa Barbara Doctor of Philosophy thesis, 200 p., 2 plates.

Fiske, R. S.; Hopson, C. A.; Waters, A. C., 1963, Geology of Mount Rainier National Park, Washington: U.S. Geological Survey Professional Paper 444, 93 p., 1 plate. [http://vulcan.wr.usgs.gov/Volcanoes/Rainier/Publications/PP444/framework.html]

Frizzell, V. A., Jr., 1979, Petrology and stratigraphy of Paleogene nonmarine sandstones, Cascade Range, Washington: U.S. Geological Survey Open-File Report 79-1149, 151 p., 3 plates. [http://pubs.er.usgs.gov/pubs/ofr/ofr791149]

Frizzell, V. A., Jr.; Tabor, R. W.; Zartman, R. E.; Blome, C. D., 1987, Late Mesozoic or early Tertiary mélanges in the western Cascades of Washington. *In* Schuster, J. E., editor, Selected papers on the geology of Washington: Washington Division of Geology and Earth Resources Bulletin 77, p. 129-148.

Fuller, R. E., 1925, The geology of the northeastern part of Cedar Lake quadrangle with special reference to the de-roofed Snoqualmie batholith: University of Washington Master of Science thesis, 96 p., 4 plates.

Hammond, P. E., 1963, Structure and stratigraphy of the Keechelus volcanic group and associated Tertiary rocks in the west-central Cascade Range, Washington: University of Washington Doctor of Philosophy thesis, 254 p., 2 plates.

Hammond, P. E., 1998, Tertiary andesitic lava-flow complexes (stratovolcanoes) in the southern Cascade Range of Washington—Observations on tectonic processes within the Cascade arc: Washington Geology, v. 26, no. 1, p. 20-30.

Hammond, P. E.; Dragovich, J. D., 2008, Tuff of Stampede Pass and tuff of Green Canyon in the central Cascade Range, King and Kittitas Counties, Washington: Washington Division of Geology and Earth Resources Open File Report 2008-3, 6 p., 1 Microsoft Excel file. [http://www.dnr.wa.gov/Publications/ger_ofr2008-3_stampedepass_greencanyon_tuff.zip]

Hartman, D. A., 1973, Geology and low-grade metamorphism of the Greenwater River area, central Cascade Range, Washington: University of Washington Doctor of Philosophy thesis, 99 p., 2 plates.

Jett, G. A., Heller, P. L., 1988, Tectonic significance of polymodal compositions in melange sandstones, western mélange belt, north Cascade Range, Washington: Journal of Sedimentary Petrology, v. 58, no. 1, p. 52-61.

Johnson, S. Y.; O'Connor, J. T., 1994, Stratigraphy, sedimentology, and provenance of the Raging River Formation (early? and middle Eocene), King County, Washington: U.S. Geological Survey Bulletin 2085-A, 33 p.

Johnson, S. Y.; Potter, C. J.; Armentrout, J. M.; Miller, J. J.; Finn, C. A.; Weaver, C. S., 1996, The Southern Whidbey Island fault—An active structure in the Puget Lowland, Washington: Geological Society of America Bulletin, v. 108, no. 3, p. 334-354, 1 plate.

Lambeck, Kurt; Yokoyama, Yusuke; Purcell, Tony, 2002, Into and out of the last glacial maximum; Sea-level change during oxygen isotope stages 3 and 2: Quaternary Science Reviews, v. 21, no. 1-3, p. 343-360.

Landau Associates, 2006, Cedar moraine safety studies final report—Cedar River watershed, King County, Washington: Landau Associates, 1 v., 1 DVD.

Le Maitre, R. W., editor, 1989, A classification of igneous rocks and glossary of terms—Recommendations of the International Union of Geological Sciences Subcommission on the Systematics of Igneous Rocks: Blackwell Scientific Publications, 193 p., 1 plate.

Ludwig, K. R., 2001, Isoplot/Ex version 2.49—A geochronological toolkit for Microsoft Excel: Berkeley Geochronology Center, Special Publication 2001, no. 1a, 58 p.

Mackin, J. H., 1941a, A geologic interpretation of the failure of the Cedar Reservoir, Washington: University of Washington Engineering Experiment Station Bulletin 107, 30 p.

Mackin, J. H., 1941b, Glacial geology of the Snoqualmie–Cedar area, Washington: Journal of Geology, v. 49, no. 5, p. 449-481.

Miller, R. B., 1989, The Mesozoic Rimrock Lake inlier, southern Washington Cascades—Implications for the basement to the Columbia Embayment: Geological Society of America Bulletin, v. 101, no. 10, p. 1289-1305.

Mullineaux, D. R.; Waldron, H. H.; Rubin, Meyer, 1965, Stratigraphy and chronology of late interglacial and early Vashon glacial time in the Seattle area, Washington: U.S. Geological Survey Bulletin 1194-O, 10 p.

Noson, L. L.; Qamar, A. I.; Thorsen, G. W., 1988, Washington State earthquake hazards: Washington Division of Geology and Earth Resources Information Circular 85, 77 p. [http://www.pnsn.org/INFO_GENERAL/NQT/welcome.html]

Paces, J. B.; Miller J. D., Jr., 1993, Precise U-Pb ages of Duluth complex and related mafic intrusions, northeastern Minnesota—Geochronological insights to physical, petrogenetic, paleomagnetic, and tectonomagmatic processes associated with the 1.1 Ga midcontinent rift system: Journal of Geophysical Research, v. 98, no. B8, p. 13,997–14,014.

Pettijohn, F. J., 1957, Sedimentary rocks; 2nd ed.: Harper & Brothers, 718 p.

Porter, S. C., 1976, Pleistocene glaciation in the southern part of the north Cascade Range, Washington: Geological Society of America Bulletin, v. 87, no. 1, p. 61-75.

Porter, S. C.; Swanson, T. W., 1998, Radiocarbon age constraints on rates of advance and retreat of the Puget lobe of the Cordilleran ice sheet during the last glaciation: Quaternary Research, v. 50, no. 3, p. 205-213.

Pratt, T. L.; Johnson, S. Y.; Potter, C. J.; Stephenson, W. J.; Finn, C. A., 1997, Seismic reflection images beneath Puget Sound, western Washington State—The Puget Lowland thrust sheet hypothesis: Journal of Geophysical Research, v. 102, no. B12, p. 27,469-27,489.

Raisz, E. J., 1945, The Olympic–Wallowa lineament: American Journal of Science, v. 243A [Daly volume], p. 479-485.

Rogers, A. M.; Walsh, T. J.; Kockelman, W. J.; Priest, G. R., 1996, Map showing known or suspected faults with Quaternary displacement in the Pacific Northwest. *In* Rogers, A. M.; Walsh, T. J.; Kockelman, W. J.; Priest, G. R., editors, Assessing earthquake hazards and reducing risk in the Pacific Northwest: U.S. Geological Survey Professional Paper 1560, v. 1, Plate 1, scale 1:2,000,000.

Rosengreen, T. E., 1965, Surficial geology of the Maple Valley and Hobart quadrangles, Washington: University of Washington Master of Science thesis, 71 p., 1 plate.

Saltonstall, J. H.; Koger, C. J; Sweet, Suzanne; Thompson, S. S., 2003, Olympia age paleotopographic influences on Vashon glaciofluvial sedimentation beneath eastern Bear Creek plateau, King County, Washington [abstract]: Geological Society of America Abstracts with Programs, v. 35, no. 6, p. 109.

Shannon & Wilson, 1978, Geotechnical report—Cedar embankment stability studies, Cedar Falls, Washington: Shannon & Wilson [prepared for City of Seattle Department of Lighting], 1 v., 1 plate, scale 1:12,000.

Sherrod, B. L.; Blakely, R. J.; Weaver, Craig; Kelsey, Harvey; Barnett, Elizabeth; Wells, Ray, 2005, Holocene fault scarps and shallow magnetic anomalies along the Southern Whidbey Island fault zone near Woodinville, Washington: U.S. Geological Survey Open-File Report 2005-1136, 35 p. [http://pubs.usgs.gov/of/2005/1136/]

Sherrod, B. L.; Blakely, R. J.; Weaver, C. S.; Kelsey, H. M.; Barnett, Elizabeth; Liberty, Lee; Meagher, K. L.; Pape, Kristin, 2008, Finding concealed active faults—Extending the Southern Whidbey Island fault across the Puget Lowland, Washington: Journal of Geophysical Research, v. 113, B05313, doi:10.1029/2007JB005060, 2008.

Tabor, R. W.; Frizzell, V. A., Jr.; Booth, D. B.; Waitt, R. B., 2000, Geologic map of the Snoqualmie Pass 30 x 60 minute quadrangle, Washington: U.S. Geological Survey Geologic Investigations Series Map I-2538, 1 sheet, scale 1:100,000, with 57 p. text.

Tabor, R. W.; Frizzell, V. A., Jr.; Booth, D. B.; Waitt, R. B.; Whetten, J. T.; Zartman, R. E., 1993, Geologic map of the Skykomish River 30-by 60-minute quadrangle, Washington: U.S. Geological Survey Miscellaneous Investigations Series Map I-1963, 1 sheet, scale 1:100,000, with 42 p. text. [http://geopubs.wr.usgs.gov/i-map/i1963/]

Tabor, R. W.; Frizzell, V. A., Jr.; Booth, D. B.; Whetten, J. T.; Waitt, R. B., Jr.; Zartman, R. E., 1982, Preliminary geologic map of the Skykomish River 1:100,000 quadrangle, Washington: U.S. Geological Survey Open-File Report 82-747, 31 p., 1 sheet, scale 1:100,000.

Tabor, R. W.; Frizzell, V. A., Jr.; Vance, J. A.; Naeser, C. W., 1984, Ages and stratigraphy of lower and middle Tertiary sedimentary and volcanic rocks of the central Cascades, Washington—Application to the tectonic history of the Straight Creek fault: Geological Society of America Bulletin, v. 95, no. 1, p. 26-44.

Turner, D. L.; Frizzell, V. A., Jr.; Triplehorn, D. M.; Naeser, C. W., 1983, Radiometric dating of ash partings in coal of the Eocene Puget Group, Washington—Implications for paleobotanical stages: Geology, v. 11, no. 9, p. 527-531.

U.S. Geological Survey Geologic Names Committee, 2007, Divisions of geologic time—Major chronostratigraphic and geochronologic units: U.S. Geological Survey Fact Sheet 2007-3015, 2 p.

Van Wagoner, T. M.; Crosson, R. S.; Creager, K. C.; Medema, G. F.; Preston, L. A.; Symons, N. P.; Brocher, T. M., 2002, Crustal structure and relocated earthquakes in the Puget Lowland, Washington, from high-resolution seismic tomography: Journal of Geophysical Research, v. 107, no. B12, 2381, DOI:10.1029/20012JB000710, p. ESE 22-1 – 22-23.

Vance, J. A.; Clayton, G. A.; Mattinson, J. M.; Naeser, C. W., 1987, Early and middle Cenozoic stratigraphy of the Mount Rainier–Tieton River area, southern Washington Cascades. *In* Schuster, J. E., editor, Selected papers on the geology of Washington: Washington Division of Geology and Earth Resources Bulletin 77, p. 269-290.

Vine, J. D., 1962, Stratigraphy of Eocene rocks in a part of King County, Washington: Washington Division of Mines and Geology Report of Investigations 21, 20 p.

Vine, J. D., 1969, Geology and coal resources of the Cumberland, Hobart, and Maple Valley quadrangles, King County, Washington: U.S. Geological Survey Professional Paper 624, 67 p., 4 plates.

Waldhauser, F.; Ellsworth, W. L., 2000, A double-difference earthquake location algorithm: Method and application to the northern Hayward fault: Bulletin of the Seismological. Society of America, v. 90, p. 1353-1368.

Walsh, T. J., 1983, Map of coal mine workings in part of King County, Washington: Washington Division of Geology and Earth Resources Open File Report 83-17, 4 p., 1 plate, scale 1:24,000.

Walsh, T. J., 1984, Geology and coal resources of central King County, Washington: Washington Division of Geology and Earth Resources Open File Report 84-3, 24 p., 2 plates.

Walsh, T. J., 1986, Age of deformation along the Olympic–Wallowa lineament near Seattle, Washington [abstract]: Geological Society of America Abstracts with Programs, v. 18, no. 2, p. 195.

Walsh, T. J.; Logan, R. L., 1985, Geological and geophysical expression of the Olympic–Wallowa lineament (OWL) near North Bend, Washington [abstract]: Geological Society of America Abstracts with Programs, v. 17, no. 6, p. 416.

Warren, W. C.; Norbisrath, Hans; Grivetti, R. M.; Brown, S. P., 1945, Preliminary geologic map and brief description of the coal fields of King County, Washington: U.S. Geological Survey Preliminary Map, 1sheet, scale 1:31,680.

Wolfe, J. A., 1968, Paleogene biostratigraphy of nonmarine rocks in King County, Washington: U.S. Geological Survey Professional Paper 571, 33 p., 7 plates.

Wolfe, J. A., 1981, A chronologic framework for Cenozoic megafossil floras of northwestern North America and its relation to marine geochronology. *In* Armentrout, J. M., editor, Pacific Northwest Cenozoic biostratigraphy: Geological Society of America Special Paper 184, p. 39-47.

Wolfe, J. A.; Forest, C. E.; Molnar, Peter, 1998, Paleobotanical evidence of Eocene and Oligocene paleoaltitudes in midlaltitude western North America: Geological Society of America Bulletin, v. 110, no. 5, p. 664-678.

Yount, J. C.; Gower, H. D., 1991, Bedrock geologic map of the Seattle 30′ by 60′ quadrangle, Washington: U.S. Geological Survey Open-File Report 91-147, 37 p., 4 plates.

Appendix A. U-Pb LA-ICP-MS Geochronology

Zircons for this study were analyzed for U and Pb using laser ablation inductively coupled mass spectrometry (LA-ICP-MS) at Washington State University. Individual ~50-lb samples were crushed to fine sand-size particles. Heavy minerals were concentrated using a MD Mineral Technologies Gemini gold table. Crushing plates and the Gemini table were thoroughly cleaned after each sample to reduce the risk of cross contamination. The zircon concentrate was then passed through a 350-mm sieve. The <350-mm fraction was cleaned by magnetic separation using a Frantz LB1. Zircons were further separated by density from the nonmagnetic fraction with methylene iodide (heavy liquid). From the zircon separate, between 5 and 30 individual zircon grains were selected from each sample and mounted in epoxy with zircon standards Peixe and FC1 (Dickinson and Gehrels, 2003; Black and others, 2004; Paces and Miller, 1993) and polished to expose the grain centers. Zircon regions suitable for analysis were identified by cathodoluminescence and optical imaging. All dated zircons are euhedral to subhedral. The analytical LA-ICP-MS setup consists of a New Wave UP-213 laser ablation system interfaced with a ThermoFinnigan™ Element-2, high-resolution magnetic sector ICPMS. The laser was operated at 10 Hz repetition rate at a fluence of 10–12 joules/cm^2. Laser beam width was 30 μm, and pit depth was 25 μm in a typical analysis.

All data were reduced offline using a Microsoft Excel–based program (Chang and others, 2006), and concordia ages were generated with Isoplot (Ludwig, 2001) and anchoring to a common Pb value of 0.86 ± 0.06 (Fig. A1–A8). Uncertainties are reported on Table A1 and are a quadratic combination of (1) uncertainty of the measured ^{206}Pb/^{238}U and ^{207}Pb/^{206}Pb for each analysis and (2) variance in the ^{206}Pb/^{238}U and ^{207}Pb/^{206}Pb determinations of the standards that bracket the unknowns. Overall uncertainty in age is conservatively estimated to be between 3 and 5 percent 2 sigma (σ). (A fuller description of this method is given in Chang and others, 2006.)

Figures A1–A8. *(p. 36)* ^{207}Pb/^{206}Pb versus ^{238}U/^{206}Pb Terra Wasserberg Concordia plots for samples for samples 07-10F, 07-14E, 07-23A, and 07-47T. Zircons for this study were analyzed for U and Pb using laser ablation inductively coupled mass spectrometry (LA-ICP-MS). See Table A1 for age data and basic sample information. Data used to generate plots are bold in Table A1, and error ellipses are 2 sigma (σ). Concordia ages were determined using Isoplot (Ludwig, 2001) by anchoring to a common ^{207}Pb/^{206}Pb value of 0.86 ±0.06. See "Description of Map Units", p. 3, for further information. We report the intercept age illustrated in the upper right corner of each figure. See "Eastern Rattlesnake Mountain Fault Zone, North Bend Basin, and the Snoqualmie River Anticlinorium", p. 25, for a discussion of sample 07-23A (unit Ꝑvr) near Snoqualmie Falls. Older zircons in Tertiary volcanic rocks (Figs. A3, A4, A6, A8) can be obtained by several intrusive (magmatic), extrusive, or depositional-erosional mechanisms such as shallow or deep-seated magmatic assimilation from enveloping wall rocks or erosion during pyroclastic extrusion and deposition. Some Tertiary sedimentary wall rocks may contain old detrital zircons; thus assimilation may incorporate Proterozoic or older zircons without the need for assimilating pre-Tertiary basement. For example, we interpret the plot in Figure A3 as zircons obtained from the Naches Formation wall rocks surrounding the tuff of Stampede Pass vent area as discussed under unit Ꝑvt on p. 14.

Fig. A1 Unit Ꝑvr Snoqualmie Falls on Fig. 2 on plate 07-23A

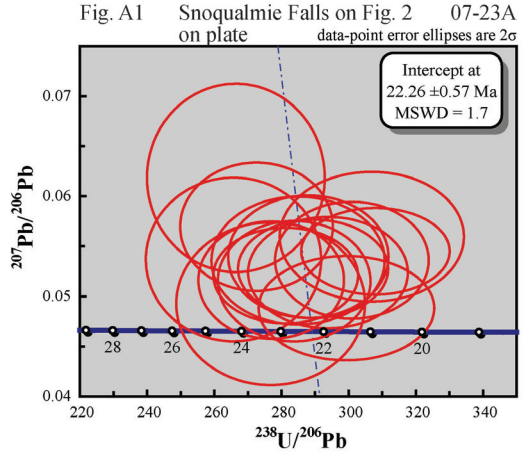

Fig. A2 Unit Ꝑvt 07-47T

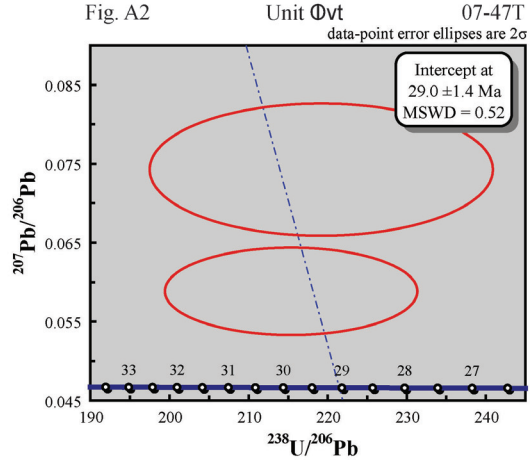

Age site 4 on plate

Fig. A3 Unit Ꝑvt 07-47T

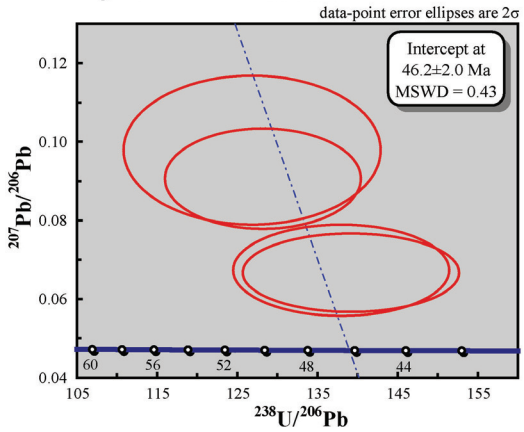

Age site 4 on plate

Fig. A4 Unit Ꝑvt 07-47T

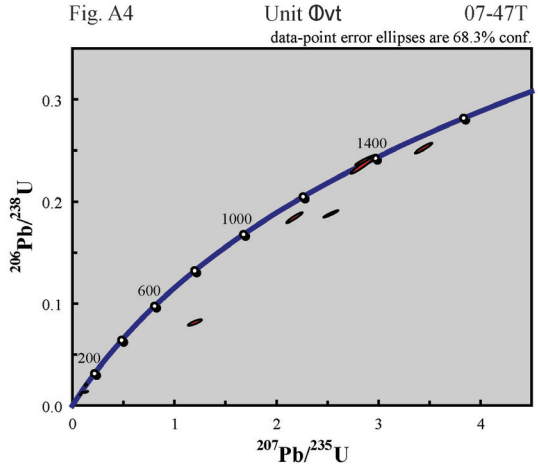

Age site 4 on plate

Fig. A5 Unit ꝐEva 07-10F

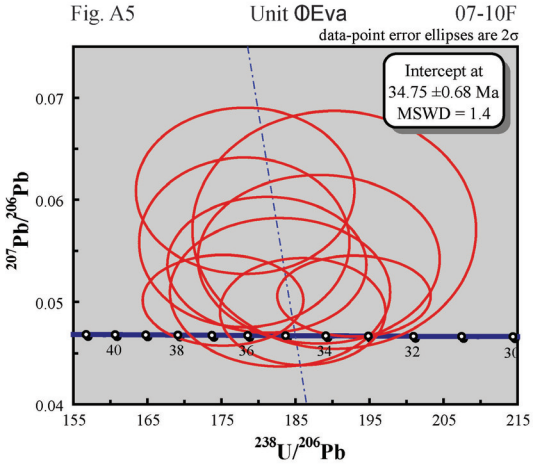

Age site 5 on plate

Fig. A6 Unit ꝐEva 07-10F

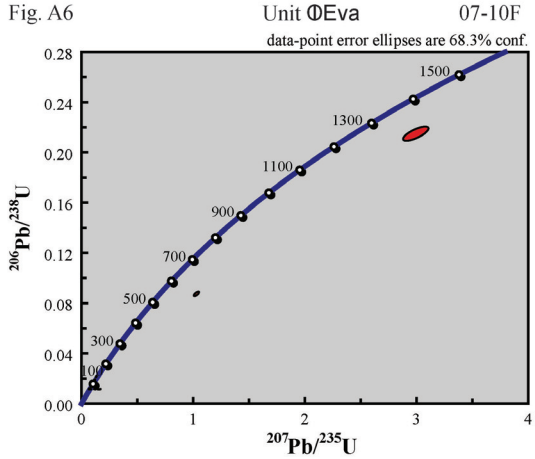

Age site 5 on plate

Fig. A7 Unit Evt$_t$ 07-14E

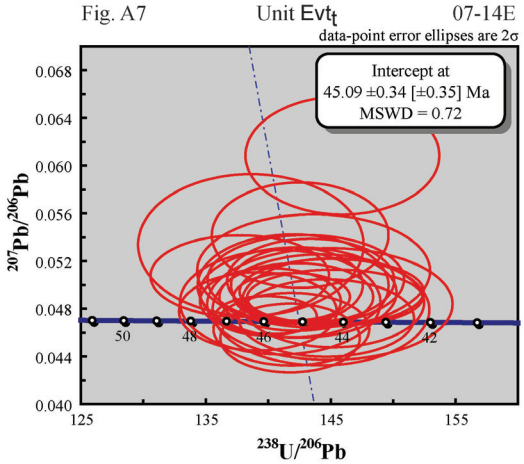

Age site 6 on plate

Fig. A8 Unit Evt$_t$ 07-14E

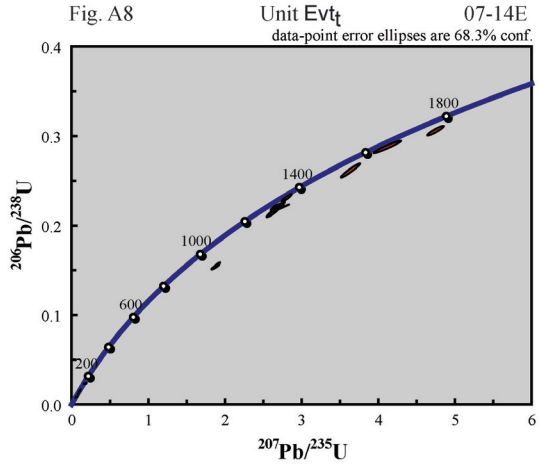

Age site 6 on plate

Table A1. U-Pb (LA-ICP-MS) geochronology data. Age sites are located on the geologic map (plate). See unit Ꝑvr near Snoqualmie Falls on Figure 2 (plate) for the general location of sample 07-23A. "Zircon grain no. and zircon spot letter" provides the number of zircons analyzed for the age, as well as the number of laser sites for each zircon. For example, "12a-3" was from the twelfth zircon analyzed from the sample at laser probe site "a" (third grain mount). Error ellipses for the bold $^{206}Pb/^{238}U$ ages are shown on Figures A1–A8. See geologic unit descriptions for further information.

Sample no.	Zircon grain no. and zircon spot letter	$^{238}U/^{206}Pb$ ratio	2σ (sigma) error (%)	$^{207}Pb/^{206}Pb$ ratio	2σ (sigma) error (%)	$^{206}Pb/^{238}U$ age (Ma)	2σ (sigma) absolute error (Ma)	$^{207}Pb/^{206}Pb$ age (Ma)	2σ (sigma) absolute error (Ma)
Sample 07-14E at "age site 6" on the plate. Unit Evtt pumiceous volcanic sandstone at small waterfall east of Brewster Lake at 47.4475°N, 121.7803°W in the east-central part of the map area.									
07-14E	5b-1	152.4211	5.16%	0.0469	8.01%	42.2	2.2	—	—
07-14E	14a-1	149.3832	4.66%	0.0501	6.66%	43.0	2.0	—	—
07-14E	15a-2	145.9348	4.34%	0.0609	6.65%	**44.0**	1.9	—	—
07-14E	5a-2	145.3229	3.95%	0.0489	3.91%	**44.2**	1.7	—	—
07-14E	3a-2	145.1779	4.11%	0.0485	6.29%	**44.3**	1.8	—	—
07-14E	6a-2	145.0780	4.15%	0.0495	4.52%	**44.3**	1.8	—	—
07-14E	2d-2	144.9359	5.54%	0.0484	7.91%	**44.3**	2.4	—	—
07-14E	2b-1	144.6484	3.96%	0.0472	5.61%	**44.4**	1.8	—	—
07-14E	2a-2	144.2184	4.91%	0.0479	7.94%	**44.5**	2.2	—	—
07-14E	11a-1	143.6294	5.31%	0.0512	7.57%	**44.7**	2.4	—	—
07-14E	12a-2	143.4026	3.81%	0.0504	5.65%	**44.8**	1.7	—	—
07-14E	7a-2	143.0068	4.49%	0.0505	6.05%	**44.9**	2.0	—	—
07-14E	6a-3	142.5557	4.05%	0.0542	6.66%	**45.1**	1.8	—	—
07-14E	2b-2	142.4078	4.51%	0.0494	6.27%	**45.1**	2.0	—	—
07-14E	11a-3	142.2950	3.03%	0.0500	5.10%	**45.1**	1.4	—	—
07-14E	6a-1	142.2412	3.54%	0.0490	4.72%	**45.2**	1.6	—	—
07-14E	10a-3	141.9905	4.40%	0.0499	7.05%	**45.2**	2.0	—	—
07-14E	3a-3	141.8890	2.68%	0.0490	3.32%	**45.3**	1.2	—	—
07-14E	5a-1	141.8489	3.59%	0.0463	5.37%	**45.3**	1.6	—	—
07-14E	7a-3	141.7458	3.22%	0.0456	5.16%	**45.3**	1.5	—	—
07-14E	2a-1	140.9528	4.65%	0.0486	7.36%	**45.6**	2.1	—	—
07-14E	13a-2	140.1705	3.29%	0.0486	4.62%	**45.8**	1.5	—	—
07-14E	1a-3	139.8329	2.36%	0.0474	2.84%	**45.9**	1.1	—	—
07-14E	3b-1	139.1661	3.71%	0.0478	5.60%	**46.2**	1.7	—	—
07-14E	5c-1	138.6074	5.32%	0.0534	9.08%	**46.3**	2.5	—	—
07-14E	2c-2	137.7224	4.24%	0.0508	5.50%	**46.6**	2.0	—	—
07-14E	1a-1	125.9324	7.95%	0.0603	17.13%	51.0	4.0	—	—
07-14E	4a-2	94.0291	4.38%	0.0515	5.79%	68.2	3.0	—	—
07-14E	12b-1	92.4231	4.58%	0.0517	5.51%	69.4	3.2	—	—
07-14E	4a-3	74.8220	2.65%	0.0479	3.59%	85.6	2.3	—	—
07-14E	14a-2	72.2416	3.31%	0.0522	4.13%	88.6	2.9	—	—
07-14E	7b-1	70.3362	3.44%	0.0483	4.45%	91.0	3.1	—	—
07-14E	10a-2	69.6675	2.86%	0.0496	2.67%	91.9	2.6	—	—
07-14E	7a-1	64.6885	3.44%	0.0465	4.34%	98.9	3.4	—	—
07-14E	8a-2	62.2659	2.86%	0.0483	3.09%	102.7	2.9	—	—
07-14E	5b-3	44.4601	2.13%	0.0495	2.28%	143.4	3.0	—	—

Sample no.	Zircon grain no. and zircon spot letter	$^{238}U/^{206}Pb$ ratio	2σ (sigma) error (%)	$^{207}Pb/^{206}Pb$ ratio	2σ (sigma) error (%)	$^{206}Pb/^{238}U$ age (Ma)	2σ (sigma) absolute error (Ma)	$^{207}Pb/^{206}Pb$ age (Ma)	2σ (sigma) absolute error (Ma)
07-14E	5a-3	43.9802	2.45%	0.0578	3.95%	144.9	3.5	—	—
07-14E	18a-2	6.5088	2.83%	0.0880	1.52%	921.3	24.3	1383.1	29.0
07-14E	8a-3	6.4270	2.49%	0.0878	1.05%	932.2	21.6	1378.9	20.0
07-14E	9a-1	4.6160	4.05%	0.0884	1.36%	1264.1	46.4	1391.3	26.0
07-14E	13a-1	4.6096	4.34%	0.0880	1.40%	1265.7	49.8	1381.6	26.8
07-14E	1a-2	4.5562	2.81%	0.0897	2.67%	1279.1	32.6	1419.7	50.6
07-14E	11a-2	4.5379	2.55%	0.0878	1.50%	1283.8	29.7	1377.8	28.8
07-14E	9a-3	4.5342	2.11%	0.0867	0.92%	1284.8	24.5	1353.1	17.8
07-14E	2a-3	4.4943	2.29%	0.0884	1.05%	1295.1	26.9	1392.1	20.1
07-14E	17a-2	4.3235	2.41%	0.0877	1.27%	1341.3	29.2	1375.3	24.2
07-14E	12a-1	3.8147	4.03%	0.1004	1.27%	1500.8	53.8	1630.6	23.5
07-14E	3a-2	3.4626	3.26%	0.1032	2.73%	1635.5	47.0	1681.9	50.1
07-14E	16a-2	3.2612	2.34%	0.1121	1.19%	1724.1	35.3	1833.2	21.5
Sample 10F at "age site 5" on the plate. Unit ΦEva felsic tuff; directly south of the Steele Creek fault at 47°24′53.056″N, 121°49′48.197″W north of the Cedar River in the south-central part of the study area.									
07-10F	5b-1	205.0732	9.17%	0.0752	12.56%	31.4	2.9	—	—
07-10F	1a-1	196.6519	9.78%	0.1894	10.10%	32.7	3.2	—	—
07-10F	1b-1	192.9089	4.39%	0.0506	6.39%	**33.3**	1.5	—	—
07-10F	7a-1	190.2532	8.23%	0.0571	16.67%	**33.8**	2.8	—	—
07-10F	16a-1	188.1636	7.09%	0.0542	12.43%	**34.2**	2.4	—	—
07-10F	8a-1	185.9893	4.91%	0.0491	8.72%	**34.6**	1.7	—	—
07-10F	3a-1	182.9251	6.64%	0.0510	11.65%	**35.1**	2.3	—	—
07-10F	15a-1	181.1500	6.06%	0.0537	10.11%	**35.5**	2.1	—	—
07-10F	14a-1	178.2165	6.77%	0.0609	10.91%	**36.1**	2.4	—	—
07-10F	10a-1	178.0983	6.52%	0.0558	12.14%	**36.1**	2.3	—	—
07-10F	13a-1	175.2236	5.06%	0.0502	7.24%	**36.7**	1.9	—	—
07-10F	11a-1	174.0355	5.97%	0.0444	9.60%	36.9	2.2	—	—
07-10F	4a-1	76.5762	3.51%	0.0496	4.98%	83.6	2.9	—	—
07-10F	6a-1	75.9806	3.11%	0.0497	5.12%	84.3	2.6	—	—
07-10F	5a-1	64.4270	3.30%	0.0474	4.82%	99.3	3.2	—	—
07-10F	12a-1	12.0357	2.75%	0.0874	2.55%	514.5	13.6	1370.1	48.6
07-10F	12b-1	4.6626	3.64%	0.1006	3.26%	1252.6	41.4	1634.9	60.0
Sample 47T at "age site 4" on the plate. Unit Φvt (Stampede Pass tuff); pumice-bearing dacitic tuff from prominent logging road cut bank at 47.3796°N, 121.7513°W in extreme southeast corner of map area.									
07-47T	17a-2	219.1896	8.09%	0.0743	9.21%	**29.3**	2.4	—	—
07-47T	4b-2	215.3791	6.05%	0.0588	7.69%	**29.9**	1.8	—	—
07-47T	4a-2	206.5298	5.35%	0.0562	7.41%	31.1	1.7	—	—
07-47T	7c-1	139.1688	7.91%	0.0667	12.20%	**46.2**	3.6	—	—
07-47T	7a-1	137.9573	7.97%	0.0673	14.07%	**46.6**	3.7	—	—
07-47T	7d-2	134.9070	11.27%	0.0992	14.64%	**47.6**	5.3	1609.6	261.2
07-47T	7b-1	128.1988	7.78%	0.0906	11.50%	**50.1**	3.9	—	—
07-47T	7d-1	126.8544	10.32%	0.0979	15.81%	**50.6**	5.2	—	—

Sample no.	Zircon grain no. and zircon spot letter	$^{238}U/^{206}Pb$ ratio	2σ (sigma) error (%)	$^{207}Pb/^{206}Pb$ ratio	2σ (sigma) error (%)	$^{206}Pb/^{238}U$ age (Ma)	2σ (sigma) absolute error (Ma)	$^{207}Pb/^{206}Pb$ age (Ma)	2σ (sigma) absolute error (Ma)
07-47T	10a-1	74.7482	3.36%	0.0510	3.27%	85.7	2.9	—	—
07-47T	15a-1	72.7561	3.99%	0.0495	4.76%	88.0	3.5	—	—
07-47T	13a-1	72.5087	2.98%	0.0495	2.75%	88.3	2.6	—	—
07-47T	9a-1	72.2767	3.15%	0.0556	4.24%	88.6	2.8	—	—
07-47T	3a-1	71.8441	2.92%	0.0491	2.42%	89.1	2.6	—	—
07-47T	6a-2	70.6489	3.19%	0.0481	3.06%	90.6	2.9	—	—
07-47T	2a-2	70.5462	2.51%	0.0474	2.01%	90.7	2.3	—	—
07-47T	6a-1	70.0404	5.00%	0.0542	5.85%	91.4	4.5	—	—
07-47T	3a-1	69.9064	3.64%	0.0469	2.73%	91.6	3.3	—	—
07-47T	3b-1	69.8120	4.16%	0.0534	3.75%	91.7	3.8	—	—
07-47T	16a-1	69.2321	3.74%	0.0504	4.10%	92.4	3.4	—	—
07-47T	1a-2	68.5371	3.45%	0.0468	2.58%	93.4	3.2	—	—
07-47T	12a-1	64.7948	2.78%	0.0490	2.63%	98.7	2.7	—	—
07-47T	5b-1	13.2144	5.56%	0.1119	4.19%	470.3	25.2	1830.6	74.9
07-47T	5a-1	5.5893	4.13%	0.0869	1.58%	1061.0	40.3	1359.2	30.2
07-47T	1a-2	5.4632	2.70%	0.0991	1.63%	1083.6	26.9	1607.3	30.3
07-47T	2a-1	4.3492	4.65%	0.0885	1.56%	1334.1	56.0	1393.7	29.8
07-47T	5b-2	4.2403	2.80%	0.0873	2.00%	1365.0	34.4	1366.7	38.2
07-47T	11a-1	4.0412	2.82%	0.0999	1.12%	1425.3	36.0	1622.8	20.8
Sample 23A. Site is north of the map area and directly north of Snoqualmie Falls along east bank of Snoqualmie River and below the wooden observation deck at 47.5431°N, 121.8396°W (Snoqualmie 7.5-minute quadrangle and Fig. 2 on plate). Rhyolite contains smokey quartz phenocrysts in hand sample. Contact relations not exposed. Coarse volcanic breccias with bombs across the river suggest proximal deposition of volcanic rocks here. Rocks at this site were earlier included in the volcanic rocks of Mount Persis by Tabor and others (1993). Rock is dark gray to slightly greenish with a glassy matrix and minor plagioclase.									
07-23A	1e-1	307.9563	5.86%	0.0545	6.48%	**20.9**	1.2	—	—
07-23A	3b-1	306.8729	7.31%	0.0560	9.48%	**21.0**	1.5	—	—
07-23A	2a-1	300.9431	6.21%	0.0536	8.90%	**21.4**	1.3	—	—
07-23A	2b-1	299.3252	7.14%	0.0488	8.72%	**21.5**	1.5	—	—
07-23A	2d-1	293.8336	6.61%	0.0524	8.68%	**21.9**	1.4	—	—
07-23A	1d-1	289.4118	6.31%	0.0528	7.63%	**22.2**	1.4	—	—
07-23A	3c-1	287.9727	6.77%	0.0540	9.27%	**22.3**	1.5	—	—
07-23A	2c-1	284.9150	7.39%	0.0536	9.75%	**22.6**	1.7	—	—
07-23A	2e-1	283.7517	6.54%	0.0515	9.57%	**22.7**	1.5	—	—
07-23A	3d-1	281.2524	6.26%	0.0521	7.49%	**22.9**	1.4	—	—
07-23A	1f-1	276.9228	6.40%	0.0516	9.30%	**23.2**	1.5	—	—
07-23A	1b-1	276.7542	8.30%	0.0493	13.48%	**23.3**	1.9	—	—
07-23A	3a-1	272.5514	6.81%	0.0570	9.20%	**23.6**	1.6	—	—
07-23A	1a-1	266.4034	8.12%	0.0618	12.44%	**24.2**	2.0	—	—
07-23A	1c-1	265.7011	8.03%	0.0537	12.46%	**24.2**	1.9	—	—